EPRI

# The Potential Effects of Single-Phase Power Electronic-Based Loads on Power System Distortion and Losses

## Volume 4: The Harmonic Impact of Electric Vehicle Battery Charging

# The Potential Effects of Single-Phase Power Electronic-Based Loads on Power System Distortion and Losses

Volume 4: The Harmonic Impact of Electric Vehicle Battery Charging

**1000664**

Final Report, September 2003

## DISCLAIMER OF WARRANTIES AND LIMITATION OF LIABILITIES

THIS DOCUMENT WAS PREPARED BY THE ORGANIZATION(S) NAMED BELOW AS AN ACCOUNT OF WORK SPONSORED OR COSPONSORED BY THE ELECTRIC POWER RESEARCH INSTITUTE, INC. (EPRI). NEITHER EPRI, ANY MEMBER OF EPRI, ANY COSPONSOR, THE ORGANIZATION(S) BELOW, NOR ANY PERSON ACTING ON BEHALF OF ANY OF THEM:

(A)  MAKES ANY WARRANTY OR REPRESENTATION WHATSOEVER, EXPRESS OR IMPLIED, (I) WITH RESPECT TO THE USE OF ANY INFORMATION, APPARATUS, METHOD, PROCESS, OR SIMILAR ITEM DISCLOSED IN THIS DOCUMENT, INCLUDING MERCHANTABILITY AND FITNESS FOR A PARTICULAR PURPOSE, OR (II) THAT SUCH USE DOES NOT INFRINGE ON OR INTERFERE WITH PRIVATELY OWNED RIGHTS, INCLUDING ANY PARTY'S INTELLECTUAL PROPERTY, OR (III) THAT THIS DOCUMENT IS SUITABLE TO ANY PARTICULAR USER'S CIRCUMSTANCE; OR

(B)  ASSUMES RESPONSIBILITY FOR ANY DAMAGES OR OTHER LIABILITY WHATSOEVER (INCLUDING ANY CONSEQUENTIAL DAMAGES, EVEN IF EPRI OR ANY EPRI REPRESENTATIVE HAS BEEN ADVISED OF THE POSSIBILITY OF SUCH DAMAGES) RESULTING FROM YOUR SELECTION OR USE OF THIS DOCUMENT OR ANY INFORMATION, APPARATUS, METHOD, PROCESS, OR SIMILAR ITEM DISCLOSED IN THIS DOCUMENT.

ORGANIZATION(S) THAT PREPARED THIS DOCUMENT

**EPRI PEAC**
**University of Texas at Austin**

## ORDERING INFORMATION

# CITATIONS

This report was prepared by

University of Texas at Austin
24th and Speedway
Engineering Science Building 346
Austin, Texas 78712-1084

Principal Investigators
W.M. Grady
P.T. Staats
A. Arapostathis

This report describes research sponsored by EPRI and Reliant Energy and Salt River Project.

The report is a corporate document that should be cited in the literature in the following manner:

# REPORT SUMMARY

Utilities have traditionally considered harmonics due to single large loads the main harmonics problem in power systems. However, the increase in size and proliferation of single-phase power electronics-based loads has created a need for developing analytical tools for analyzing the impact of distributed nonlinear loads on electrical equipment and on the distribution system as a whole. This report focuses on the harmonic impact of electric vehicle battery charging.

## Background

The number and effect of single-phase nonlinear harmonic-producing devices connected to the power system have increased significantly over the past few years. While individual large single-phase power electronic loads do not pose a problem for electric utilities, harmonics generated by many distributed loads accumulate in the power system. The possible implications of large numbers of single-phase devices in distribution systems and in customer facilities are a growing concern for utilities and customers. This volume is the fourth part of a five-volume report that summarizes the results of an extensive research effort to analyze the impact of distributed harmonic sources on the utility system and on equipment. It focuses on the development of theory required to evaluate Electric Vehicle (EV) battery chargers as harmonic-producing loads and their possible impact on various aspects of power distribution systems.

## Objective

To evaluate the harmonic impact of electric vehicle battery charging.

## Approach

The project team attempted to predict the net harmonic current injection of a concentration of EV battery chargers operating in parallel. Previous studies have evaluated this problem by examining a 'worst-case' situation in which all of the battery chargers begin operation at the same time on fully discharged batteries. This method overstates the likely impact of EV battery charging by discounting any diversity in power level and harmonics among individual chargers that might result in partial harmonic current cancellation. The method presented in this report seeks to more accurately predict the net harmonic currents by accounting for uncertainty in both start-time and initial battery state-of-charge of an individual charger. The team accomplished this by formulating the problem stochastically and modeling the start-time and the initial battery state-of-charge of each charger in the concentration as random variables.

**Results**

The stochastic method used in this study indicates that EV harmonic currents are considerably less than the peak values that would be expected if the same number of chargers were operated in unison. The expected net magnitudes of harmonic currents per-charger from an EV concentration operating with a uniform start time probability distribution function lasting 8 hours are roughly one-half those of the full-load harmonic current magnitude of a single charger. The report also presents results quantifying the effect of an EV battery charging on a substation transformer that supplies commercial, residential, and EV load on a peak summer day. This analysis shows that the time of day and the length of time during which the EVs begin charging are critical in determining the amount of transformer derating required. Results show that with proper control, EV charging may have very little effect on power system components at the substation level.

**EPRI Perspective**

By providing utilities with analytical tools and methodologies to assess the impact of single-phase nonlinear loads, EPRI is enabling utilities to understand how these loads may impact the power system in the future. The results of this research should also help industries and utilities define meaningful and practical limits for harmonic current injection from single-phase nonlinear loads. These limits will ultimately benefit end users by improving the quality of the voltage supplied to end-use loads and minimizing the impact of harmonics voltage on equipment performance.

**Keywords**

Power Quality
Electric Vehicle
Harmonics
Transformer
Induction Motor

# ABSTRACT

The potential widespread use of electric vehicles (EVs) presents a potential danger to electric power distribution systems in the form of excessive harmonic currents. This report develops and presents the theory required to evaluate EV battery chargers as harmonic current distorting loads and their possible harmonic impact on various aspects of power distribution systems.

The report presents a method for evaluating the net harmonic current injection of a large collection of EV battery chargers. This method accounts for variation in start-time and initial battery state-of-charge (SOC) among individual chargers. Next, this method is used to evaluate the effect of input parameter variation on the net harmonic currents predicted by the model. We then turn to an evaluation of the impact of EV charger harmonic currents on power distribution systems by considering the effect that these currents have on substation transformers and system harmonic voltages.

The results indicate that accounting for variations in start-time and SOC in the analysis leads to reduced estimates of harmonic current injection when compared to more traditional methods that do not account for these variations. Our analysis shows that from the point of view of substation transformers, the impact of EVs is mainly one of power and energy, rather than harmonics. Furthermore, our evaluation of several typical power distribution systems leads us to believe that from a harmonics perspective, most distribution systems can withstand at least a 15% penetration level of EVs while meeting IEEE guidelines for voltage distortion at almost all buses.

Thus, while localized harmonic problems at individual service transformers may occur, from a system perspective, most existing distribution systems should be able to accommodate the introduction of EV battery charging without widespread harmonic problems.

# CONTENTS

# LIST OF FIGURES

# LIST OF TABLES

# 1
# INTRODUCTION

---

Electric vehicle (EV) battery charging is a potentially large power system load that presents both opportunities and challenges to power engineers. With proper control, EV battery charging could raise load factor and profits for electric utilities. However, because EV battery chargers utilize AC/DC converters, unless deliberate and expensive design efforts are made, EV battery chargers can produce excessive harmonic currents.

Harmonic distortion of power system currents and voltages is not a new problem. Indeed, since the 1920s when static converters forced the study of waveform distortion in Germany, evaluating and mitigating power system harmonics has been a task of the power engineer. The mathematical basis for harmonic analysis dates to 1822 when the French mathematician Jean Babtiste Joseph Fourier postulated that any periodic waveform could be represented by a sum of sinusoids, each sinusoid having an integer multiple frequency of the fundamental [1]. Harmonic analysis is then the process of determining the magnitudes and phase angles of the individual harmonics of the periodic waveform [2].

In recent years, increasing attention has focused on current and voltage harmonic distortion in power systems caused by the use of non-linear power electronic loads. Though linear loads continue to make up the bulk of the total power system load, the composition of power system loads is changing rapidly as the use of high-efficiency non-linear power electronic loads becomes more common. The harmonic currents these loads produce do little or no useful work and cause extra power losses in distribution transformers, feeders and some conventional loads such as AC motors [3-5]. In the case of motors, transformers, and power capacitors, increased losses translate into lower efficiency and reduced life expectancy of the equipment. Harmonics can also cause interference with telephone communications, and result in the abnormal operation of important control and protection equipment [1]. Finally, harmonics adversely affect many loads designed to receive pure 60Hz electric power [6].

Frequently, harmonic distortion is detected on a power system only when expensive and destructive problems begin to occur [7]. Examples of these problems include the shutdown of industrial processes, or the catastrophic failure of power-factor correction capacitors [8]. Thus it is the concern of the power engineer to study the harmonic distorting properties of power system loads and to predict their effect on the power network.

One such harmonic distorting load is the EV battery charger. Recent studies of the current total harmonic distortion (THDI) of several commercially-available EV battery chargers indicate that many of the chargers currently on the market draw highly distorted currents. Table 1-1 details the THDI of several such chargers operating at full power [9].

Though many single-phase power electronic loads common to power systems currently draw currents with THDI higher than those listed in Table 1-1, EV battery chargers may contribute heavily to power system distortion because they operate at very high power levels. In contrast to a computer which operates around 100W, an EV battery charger can be expected to operate at full power anywhere between three and eight kW. Thus, similar levels of THDI result in much higher harmonic current injections for the EV battery charger than for the computer.

**Table 1-1**
**Commercially Available EV Battery Charger Current Distortions**

| Charger | THD$_I$ - % |
|---------|-------------|
| 1 | 7.0 |
| 2 | 17.2 |
| 3 | 56.7 |
| 4 | 8.1 |
| 5 | 15.7 |
| 6 | 21.4 |
| 7 | 27.6 |
| 8 | 99.0 |

This report develops and presents the theory and solution methodology for evaluating the EV battery charger as a harmonic distorting load, its effect on power distribution system voltages, and its effect on certain power system components.

The main theory is presented in Chapter 2 and yields a method for predicting the net harmonic currents generated by a concentration of similar EV battery chargers operating in parallel. Figure 1-1 describes this situation.
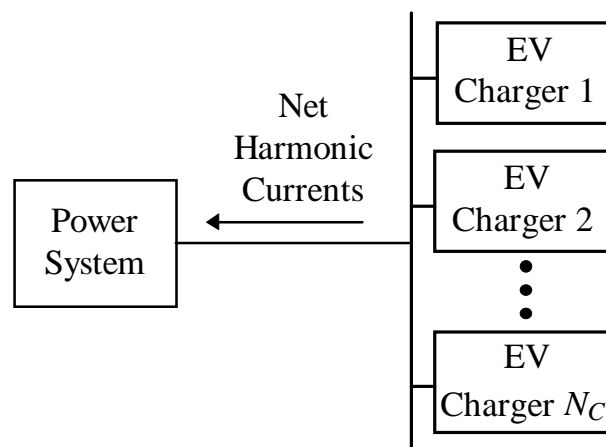


**Figure 1-1**
**$N_c$ Electric Vehicle Chargers in Parallel**

Previous studies have evaluated this problem by examining a 'worst-case' situation in which all of the battery chargers begin operation at the same time, and all have fully discharged batteries [9]. This prediction overstates the likely impact of EV battery charging by discounting any diversity among individual chargers in the concentration, which will lead to partial harmonic current cancellation. The method presented in this work seeks to more accurately predict the net harmonic currents by accounting for uncertainty in both the start-time and initial battery state-of-charge of each individual charger. This is done by formulating the problem stochastically; the start-time and the initial battery state-of-charge of each charger in the concentration are modeled as random variables. The statistics of net harmonic injection current generated by the method indicate that peak expected EV harmonic currents are considerably less than the peak values that would be expected if the same number of chargers are operated in unison.

Chapter 3 studies the sensitivity to parameter variation of the net harmonic current statistics generated by the aforementioned method. The density functions of the random variables that model start-time and initial battery state-of-charge of an individual EV battery charger are varied in order to determine their effect on the predicted net harmonic currents. Also, the parameters describing the individual EV battery charger are varied to account for EVs with varying fuel-efficiencies.

Subsequently, Chapter 4 studies the effect of EV battery charging on a substation transformer that supplies commercial, residential, industrial, and EV load on a peak summer day. Figure 1-2 describes this situation.
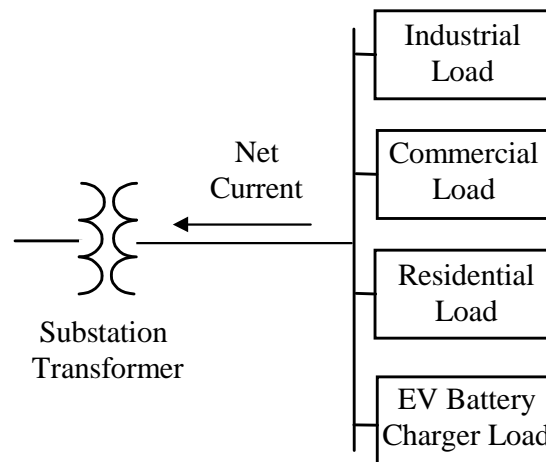


**Figure 1-2**
**Loaded Substation Transformer**

This analysis models non-EV load with typical utility load shapes. EV load is modeled using statistics generated by the method presented in Chapter 2. The effect of net load on the substation transformer is evaluated using ANSI/IEEE standards for transformer loading and the effect of nonlinear currents on power system devices [20-21]. For specific non-EV load, EV charging is introduced, and the amount of transformer derating required to maintain a constant daily transformer loss-of-life, with and without EV charging, is computed. The time of day when the EV chargers and the amount of time during which the chargers may begin operation are found to

be critical in determining the amount of transformer derating required to maintain a constant transformer life-expectancy.

Chapter 5 presents a statistical method for predicting the effect that widespread EV battery charging will have on power distribution system harmonic voltage levels. The method relies on a statistical description of nonlinear load currents and data for actual power distribution networks to determine the statistics of network harmonic voltages. To describe the nonlinear load currents generated by the EV chargers, the work relies on the method presented in Chapter 2. Using the voltage statistics computed, this chapter presents the probabilities of exceeding certain specific levels of voltage total harmonic distortion at various points in the example systems.

Also presented in Chapter 5 are the results of several analyses of three different actual power distribution networks. By varying the EV penetration, or number of residences with EV chargers, the method generates, with varying degrees of confidence, plots of the fraction of buses whose voltage total harmonic distortion ($THD_v$) will not exceed 5%. The results of analysis of several different networks under different conditions indicate that there is a threshold penetration below which EV charging has negligible impact on the number of buses whose $THD_v$ exceed 5%.

Chapter 6 concludes this report, highlighting the significant contributions and suggesting possible future research. The Appendices include data on the EV charger used in this study and the results of a statistical analysis of the net harmonic currents generated by a concentration of EV battery chargers. Also included are the FORTRAN implementations of the methods presented in Chapters 2, 4, and 5, as well as the data describing the three power distribution networks evaluated in Chapter 5.

# *2*
# PREDICTING NET POWER AND HARMONIC CURRENTS

## Introduction

Electric vehicle (EV) battery charging presents a potential problem to power systems in the form of excessive harmonic currents. Thus, it is important to develop a technique for predicting the net harmonic currents injected by a large number of EV chargers, so that an accurate and realistic assessment can be made of the impact EV charging may have on power systems.

Orr, et al. [11], using a Monte Carlo simulation, analyzed the harmonic currents associated with a cluster of EV battery chargers connected to a common bus. This chapter presents an analytical solution technique for predicting the harmonic currents produced by a group of EV battery chargers. It has been shown previously [10] that ignoring diversity among distributed harmonic sources leads to a significant overestimation of the harmonic problem. The technique presented in this chapter accounts for the diversity caused by variations in individual charger start-time and battery state-of-charge. The results are validated using Monte Carlo trials.

## Formulation of the Net Harmonic Current Problem

We analyze the net harmonic current injection induced by a number $N_c$ of similar EV chargers operating in parallel. Figure 2-1 describes this situation. We study the problem in as realistic a fashion as possible, taking into account diversity among the operating characteristics of the chargers. The analysis begins by characterizing the individual chargers.
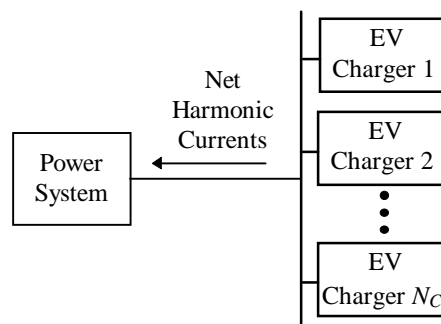


**Figure 2-1**
**$N_c$ Electric Vehicle (EV) Chargers in Parallel**

## Individual EV Charger Model

We adopt a generic model of an EV charger using actual data from a commercially-available EV charger and battery. The power profile of this charger, which is also typical of other EV chargers we have seen, is displayed in Figure 2-2. When the battery state-of-charge is low, the charger operates at maximum rated current. This continues until the battery voltage nears its gassing limit, at which time current drops as the charger maintains a constant voltage, and as battery receptivity drops. Charging ceases at a predetermined battery voltage in order to prevent damage to the battery [12]. The total energy in Figure 2-2 is approximately 20 kWh.

Though the battery gassing voltage is variable, this variation is relatively small. It is reasonable then to expect that, for a partially charged battery, charger power follows a time-shifted original power profile. In other words, the charger begins operation at the point $t_0$ on the fully discharged power profile so that the area under the profile curve to the right of $t_0$ equals the energy required by the battery.
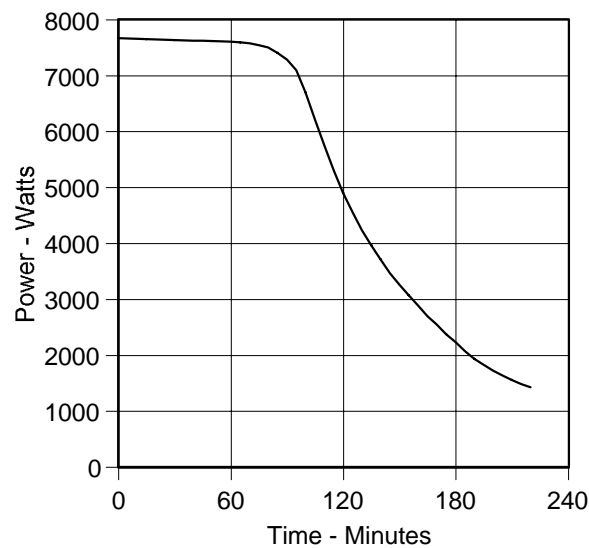


**Figure 2-2**
**Typical Power Profile of EV Charger**

## Charger Harmonic Currents

It is necessary to have information on both the harmonic current magnitudes and phase angles in order to account for cancellation when computing the net harmonic currents. These data were recorded for the example charger at specific time intervals using a spectrum analyzer which provides magnitude and phase angle information for each harmonic.

The particular 480V single-phase charger studied is a flat-plate inductive system using parallel diode bridges and an input transformer with variable taps to maintain constant DC voltage. For 240V operation, the DC circuit is the same, a 240V transformer is used, and the AC current magnitudes double. It is expected that most residential EV chargers will operate at 240V [13]; hence, we double all measured currents.

Harmonic composition varies, and $THD_I$ increases, as battery state-of-charge increases. Furthermore, for different chargers, $THD_I$ can range as high as 100%, or as low as 7% at full load [9], [14]. Using the terminology in [9], the study charger is appropriately classified as a "medium" distorting charger. Figure 2-3 shows how the shape of the input current varies with battery state-of-charge with zero degrees referenced to zero voltage.
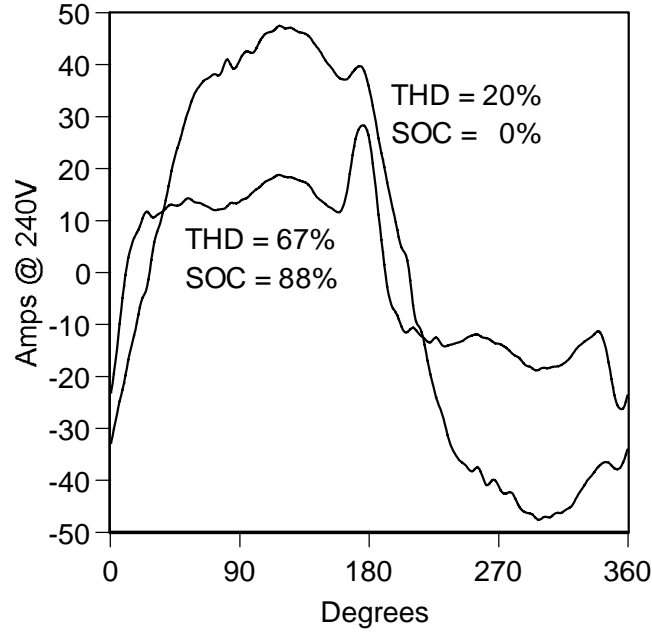


**Figure 2-3**
**Individual Charger Current Waveforms and Their Respective *THD$_I$* at Two Different States-of-Charge (SOC)**

By decomposing the harmonic currents into their real and imaginary components, plotting each real and imaginary harmonic current versus power, and subsequently interpolating their graphs by polynomial curves at a sufficient number of points, we obtain a continuous approximation of the harmonic current injections for each power level. We define $\hat{X}_h(P)$ and $\hat{Y}_h(P)$ to be the values of the real and imaginary harmonic currents of order *h* in Amps for an individual charger operating at power *P*. The coefficients of the approximating polynomials are shown in Table A-1 of Appendix A. Harmonics above the 15th multiple are small in magnitude and are ignored in this study.

### *Initial State-of-Charge and Start-Time Distributions*

Any diversity among individual chargers in the concentration will lead to partial harmonic current cancellation. Orr, et al. [11], showed that diversity is introduced among chargers because of two effects:

- Variable charger starting time.

- Variable initial battery state-of-charge (SOC).

2-3

Because not all EVs in the concentration will begin charging simultaneously, different chargers will likely be operating at different points in their charging profiles at any given instant. It is, however, impossible to know with certainty when a particular charger will begin operation. Therefore, we treat the start-time of an individual charger as a random variable with probability density function (pdf) $g(t)$. Likewise, not all chargers will begin operation on a fully discharged battery. Initial SOC of the battery is a function of the total distance the EV has traveled since its last charge, which also cannot be known deterministically. Hence, we model initial battery SOC as a random variable with pdf $f(E)$ where $E$ is the initial battery SOC expressed in percent.

Using the probability density function $d(m)$ of the typical miles traveled by an American commuter automobile presented in [11], it is possible to estimate the density function of initial battery SOC. According to [15], average trip length increased 11% from 1983 to 1990. To account for growth, we scale the mean and variance by the factor 1.11. Assuming that the pdf is representative of the EV in question, that each EV is recharged only once daily, that the typical EV battery has a set range in miles $R$, and that we can scale $d(m)$ so as to ignore vehicles that travel further than $R$, the pdfs $f(E)$ and $d(m)$ are related by

$$f(E) = \frac{R}{100} d\left( R - \frac{R \cdot E}{100} \right). \qquad \textbf{Eq. 2-1}$$

Assuming a typical EV battery range of 75 miles [16], the actual density $f(E)$ used in the calculations becomes that shown in Figure 2-4. This range matches the expected range for a 20 kWH battery [17].
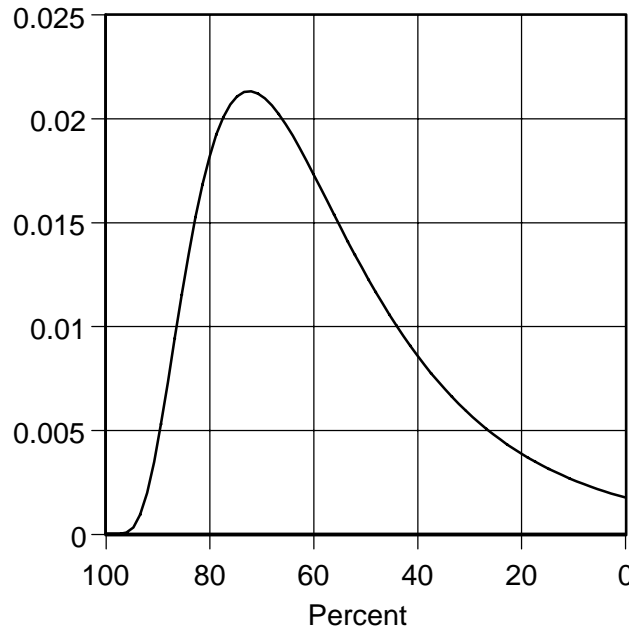


**Figure 2-4**
**Probability Density Function of Initial Battery SOC**

## *Net Power and Harmonic Currents for One Charger*

Before analyzing the net power and harmonic current injections of the concentration, we first evaluate the power drawn by an individual charger. The time period of interest is the interval of non-zero probability density of start-time augmented by the interval of time necessary to charge a fully discharged battery.

In order to facilitate the numerical calculations we discretize both the time domain and the power range. This is accomplished by selecting a fixed time interval, $\Delta t$, so that there are a suitable number, *N*, of discrete power levels $P_i$, $i = 1,..., N$, from the power profile. These are given by

$$P_i = \frac{p(i\Delta t) + p((i-1)\Delta t)}{2}.$$

**Eq. 2-2**

Thus, we obtain the corresponding charger energy levels $E_i$, defined by

$$E_i = \sum_{k=i}^{N} P_k \Delta t.$$

**Eq. 2-3**

Discretizing *f(E)* at these energy levels and *g(t)* at the time-partition, respectively, we define

$$f_i = \frac{f(E_{i+1}) + f(E_i)}{2}(E_{i+1} - E_i),$$

**Eq. 2-4**

$$g_j = \frac{g(j\Delta t) + g((j-1)\Delta t)}{2}\Delta t .$$

**Eq. 2-5**

Next, we calculate the probability of a charger operating at power level $P_i$ at time $j$, which we denote by $\phi(P_i, j)$. If charging started at time $k \leq j$, then it follows that the operation commenced at power level $P_{i-(j-k)}$, or in other words, at an initial battery SOC $E_{i-(j-k)}$, which according to the model has probability $f_{i-(j-k)}$. Imposing the natural assumption that charging start-time and battery SOC are independent, we deduce that the probability of a charger starting operation at time *k* and operating at power $P_i$ at some later time *j* is the product of $g_k$ and $f_{i-(j-k)}$. Therefore, we obtain the discrete pdf

$$\phi(P_i, j) = \sum_{k=1}^{j} g_k f_{i-(j-k)},$$

**Eq. 2-6**

from which we compute the expected value $\hat{\mu}_P(j)$ and variance $\hat{\sigma}_P^2(j)$ of power at each time *j*.

It is also possible to compute the statistics describing the harmonic currents at each discrete time $j$. We define $\hat{\mu}_{X_h}(j)$ and $\hat{\sigma}^2_{X_h}(j)$ to be the mean and variance, respectively, of the real component of the $h$-order harmonic current at time $j$ for a single charger. Thus,

$$\hat{\mu}_{X_h}(j) = \sum_{k=1}^{N} \phi(P_k, j)\hat{X}_h(P_j),$$  **Eq. 2-7**

$$\hat{\sigma}^2_{X_h}(j) = \sum_{k=1}^{N} \phi(P_k, j)\hat{X}^2_h(P_k) - \hat{\mu}^2_{X_h}(j).$$  **Eq. 2-8**

The mean and variance, $\hat{\mu}_{Y_h}(j)$ and $\hat{\sigma}^2_{Y_h}(j)$, of the imaginary component of the $h$-order harmonic current at time $j$ are similarly computed.

## Net Power and Harmonic Current for $N_c$ Chargers

We now embark on the study of the net power and harmonic currents for a concentration of chargers using the statistics of an individual charger that were derived in the previous section. We make the reasonable assumption that chargers are operated independently of each other but in a similar fashion. More precisely, we assume that the start-times are independent, identically distributed random variables.

We also assume that the initial battery SOCs presented to different chargers are independent and identically distributed according to the discrete density $f_i$. It then follows by the Central Limit Theorem that if the number of chargers in the concentration is sufficiently large, the total power drawn at each instant $j$ may be approximated by a Gaussian random variable. Net mean power, $\mu_P(j)$, and the variance of net power, $\sigma^2_P(j)$, equal the product of $N_c$ and the individual power mean and variance, respectively.

Likewise, net real and imaginary harmonic currents may be approximated by Gaussian random variables with means and variances equal to the product of $N_c$ and the appropriate individual means or variances. In fact, the net real and imaginary harmonic currents $X_h$, and $Y_h$ have an approximately joint Gaussian distribution with density

$$f_{X_h Y_h}(x, y, j) = \frac{\exp\left(\dfrac{-\eta}{2(1-\gamma^2)}\right)}{2\pi\sigma_{X_h}(j)\sigma_{Y_h}(j)\sqrt{1-\gamma^2}}.$$  **Eq. 2-9**

The correlation coefficient $\gamma$ is given by

$$\gamma = \frac{\text{Cov}(X_h, Y_h; j)}{\hat{\sigma}_{X_h}(j)\hat{\sigma}_{Y_h}(j)},$$  **Eq. 2-10**

where

$$\text{Cov}(X_h, Y_h; j) = N_C\left[\sum_{k=1}^{N}\hat{X}_h(P_k)\hat{Y}_h(P_k)\phi(P_k, j) - \hat{\mu}_{X_h}(j)\hat{\mu}_{Y_h}(j)\right].$$  **Eq. 2-11**

Also,

$$\eta = \frac{(x - \mu_{X_h}(j))^2}{\sigma_{X_h}^2(j)} - \frac{2\gamma(x - \mu_{X_h}(j))(y - \mu_{Y_h}(j))}{\sigma_{X_h}\sigma_{Y_h}} + \frac{(y - \mu_{Y_h}(j))^2}{\sigma_{Y_h}^2}.$$  **Eq. 2-12**

Transforming $(X_h, Y_h)$ into polar coordinates $(Z_h, \theta_h)$ [18], we compute the pdf of the harmonic magnitude at $j$ by

$$f_{Z_h}(z, j) = \int_0^{2\pi} z f_{X_h Y_h}(z\cos\theta, z\sin\theta, j)d\theta,$$  **Eq. 2-13**

from which we calculate the mean, $\mu_{Z_h}(j)$, and variance, $\sigma_{Z_h}^2(j)$, of the magnitude of the $h$-order harmonic current at time $j$.

## Example and Analysis of Method

To confirm our analytical results, we developed a computer algorithm to perform Monte Carlo trials to evaluate the concentration of chargers. This algorithm evaluates the net power and harmonic currents by selecting a random start-time and initial battery SOC according to the appropriate pdf for each of the $N_c$ chargers. After performing many Monte Carlo trials, this algorithm generates the relevant statistics. The FORTRAN implementation of this algorithm is found in Appendix C.

While the procedure described can support any start-time pdf, we choose a uniform pdf over an eight hour period. Using the charger model and initial battery SOC pdf presented earlier, we execute both the analytical and the Monte Carlo solutions. The FORTRAN implementation of the analytical method is found in Appendix B.

We now evaluate the net power and harmonic current characteristics. The distributions shown in Figures 2-5, 2-6, and 2-7 are characteristic of a concentration operating with uniform start-time pdf. Means and variances increase from zero, reaching a maximum value over a period of time

less than or equal to the on-time M of a charger operating on a fully discharged battery. They then remain at this maximum level, creating a plateau, throughout the remaining interval of support of the start-time distribution, after which they decrease monotonically to zero over a length of time *M*. Harmonics 11-15 exhibit the same type of characteristics as those shown in Figures 2-6 and 2-7.

As an indication of the value of $N_C$ required to validly apply the Central-Limit-Theorem, we compare the discrete pdf of power on the plateau generated by the Monte Carlo solution to that of the analytical solution. Defining the summed absolute error per charger (SAET) as the sum of the absolute values of the differences between the two densities, divided by the square root of $N_C$, we plot SAET in Figure 2-8. We see that the error between the two densities is sufficiently small for $N_C$ between 10 and 15. The densities of power on the plateau, for $N_C = 15$, as calculated by the Monte Carlo and analytical solution, are shown in Figure 2-9.
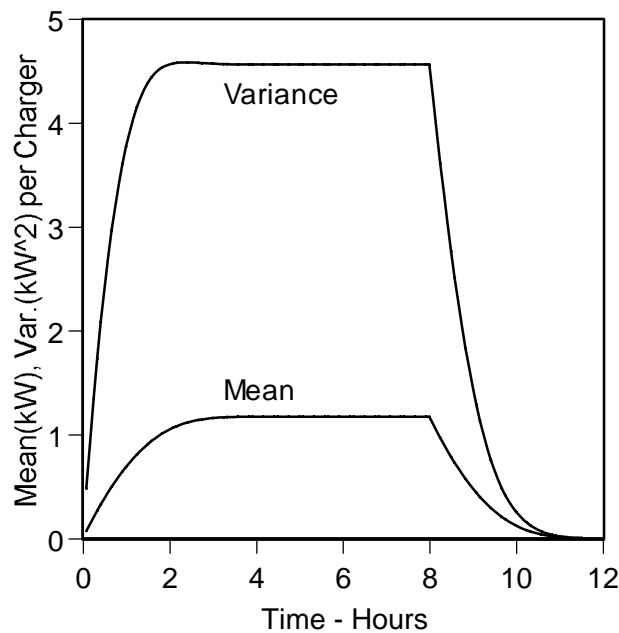


**Figure 2-5**
**Mean and Variance of Net Power vs. Time**
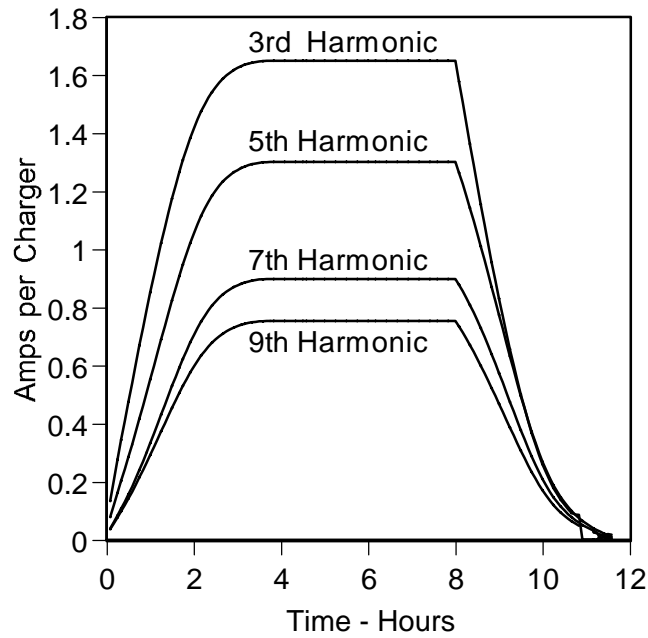
**Figure 2-6**
**Mean of Net Harmonic Current Magnitudes for Orders 3, 5, 7, 9 vs. Time**
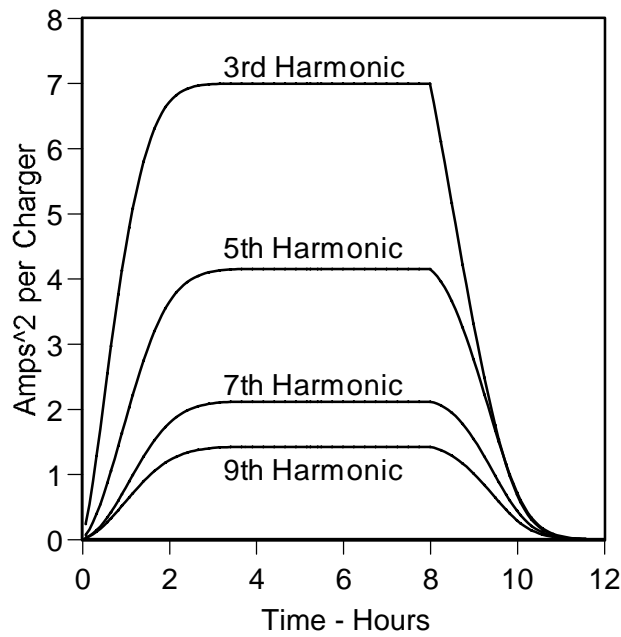


**Figure 2-7**
**Variance of Net Harmonic Current Magnitudes for Orders 3, 5, 7, 9 vs. Time**
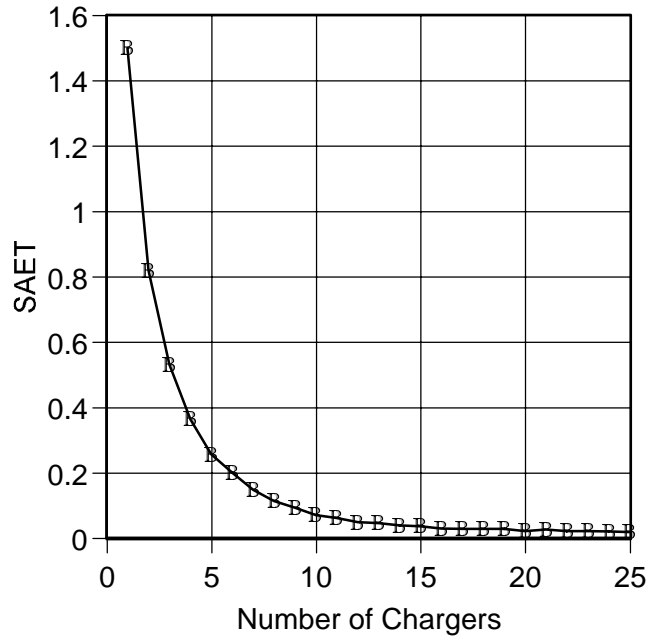
**Figure 2-8**
**Normalized Error between Monte Carlo and Analytical Power Densities on the Plateau**
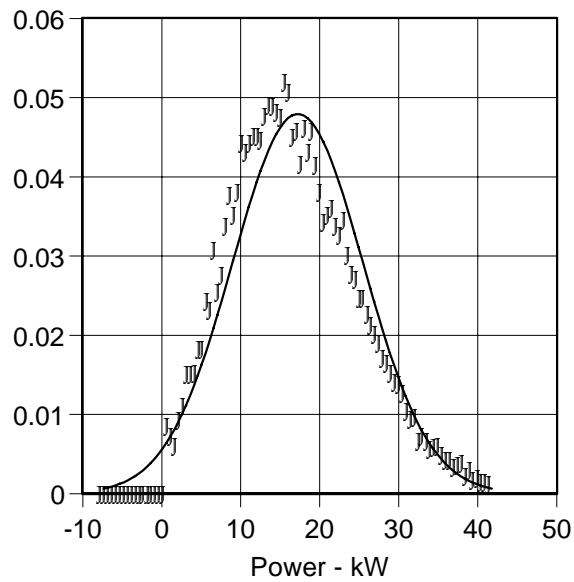


**Figure 2-9**
**Monte Carlo and Analytical PDF of Power on the Plateau, $N_c$ = 15**

Figures 2-10, 2-11 and 2-12 show the statistics of harmonic current magnitudes on the plateau calculated using the Monte Carlo and analytical method. The analytical solution converges to that of the Monte Carlo, and mean power and mean harmonic currents per charger remain constant for $N_C \geq 7$.
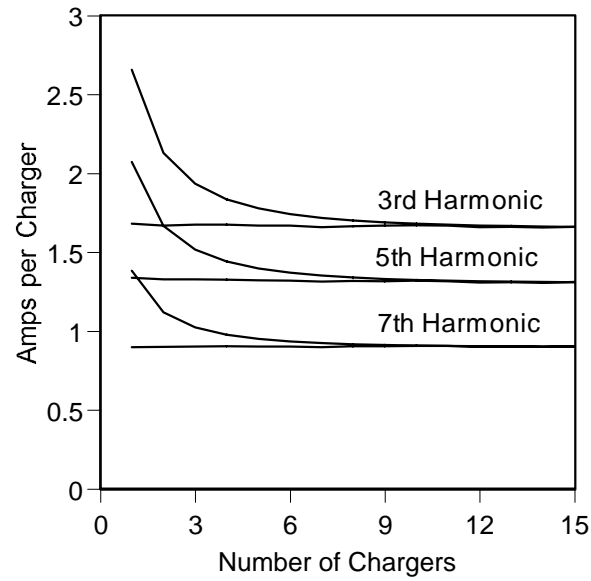
**Figure 2-10**
**Mean Harmonic Current Magnitude on the Plateau vs. Number of Chargers $N_c$ for Orders 3, 5, 7**
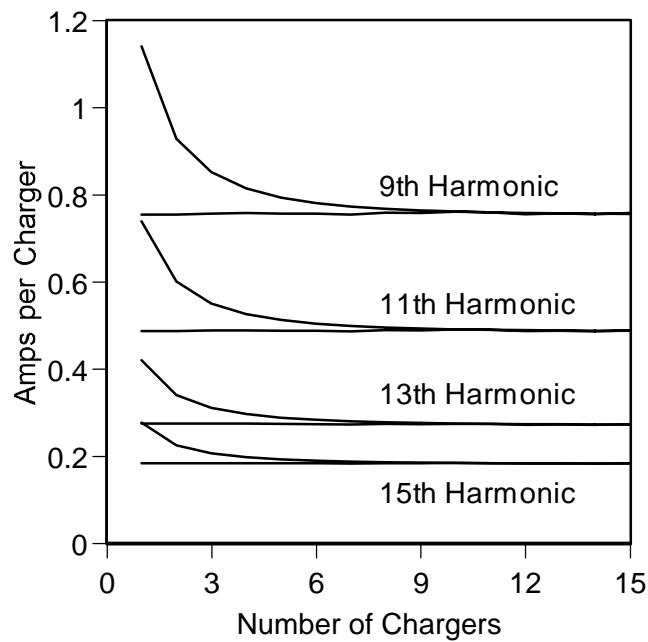


**Figure 2-11**
**Mean Harmonic Current Magnitude on the Plateau vs. Number of Chargers $N_c$ for Orders 9, 11, 13, 15**
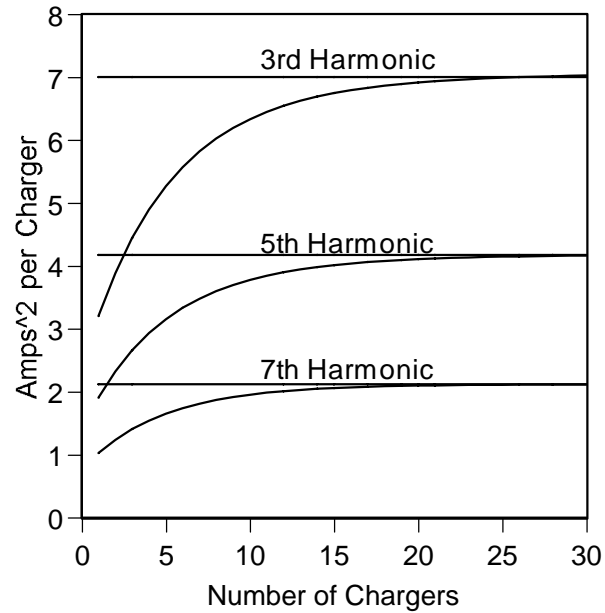
**Figure 2-12**
**Variance of Harmonic Current Magnitudes on the Plateau vs. Number of Chargers $N_c$**
**for Orders 3, 5, 7**

We now define the diversity factor of power, $DF_P$, as the ratio of the mean-per-charger power on the plateau to the full-load power of a single charger. Similarly, we define $DF_h$, the diversity factor of harmonic current, as the ratio of the mean-per-charger harmonic current magnitude on the plateau to the full-load harmonic current magnitude of a single charger.

For the example charger and distributions chosen, power on the plateau is normally distributed with mean 1.169 kW per charger, and variance 4.56 $(\text{kW})^2$ per charger. The $DF_P$ is 0.15, and mean current $THD_I$ on the plateau, calculated from Monte Carlo trials, is 49%. The statistics describing the net harmonic currents on the plateau, using a Fourier sine series reference, are shown in Table 2-1, and the corresponding current waveform is shown in Figure 2-13.

**Table 2-1**
**Statistics of Net Harmonic Currents on the Plateau**

| Harm | Exp. Mag. A/Chgr | Exp. Phase Angle - deg. | Var. Mag. $A^2$/Chgr | $DF_h$ |
|------|------------------|-------------------------|----------------------|--------|
| 1    | 5.30             | -26                     | 95                   | 0.15   |
| 3    | 1.65             | -52                     | 7.02                 | 0.24   |
| 5    | 1.30             | -94                     | 4.15                 | 0.44   |
| 7    | 0.90             | -67                     | 2.11                 | 0.71   |
| 9    | 0.75             | -66                     | 1.42                 | 0.59   |
| 11   | 0.49             | -67                     | 0.58                 | 0.61   |
| 13   | 0.27             | -46                     | 0.18                 | 0.52   |
| 15   | 0.18             | -56                     | 0.08                 | 0.48   |

Using the results presented in Table 2-1, we can conclude that a concentration of the type of chargers studied in this paper, operating from a transformer with 4% impedance, can be no more than 17% of the operating load in order to comply with IEEE 519 harmonic current limits [19]. The binding constraint is total demand distortion (TDD).
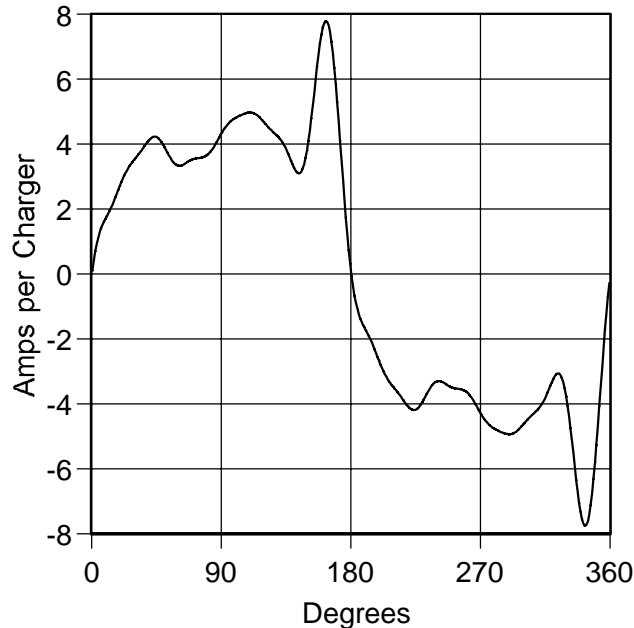


**Figure 2-13**
**Expected Waveform of Net Current**

## Summary

This chapter presents a general method for predicting the harmonic currents generated by a concentration of EV battery chargers. The method accounts for uncertainties in starting time of individual chargers and initial battery state-of-charge by modeling both as random variables. FORTRAN implementations of the analytical and Monte Carlo methods are located in Appendices B and C.

The solution method relies on the Central Limit Theorem and this, in turn, requires that there be a sufficiently large number of chargers in the concentration. The densities of decomposed harmonic currents and power are approximately normal for as few as fifteen chargers. However, Monte Carlo simulations show that the computed means and variances are accurate for as few as seven chargers.

The net harmonic injection currents and diversity factors for our example are shown in Table 2-1. These diversity factors demonstrate that evaluating the charger concentration as the simple algebraic sum of individual charger full-load harmonic currents will lead to significant overestimation of the effect of EV charging. The particular densities and charger model chosen for this example indicate a reduction of harmonic currents of approximately 50% from the full-power algebraic solution.

The values in Table 2-1 are based on a uniform start-time pdf of eight hours. Varying the uniform start-time pdf between four and ten hours does not result in any qualitative changes in the spectra; however, the net expected power changes inversely with the duration of the start-time pdf.

While we show results for only one typical charger, the method presented in this chapter is capable of accepting any input density and charger model.

# 3
# SENSITIVITY OF NET HARMONIC CURRENTS TO PARAMETER VARIATION

## Introduction

In the previous chapter, we presented an analytical solution technique for predicting the harmonic currents produced by a group of EV battery chargers. This technique, which accounts for the diversity caused by variations in individual charger start-time and battery state-of-charge by modeling both as random variables, was verified using Monte Carlo trials. An example analysis was performed using a particular charger model, charger start-time probability density function (pdf), and initial battery state-of-charge (SOC) pdf. The first- and second-order statistics of harmonic currents and power were derived.

Here, we study the effect of variations in start-time pdf, SOC pdf, and charger model on net power and harmonic currents. Maintaining the uniform start-time pdf and the charger model presented in Chapter 2, we first vary the mean and variance of the pdf of daily miles traveled by a typical vehicle. This changes the pdf of the initial battery SOC. We then fix the original SOC pdf and charger model, and vary the uniform start-time pdf by changing the length of time during which the chargers may begin operation. Next, we vary the charger model while maintaining the pdfs presented in Chapter 2 by adding additional energy to the charger full-load power profile to simulate a less fuel-efficient vehicle. Finally, we use the results of these analyses to present the worst-case expected value of the harmonic currents generated by the concentration of EV chargers.

## Parameters Affecting Net Harmonic Currents

After first selecting a model to describe an individual EV battery charger, the solution process presented in Chapter 2 begins by discretizing both the time domain and power range to yield discrete power levels $P_i$ (2-2) from the power profile, and a discrete pdf of start-time $g_k$ (2-5). The discrete pdf of initial battery SOC, $f_i$, is found by discretizing $f(E)$, the continuous pdf of initial battery SOC, at the energy levels defined by the power levels $P_i$ and the power profile (2-3, 2-4). Analysis shows that at each time $j$ the statistics describing power, and the statistics describing the h-order harmonic current magnitude, are given in (2-6).

In order to gain greater insight on the net harmonic current injection of the EV battery charger concentration it is, therefore, necessary to consider the effects of variations $f_i$ of and $g_k$ on net power and net harmonic currents. The particular choice of charger model also affects the solution and should be examined.

## Varying Initial State-of-Charge

The pdf of battery initial SOC is a function of the number of miles the vehicle has traveled between consecutive charges. It is assumed in Chapter 2 and [11] that the batteries are charged only once daily and that they are charged to completion. A pdf, $d(m)$, of daily distance driven by a typical U.S. automobile is introduced in [11]. This takes the form

$$d(m) = \frac{\ln(m)}{\sqrt{2\pi}\beta\eta} \exp(-\frac{1}{2\beta^2}(\ln(m)-\alpha)^2),$$

<div align="right">**Eq. 3-1**</div>

where $\eta$ is the normalization constant and equals

$$\eta = (\alpha + \beta^2)\exp\left(\frac{1}{2}\beta^2 + \alpha\right).$$

<div align="right">**Eq. 3-2**</div>

The n-th order moments are given by

$$E(X^n) = \frac{(\alpha + (n+1)\beta^2)}{\eta} \exp\left(\frac{(n+1)^2}{2}\beta^2 + (n+1)\alpha\right).$$

<div align="right">**Eq. 3-3**</div>

Determining the specific values of $\alpha$ and $\beta$ to yield particular values of the mean and variance of $d(m)$ is very difficult to do analytically. Rather, $d(m)$ is solved to yield specific means and variances using a Newton-Raphson technique. Given a desired mean and variance, and arbitrary starting values for $\alpha$ and $\beta$, the technique numerically determines the partial derivative of the mean and variance of a discretized $d(m)$ with respect to $\alpha$ and $\beta$. These derivatives are used to determine new values for $\alpha$ and $\beta$ that yield a mean and a variance closer to the desired. The method continues to iterate in this fashion until the computed mean and variance of $d(m)$ are sufficiently close to the desired values.

Assuming the battery has a set range $R$ miles, and recalling that $E$ is expressed in percent of complete charge, $m$ is related to $E$ by

$$m = R - \frac{R\,E}{100}.$$

<div align="right">**Eq. 3-4**</div>

Initial SOC $f_i$ is found by first redefining $d(m)$ so that all trips greater than the range $R$ have probability zero and proportionately rescaling the remaining discrete non-zero probabilities so that their sum remains one. The daily distance $d(m)$ can then be discretized at the levels $m_i$ corresponding to the required energy level $E_i$. This yields the discrete pdf of $f_i$.

The mean and standard deviation of $d(m)$ were presented in [11] as 34.2 miles and 21.1 miles, respectively. This pdf is shown in Figure 3-1. The increase in average trip length of 11% between 1983 and 1990, reported in [15], was accounted for in Chapter 2 by increasing both the

mean and variance of $d(m)$ by a scaling factor of 1.11. Under the assumption that the EV battery range $R$ is 75 miles, and applying a uniform start distribution over an 8 hour period to the EV charger model presented in Chapter 2, we evaluate the effect of varying the scaling factor to represent growth in daily travel. This is accomplished by applying the scaling factor to both the original mean of 34.2 miles and the original variance of 445.2 miles$^2$ to determine new values. A new $d(m)$ is then found with these statistics utilizing the Newton-Raphson technique described earlier. The solution procedure presented in Chapter 2 is then used to compute the net power and harmonic currents.
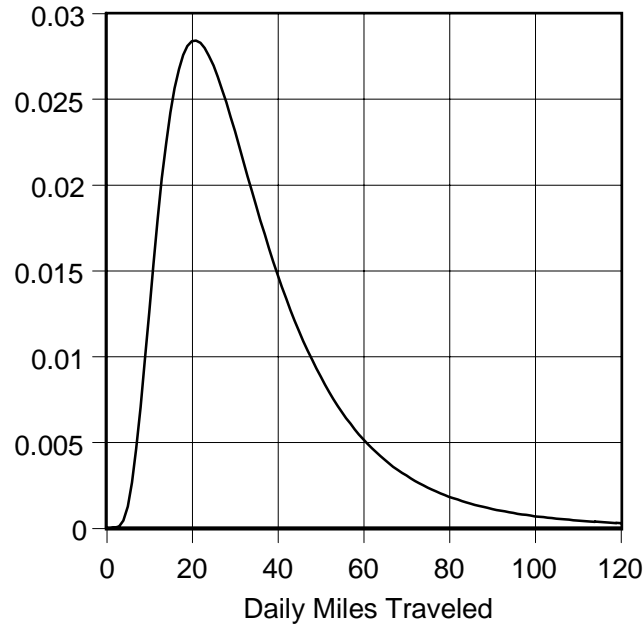


**Figure 3-1**
**PDF of Miles Traveled by a Single EV**

Power and harmonic current magnitudes on the plateau are determined, and their maximum means and variances are shown in Figures 3-2, 3-3, and 3-4. For the sake of clarity, expected values of current harmonic magnitudes of order higher than 9 are not presented, though they follow the same pattern as do the lower-order harmonics. Results are presented as per charger values since these were shown in Chapter 2 to remain constant for groups of chargers greater in number than six. The expected value of $THD_I$ is computed using the Monte Carlo algorithm described in Chapter 2.
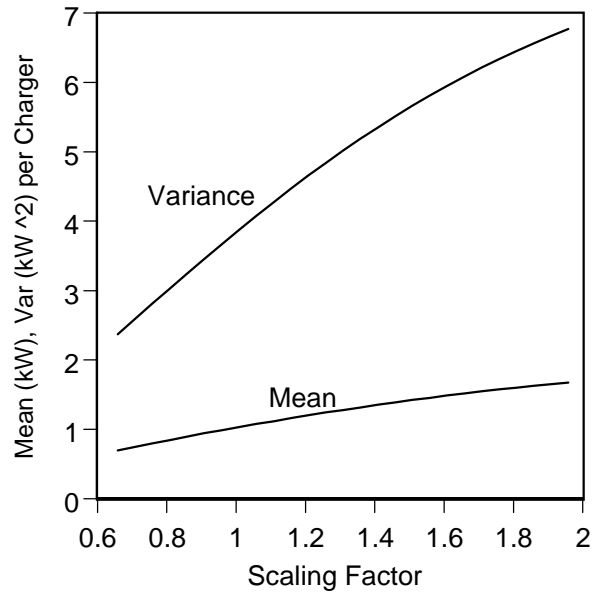
**Figure 3-2**
**Mean and Variance of Power vs. Scaling Factor**

The expected values of power and of net harmonic current magnitudes grow as we increase scaling factor due to the rise in the expected value of energy that each charger must deliver. Recalling that the $THD_I$ for this individual charger, is inversely related to operating power, and realizing that each charger is now more likely to be operating at a higher power, it is reasonable to expect that the net expected $THD_I$ should decrease with increasing scaling factor.
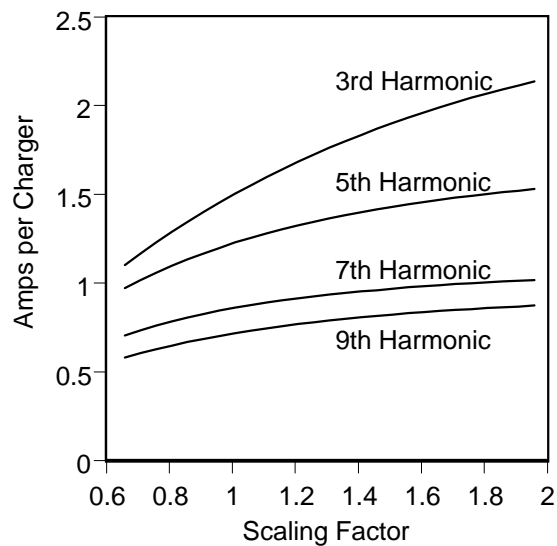


**Figure 3-3**
**Mean of Harmonic Current Magnitudes for Order 3, 5, 7, 9 vs. Scaling Factor**
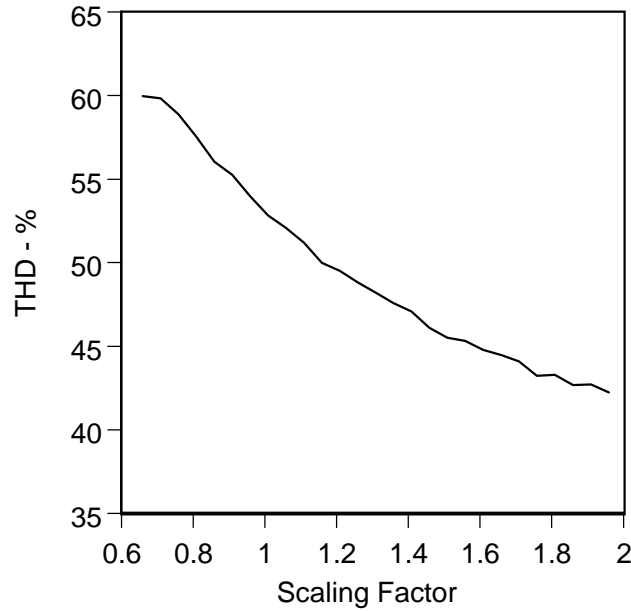
**Figure 3-4**
**Expected Value of *THD$_I$* vs. Scaling Factor**

## Varying Start-Time Distribution

Net power and harmonic currents depend also on the discrete pdf $g_k$. Earlier we used a uniform density of start-time over an eight-hour period. Eight hours was selected as the duration of start-time in order to restrict EV charging to a twelve hour off-peak period. If, however, the off-peak window is smaller, it would be desirable to restrict EV charging to a smaller window in time. It is also important to understand the sensitivity of the EV charging to the pdf chosen for charger start-time.

With this in mind, and maintaining a uniform start-time density, we vary the duration of $g_k$ from four hours to ten hours. Selecting the pdf of initial battery SOC and the charger model presented earlier, we perform the analysis. The maximum expected values of net power and net harmonic current magnitudes as well as expected *THD$_I$* are shown in Figures 3-5, 3-6, and 3-7.
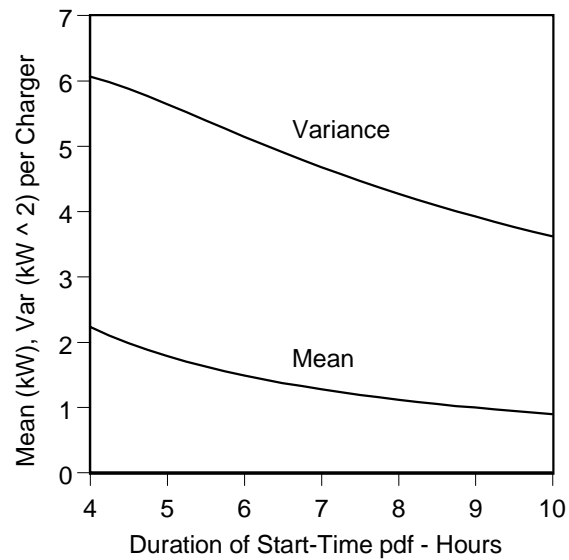
**Figure 3-5**
**Mean and Variance of Power vs. Duration of Start-Time pdf**
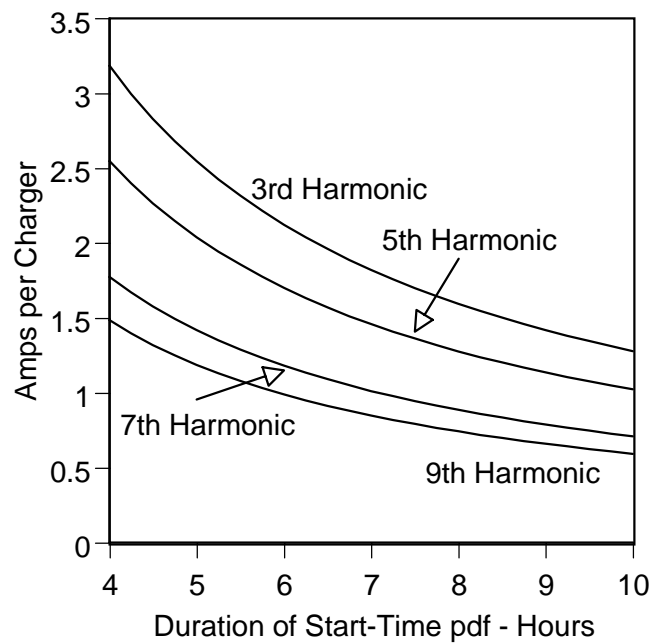


**Figure 3-6**
**Mean of Net Harmonic Current Magnitudes for Orders 3, 5, 7, 9 vs. Duration of Start-Time pdf**
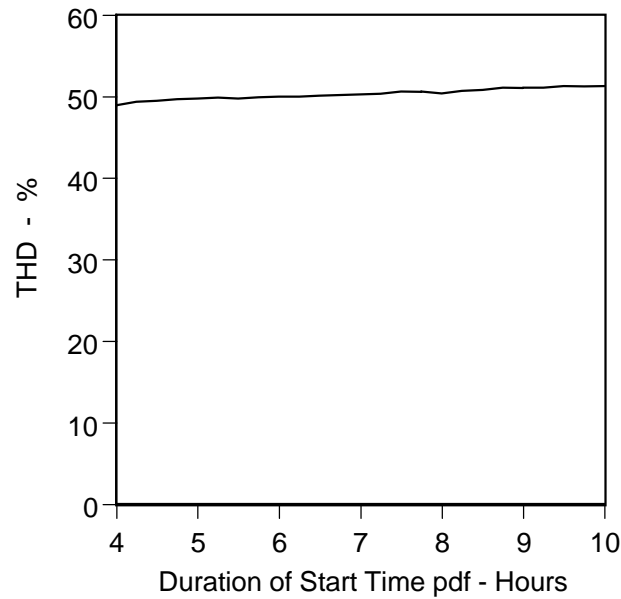
**Figure 3-7**
**Expected Value of  *THD$_I$* vs. Duration of Start-Time pdf**

As we increase the time the chargers are allowed to begin operation, fewer chargers are likely to be operating at any given instant. Therefore, the maximum values of mean harmonic current magnitude and power decrease with increasing duration of start probability. Expected *THD$_I$* is largely unaffected.

## Varying Vehicle Fuel-Efficiency

The EV battery charger profile presented in Figure 2-2 and used thus far in the analysis consumes approximately 20 kWh when operating on a fully discharged battery. Given the range  *R*  of the EV battery to be 75 miles, the vehicle thus travels roughly 3.75 mile per kWh. However, some variation in vehicle fuel-efficiencies can be expected. With this in mind, we vary the energy contained within the power profile in order to account for vehicles with lower fuel-efficiencies. This is accomplished by reshaping the power profile by adding additional operation at full-power at the beginning of the charging cycle.

It is reasonable to add additional energy to the profile in this fashion because of the physical processes occurring in the battery during charging. When the battery SOC is low, the charger operates at maximum rated current. This continues until the battery voltage nears its gassing limit, at which time current drops as the charger maintains a constant voltage, and as battery receptivity drops [12]. Resizing the battery system to supply more energy likely means adding more batteries. It is thus reasonable to expect that the charger will operate at maximum rated current longer, before it charges the battery system to sufficient voltage to force a current decrease.

We present the maximum expected values of net power, harmonic current magnitudes, and $THD_I$ using the original eight hour pdf of charger start-time and the original pdf of initial battery SOC. The results of this analysis are presented in Figures 3-8, 3-9, and 3-10, and are similar to those found by varying the initial battery SOC.
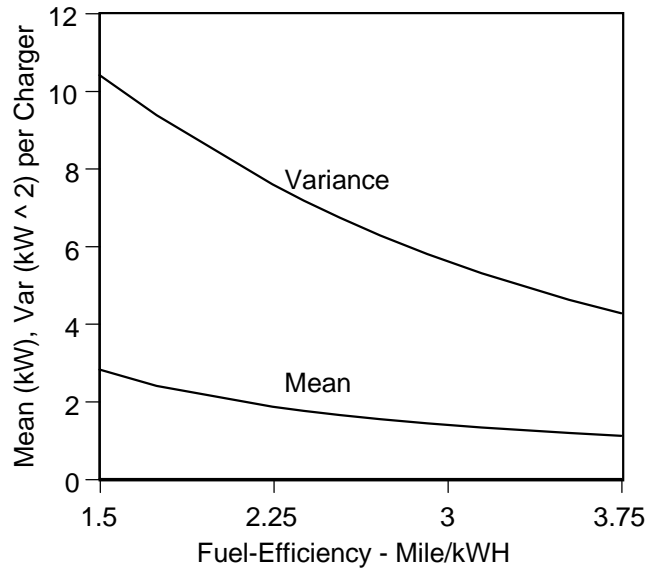


**Figure 3-8**
**Mean and Variance of Power vs Fuel-Efficiency**
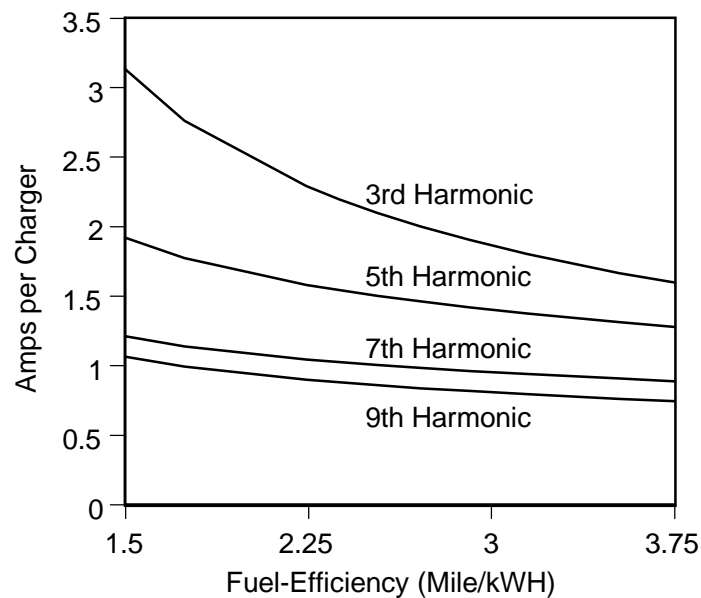


**Figure 3-9**
**Mean of Net Harmonic Current Magnitudes for Orders 3, 5, 7, 9 vs Fuel-Efficiency**
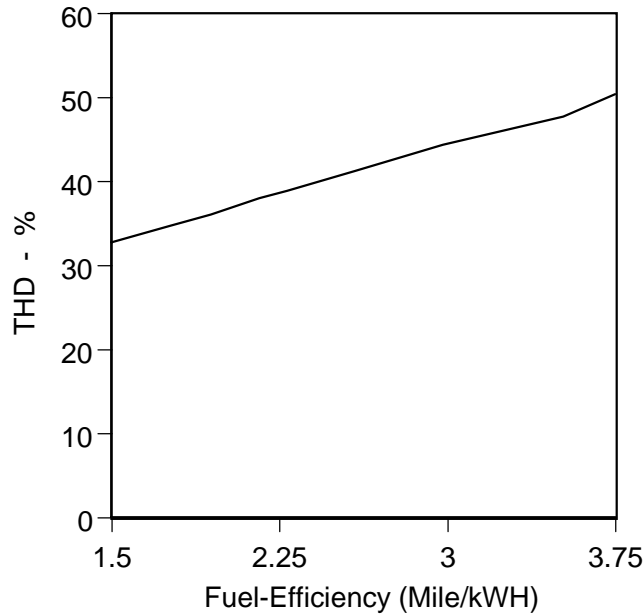
**Figure 3-10**
**Expected Value of *THD*$_I$ vs. Fuel-Efficiency**

As vehicle fuel-efficiency drops, any given charger operates at high power for a longer period. This explains why the expected values of power and harmonic currents increase with decreasing fuel-efficiency. *THD*$_I$ decreases with decreasing fuel-efficiency for the same reason.

## Bounding Net Power and Harmonic Currents

Finally, we seek to establish reasonable bounds for the net power and harmonic currents generated by the cluster of EV chargers. We accomplish this by performing two distinct analyses. In the first test, which we label 'Worst-Case,' each of the batteries is assumed to have been driven to complete discharge while operating on a vehicle with range 75 miles and fuel-efficiency 2 mile/kWh. We vary the duration of the uniform start-time pdf. Then, using the original charger model and pdf of battery SOC, we vary the duration of start-time pdf. This is our best estimate of the actual situation, and we label this test 'Best-Guess'. We present the results of the two tests in Figures 3-11, 3-12 and 3-13 by detailing the maximum expected values of power, harmonic currents, and *THD*$_I$.

We predict that a collection of chargers will operate somewhere in the range bounded by the two curves. Assuming a reasonable worst-case operation of the concentration, we present the expected values of harmonic currents in Table 3-1 using a Fourier sine series reference. The corresponding current waveform is shown in Figure 3-14. Diversity factor for power $DF_P$ and harmonic currents of order $h$, $DF_h$ are defined as in Chapter 2. Worst case operation corresponds to a collection of chargers operating on vehicles with range 75 miles, fuel-efficiency 2 Mile/kWh, with charger start-time pdf of duration 6 hours. The expected value of power is 2.9 kW per charger with variance 9.51 (kW)$^2$. $DF_P$ is 0.38, and mean *THD*$_I$ is 36%.
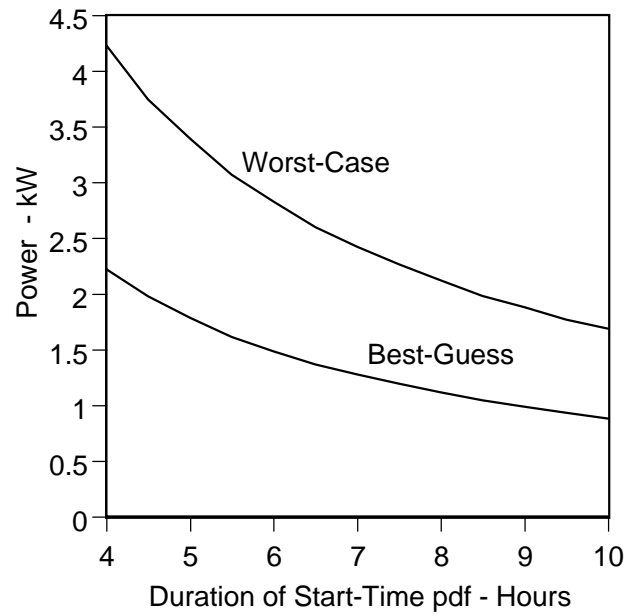
**Figure 3-11**
**Expected Value of Power**
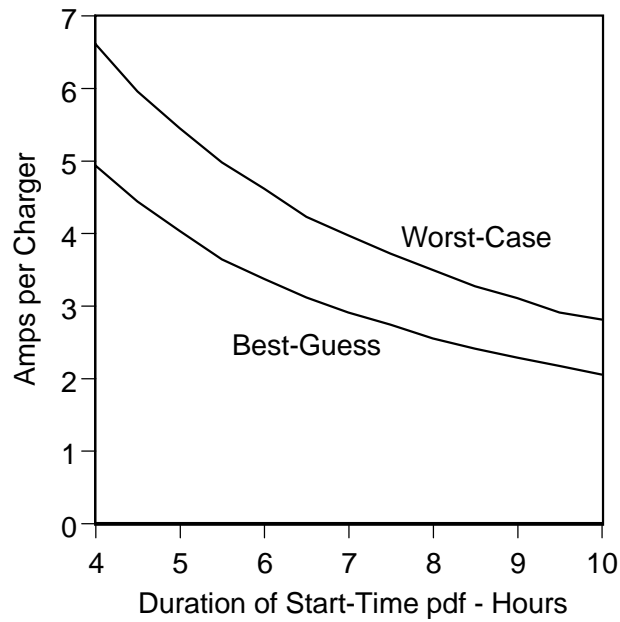


**Figure 3-12**
**Expected Value of Harmonic Amps**
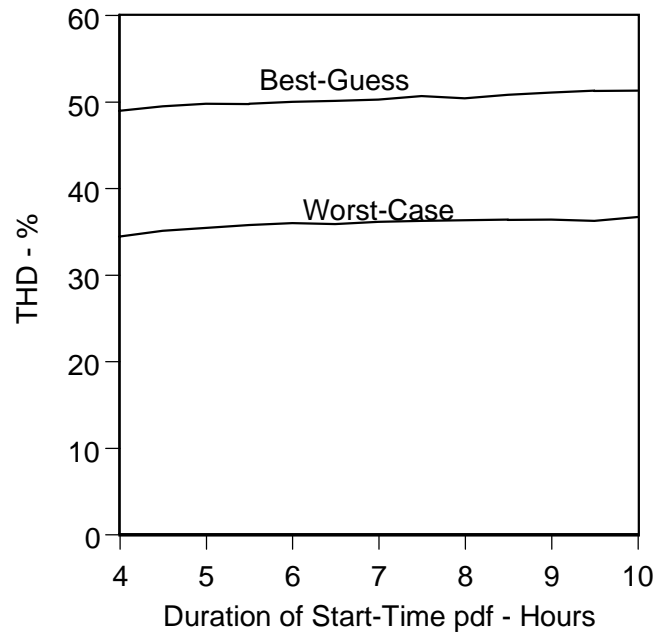
**Figure 3-13**
**Expected Value of** *THD$_I$*

**Table 3-1**
**Statistics of Worst-Case Net Harmonic Currents**

| Harm | Exp. Mag. A/Chgr | Exp. Phase Angle - deg. | Var. Mag. A$^2$/Chgr | *DF$_h$* |
|------|------|------|------|------|
| 1 | 13.18 | -26 | 190.1 | 0.37 |
| 3 | 3.42 | -58 | 9.87 | 0.49 |
| 5 | 2.25 | -101 | 4.23 | 0.76 |
| 7 | 1.46 | -66 | 2.20 | 1.15 |
| 9 | 1.27 | -66 | 1.46 | 1.00 |
| 11 | 0.81 | -67 | 0.58 | 1.02 |
| 13 | 0.46 | -42 | 0.18 | 0.88 |
| 15 | 0.32 | -56 | 0.08 | 0.86 |
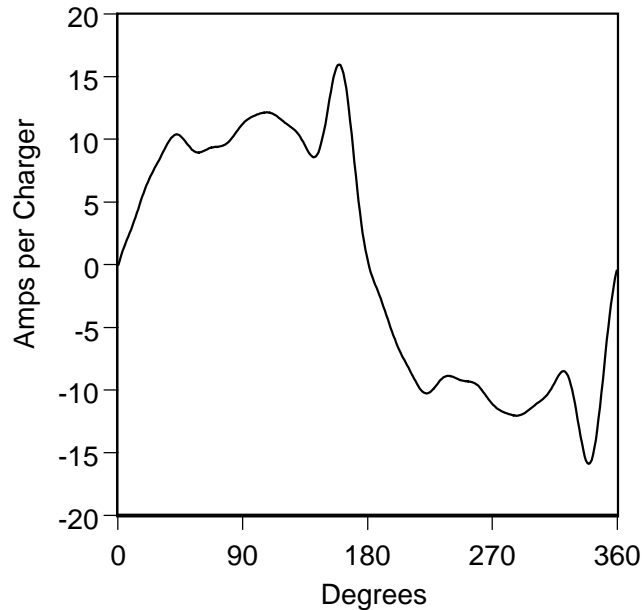
**Figure 3-14**
**Expected Waveform of Net Current**

## Summary

This chapter presents a sensitivity analysis of a general method for evaluating the harmonic currents generated by a concentration of EV battery chargers. Both initial battery SOC and individual charger start time are modeled as random variables. It is shown that the pdfs chosen to describe these random variables and the charger power profile used to model each individual charger are critical in determining the net harmonic injection of the collection of EV battery chargers. To determine the nature of their effect, we first vary, independently from the other parameters, the pdf of initial battery SOC. Results show that the expected values of power and of harmonic current magnitudes increase, and the expected value of $THD_I$ decreases, as the pdf of battery SOC approaches that of a fully discharged battery.

Similarly, the duration of charger start-time is varied while maintaining the original pdf of initial battery SOC and charger model. The expected values of power and of net harmonic current magnitudes decrease as the duration of charger start-time increases; yet the expected value of $THD_I$ remains constant.

The charger model itself is varied in order to account for vehicles with varying fuel-efficiencies. Vehicle fuel-efficiency is shown to be inversely related to the expected values of harmonic current and directly related to the expected value of $THD_I$. The direct relationship between $THD_I$ and fuel-efficiency is a result of the fact that a more fuel-efficient vehicle will be more likely to begin charging at the end of the charging cycle where $THD_I$ is highest.

Finally, an attempt to bound the net harmonic currents, power, and $THD_I$ is made by comparing the results of a worst-case analysis to those of the original study. Using reasonable worst-case assumptions, though expected values of net harmonic currents and power rise over those presented in Chapter 2, there is still a significant reduction in these quantities for the concentration as compared to the sum of their rated values. For example, fundamental current magnitude is expected to be only 37% of the sum of the rated current values. For the third harmonic current magnitude the figure is only 49%.

# 4
# DERATING A SUBSTATION TRANSFORMER

## Introduction

Harmonic currents lead to increased losses in distribution transformers, feeders, and some conventional loads such as ac motors. Because EV charging is a potentially large power system load, it is important to evaluate the impact that harmonic currents generated from EV battery charging may have on power distribution equipment. Previous chapters have developed a method for evaluating the net harmonic current injection of a concentration of electric vehicle battery chargers. This chapter studies the effect of EV battery charging on a substation transformer that supplies commercial, residential, industrial, and EV load on a peak summer day.

We evaluate the effect of net load on the substation transformer using ANSI/IEEE standards for transformer loading [20], and we also account for the effect of nonlinear currents on the transformer [21]. For specific non-EV load, we introduce EV charging and evaluate the amount of transformer derating needed to maintain a constant daily transformer loss-of-life, with and without EV charging. This analysis shows that the time of day and the length of time during which the EVs begin charging are critical in determining the amount of transformer derating required. Results show that with proper control, EV charging may have very little effect on power system components at the substation level.

## Substation Transformer Loading

Figure 4-1 depicts the situation we study, which involves a single substation transformer that supplies all types of distribution system loads.
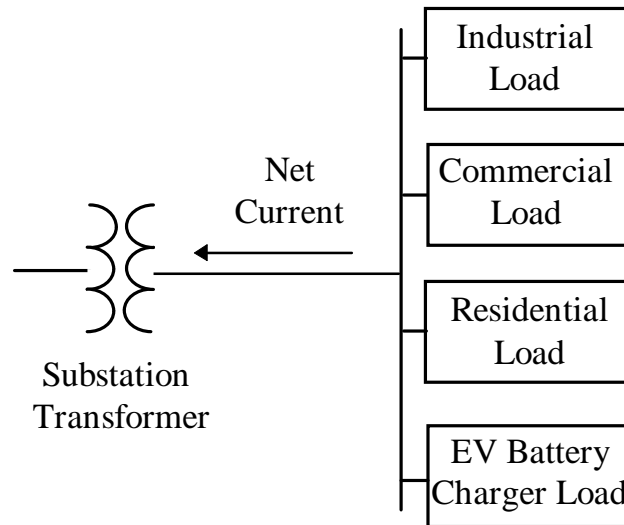
**Figure 4-1**
**Loaded Substation Transformer**

Non-EV load is expressed in percent of transformer rating. As it is expected that most EV battery charging will occur in residences during evening hours [13], EV load is expressed as a penetration of residences. This penetration is the ratio of the total number of EV chargers to the total number of residences. We show how the transformer should be derated in order to maintain a constant transformer expected life-time as EV penetration increases.

## Non-EV Load and Temperature Profiles

We begin our load analysis by examining Figure 4-2 where we present a typical load shape and temperature profile for a peak summer day. This profile represents the non-EV load.
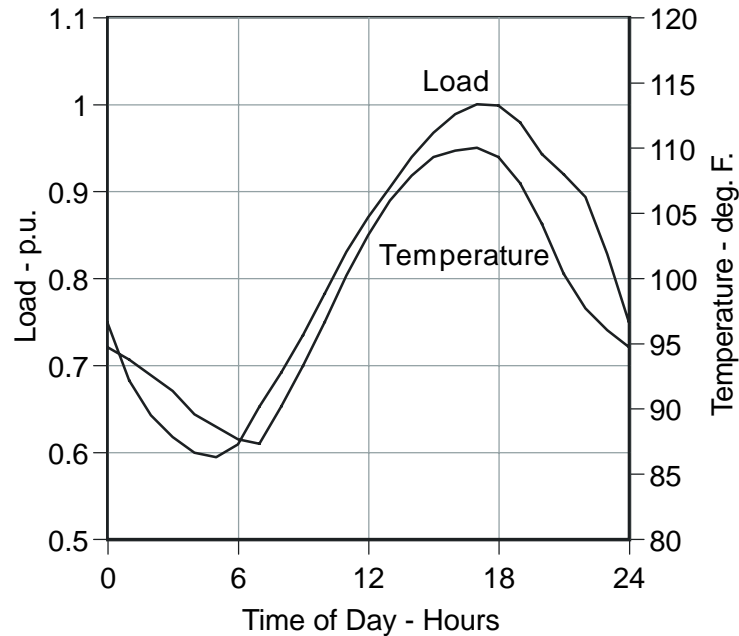
**Figure 4-2**
**Profiles of Load and Temperature for Hot Summer Day**


## *Electric Vehicle Battery Charger Load*

Because we have no actual data for concentrations of EV chargers, modeling the EV load is more difficult than is modeling the base load. However, we have already shown in Chapter 2 that the net currents generated by a concentration of EV battery chargers can be predicted if the randomness of individual charger start-time and initial battery-state-of-charge (SOC) are properly considered.

The method in of Chapter 2 determines the first- and second-order statistics of the net power and harmonic current magnitudes associated with a concentration of EV battery chargers. It uses a specific charger model and particular user-defined probability density functions (pdf) for charger start-time and initial battery SOC. Applying the method with the charger model and initial battery SOC pdf presented in Chapter 2, along with a uniform pdf of start-time lasting four hours, we determine the expected values of EV power (Figure 4-3) and harmonic current magnitudes (Figure 4-4) for the concentration. Extending the support interval of the start-time pdf to six hours yields the expected values of EV power and harmonic current magnitudes shown in Figures 4-3 and 4-5. Each charger operates at a displacement power factor (DPF) of 0.9 throughout the entire charging cycle.

This per charger model is useful because each substation transformer can be expected to serve thousands of residences. Assuming that homes with EV chargers have only one charger, it is reasonable to apply the Law of Large Numbers and model the total EV power as the product of the number of residences with EVs and the expected value of EV power per charger. Similarly, total EV harmonic current is the product of the number of residences with EVs and the expected value of harmonic current magnitude per charger.
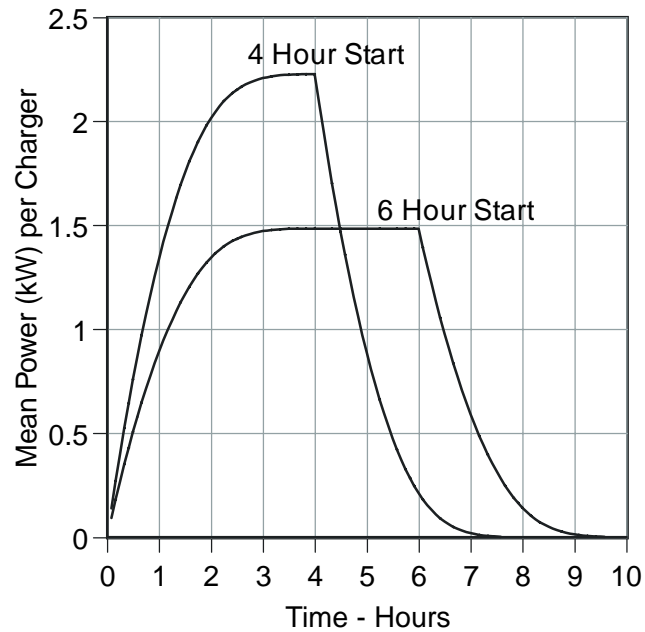
**Figure 4-3**
**Expected Power per EV Charger**
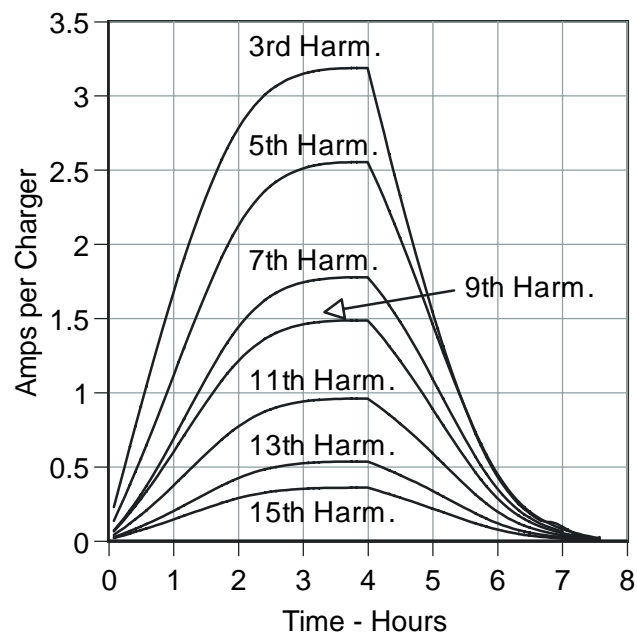


**Figure 4-4**
**Expected Harmonic Current Magnitude – Uniform Four Hour Start PDF**
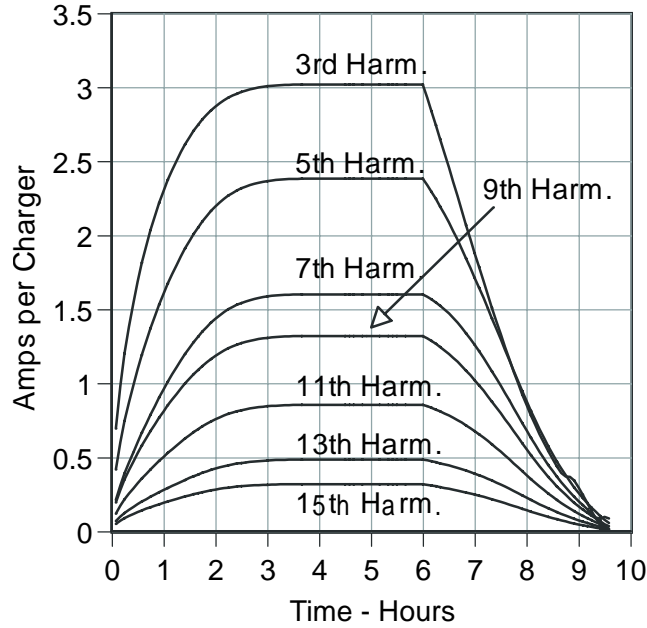
**Figure 4-5**
**Expected Harmonic Current Magnitude – Uniform Six Hour Start PDF**

### Expressing the Loads on the Transformer Base

In order to determine the total loading of the transformer we must express the non-EV and EV load on the transformer base. To begin, we specify the peak loading of the transformer without EV load, $\Phi$, expressed in p.u. on the transformer rated MVA. Non-EV load, $S(t)$, as a function of time $t$ is then the product of the typical summer load curve of Figure 4-2 and $\Phi$. EV complex power in p.u. of transformer rated MVA, $S_{EV}(\tau)$, is given by

$$S_{EV}(\tau) = \frac{P_{EV}(\tau)}{PF_{EV}\,S_R}\Phi\frac{\pi}{100},$$   **Eq. 4-1**

and EV harmonic current magnitudes of harmonic order $h$, in p.u. of transformer rated current, are given by

$$I_h(\tau) = \tilde{I}_h(\tau)\frac{V_{EV}}{S_R}\Phi\frac{\pi}{100},$$   **Eq. 4-2**

where

$\tau$ :    Time variable relative to first instant of non-zero probability of charger start-time pdf.

$P_{EV}$ :    Expected EV power in kW per charger.

$PF_{EV}$ : EV displacement power factor.

$S_R$ :    Peak non-EV substation load in kVA per residence.

$\tilde{I}_h(t)$ : Expected current magnitude of harmonic order $h$ in Amps per charger.

$\pi$ :    Percent EV penetration.

$V_{EV}$ :    Operating voltage of EV charger in kV.

## Transformer Heating

Aging and the long-term mechanical degeneration of winding insulation have historically been the basis for transformer loading and are time functions of temperature, moisture content, and oxygen content [20]. Since modern oil preservation systems minimize the contributions of moisture and oxygen, the dominant factor in insulation degeneration is temperature. The temperature distribution is not constant within most transformers. Therefore, it is common to focus on the location of the hot-spot temperature where the greatest degeneration will occur.

### *Hot-Spot Temperature Equations*

A method for determining the transformer hot-spot temperature as a function of ambient temperature, transformer loading, and certain specific transformer parameters is presented in [20]. To find the hot-spot temperature profile, we first discretize the load profile at constant time intervals $\Delta t$ for the 24 hour load profile of interest. At each discrete time, the method assumes that the hot-spot temperature $\theta_H$ consists of the following three components (All temperatures are in degrees Celsius.):

$\theta_A$,    ambient temperature,

$\Delta\theta_{TO}$, top-oil rise over ambient temperature,

$\Delta\theta_H$, hot-spot temperature over top-oil,

where

$$\theta_H = \theta_A + \Delta\theta_{TO} + \Delta\theta_H .$$    **Eq. 4-3**

The following subscripts are defined in [20].

$A$:    Ambient.

$R$:    Rated.

*i*:  Initial. Value of the variable at the beginning of the discrete time interval.

*U*:  Ultimate. Value of the variable at the end of the discrete time interval.

*H*:  Winding hot-spot.

*TO*:  Top-oil.

*W*:  Winding.

Other parameters defined in [20] are

*R*:  Ratio of load loss (at rated load) to no-load loss.

*K*:  Modified ratio of supplied load to rated load.

$\tau_{TO,R}$:  Oil time constant for rated load, hours.

$\tau_W$:  Winding time constant at hot-spot location, hours.

*m*:  Empirically derived exponent to account for changes in resistance and oil viscosity with changes in load.

*n*:  Empirically derived exponent to account for effects of change in resistance with change in load.

The top-oil temperature rise over ambient at the end of any discrete time interval of length $\Delta t$ hours is given by

$$\Delta\theta_{TO} = (\Delta\theta_{TO,U} - \Delta\theta_{TO,i})\left(1 - \exp(-\frac{\Delta t}{\tau_{TO}})\right) + \Delta\theta_{TO,i} \qquad \textbf{Eq. 4-4}$$

where the initial top-oil temperature rise over ambient is the corresponding value computed for the preceding discrete time interval. The ultimate top-oil temperature rise over ambient is given by

$$\Delta\theta_{TO,U} = \Delta\theta_{TO,R}\left[\frac{(K_U^2 R + 1)}{(R + 1)}\right]^n, \qquad \textbf{Eq. 4-5}$$

and the top-oil time constant varies with each time interval according to

$$\tau_{TO} = \tau_{TO,R} \frac{\left(\dfrac{\Delta\theta_{TO,U}}{\Delta\theta_{TO,R}}\right) - \left(\dfrac{\Delta\theta_{TO,i}}{\Delta\theta_{TO,R}}\right)}{\left(\dfrac{\Delta\theta_{TO,U}}{\Delta\theta_{TO,R}}\right)^{\frac{1}{n}} - \left(\dfrac{\Delta\theta_{TO,i}}{\Delta\theta_{TO,R}}\right)^{\frac{1}{n}}},$$

<div align="right">**Eq. 4-6**</div>

Similarly, the transformer winding hot-spot temperature rise over top-oil temperature is given by

$$\Delta\theta_H = (\Delta\theta_{H,U} - \Delta\theta_{H,i})\left(1 - \exp(-\frac{\Delta t}{\tau_W})\right) + \Delta\theta_{H,i},$$

<div align="right">**Eq. 4-7**</div>

and the ultimate top-oil temperature rise over top-oil is given by

$$\Delta\theta_{H,U} = \Delta\theta_{H,R} K_U^{2m}.$$

<div align="right">**Eq. 4-8**</div>

Ambient temperature is a user-defined function of time. We choose the hot summer day temperature profile shown in Figure 4-2.

To compute the hot-spot temperature profile, initial values for hot-spot temperature rise over top-oil, and top-oil temperature rise over ambient, are set at zero. The solution proceeds by successively computing the value of hot-spot temperature during each discrete time interval for a series of 24 hour periods with the same loading and ambient temperature profile as the day of interest. A solution is reached when the hot-spot temperature profiles between subsequent 24 hour periods converge.

Computation of the modified load ratio $K$ must account for the nonlinear currents introduced by EV charging. Provision for the supply of harmonic currents beyond simply accounting for the increase in total amperage supplied by the transformer should be made. This is because the winding eddy-current loss is proportional to the square of frequency. Thus, harmonic currents should be weighted by the square of the harmonic order to account for the increase in winding loss and the corresponding winding temperature rise [21].

We define $K_{NH}$, the value of $K$ that would be computed if no harmonic currents were present, and $K_H$, so that $K = K_{NH} K_H$. The value of $K_{NH}$ is the magnitude of the phasor sum of $S_{EV}$ and $S$, in per-unit of transformer rated MVA. We compute $K_{NH}$ using the technique described in [21] so that

$$K_{NH} = \left[\frac{\sum_h I_h^2 + P_{EC-R}\sum_h h^2 I_h^2}{(1 + P_{EC-R})I_1^2}\right]^{\frac{1}{2}}.$$

<div align="right">**Eq. 4-9**</div>

The winding eddy-current loss, $P_{EC-R}$, and harmonic current magnitudes of harmonic order $h$, $I_h$, are given in per-unit on the transformer base. $I_1$ is the fundamental current supplied by the transformer to all load.

## Parameters for the Test Transformer

For subsequent study, we choose an actual substation transformer. This transformer is rated 16.8/22.4/28 MVA (OA/FA/FA), and its thermal characteristics are described in Table 4-1. We select a representative value of $P_{EC-R}$ from [4].

**Table 4-1**
**Transformer Thermal Characteristics**

| | |
|---|---|
| $P_{EC-R}$ | 0.10 |
| $\Delta\theta_{TO-R}$ | 44.6°C |
| $\Delta\theta_{H,R}$ | 18.8°C |
| $R$ | 4.87 |
| $\tau_R$ | 2.58 hr. |
| $n$ | 0.9 |
| $m$ | 0.8 |
| $\tau_W$ | 0.08 hr. |

## Transformer Life Expectancy

Normal life expectancy for a transformer as described in [20] is the expected lifetime when operated with a continuous hot-spot temperature of 110°C. Tests on both distribution and power transformers indicate that this corresponds to a normal life expectancy of approximately 20.5 years [20]. Insulation degeneration is the typical cause for transformer failure. It has been determined experimentally that insulation degeneration is a function of time and temperature and this relation is presented in [20] where the aging acceleration factor, $F_{AA}$, is defined as

$$F_{AA} = \exp\left[\frac{15000}{383} - \frac{15000}{\theta_H + 273}\right].$$

**Eq. 4-10**

For a series of time intervals with varying temperatures indexed by $j$, each lasting $\Delta t_j$ hours, the equivalent aging factor for the transformer is defined in [20] as the average of the aging acceleration factors at each interval, given by,

$$F_{EQA} = \frac{\sum_j F_{AA,j} \Delta t_j}{\sum_j \Delta t_j}.$$

**Eq. 4-11**

These equations are such that continuous 24 hour operation of the transformer with hot-spot temperature of 110°C yields an equivalent aging factor of one.

## Method and Evaluation of Transformer Derating

We seek to determine the relation between EV penetration and substation transformer derating. The method for this analysis and the results are summarized in Figure 4-6 and Figures 4-7 to 4-12 respectively. We first select one of the two charger models described in Figures 4-3, 4-4 and 4-5, an initial start-time for the chargers, and the ambient temperature profile shown in Figure 4-2 which allows for a "worst-case" peak ambient temperature of 110°F. We also choose a peak value for the non-EV load and model this load using the load-profile of Figure 4-2. This peak is expressed as percent of the transformer rating. We assume a peak non-EV substation load of 4 kVA per residence and that the DPFs for both non-EV and EV load are 0.9.

Next, we perform a hot-spot temperature analysis as described previously assuming no EV charging. Using these hot-spot temperature values we compute the equivalent aging factor for the 24 hour period. This factor serves as the base value for $F_{EQA}$.

Subsequently, we select a value for EV penetration and compute the new total load. Performing an evaluation with this new load yields a hot-spot temperature curve and equivalent aging factor. Peak non-EV load is then decreased, the new load is computed, and the preceding analysis is repeated until the value of $F_{EQA}$ is sufficiently close to that of the non-EV load alone, thus maintaining constant transformer loss-of-life. By varying the penetration from zero to 100%, a curve is generated describing the derating of the transformer needed to accommodate for EV charging. The FORTRAN implementation of this method is included in Appendix D.

Figures 4-7 to 4-12 shows the relation between non-EV loading and EV penetration for collections of chargers with uniform start-time pdfs of four or six hours, starting at 6, 8 and 10 p.m. Each penetration corresponds to a value of peak EV load relative to peak non-EV load. For the four-hour charger start problem, this value at 100% EV penetration, is 0.62. The corresponding value for the six-hour charger start problem is 0.41. These values scale linearly from zero to the maximum values above (i.e. 0.62, 0.41) and can serve as an alternative ordinate axis to Figures 4-7 to 4-12.

To illustrate the usefulness of these figures, suppose that the particular charging scenario of interest and a particular peak value of transformer loading traditionally designed into the system without EV charging have been chosen. A particular EV penetration and the appropriate curve yields the new value of peak load without EV that will maintain constant transformer life expectancy.

For example, Figure 4-7 shows that a transformer previously designed to supply 100% of its rated load at peak without EVs should now be designed to supply, in the case of a 50% penetration of chargers all of which start between six and ten p.m., only 90% of its rated load at peak without EV charging. Here, 50% penetration corresponds to an EV load that is 31% of the non-EV load.

```
                        ┌─────────────────────────┐
                        │   Select Peak Base Load  │
                        └────────────┬────────────┘
                                     ↓
                        ┌─────────────────────────┐
                        │   Compute base F_EQA     │
                        └────────────┬────────────┘
                                     ↓
                        ┌─────────────────────────┐
                        │   Penetration = 1%       │
                        └────────────┬────────────┘
                                     ↓
  ┌──────────────┐     ┌─────────────────────────┐    ┌──────────────────┐
  │  Increment   │────→│  Compute New Load and    │←───│  Decrement Peak  │
  │  Penetration │     │        F_EQA             │    │   non-EV Load    │
  └──────┬───────┘     └────────────┬────────────┘    └─────────┬────────┘
         │                          ↓                            │
         │             ┌─────────────────────────┐    Yes        │
         │             │ non-EV F_EQA < new F_EQA │───────────────┘
         │             └────────────┬────────────┘
         │                     No   ↓
         │             ┌─────────────────────────┐
         │             │  Record Peak Base Load   │
         │             │     and Penetration      │
         │             └────────────┬────────────┘
    No   │                          ↓
         │             ┌─────────────────────────┐
         └─────────────│  Penetration = 100%      │
                       └────────────┬────────────┘
                              Yes   ↓
                        ┌─────────────────────────┐
                        │          Done            │
                        └─────────────────────────┘
```

Variables: $F_{EQA}$
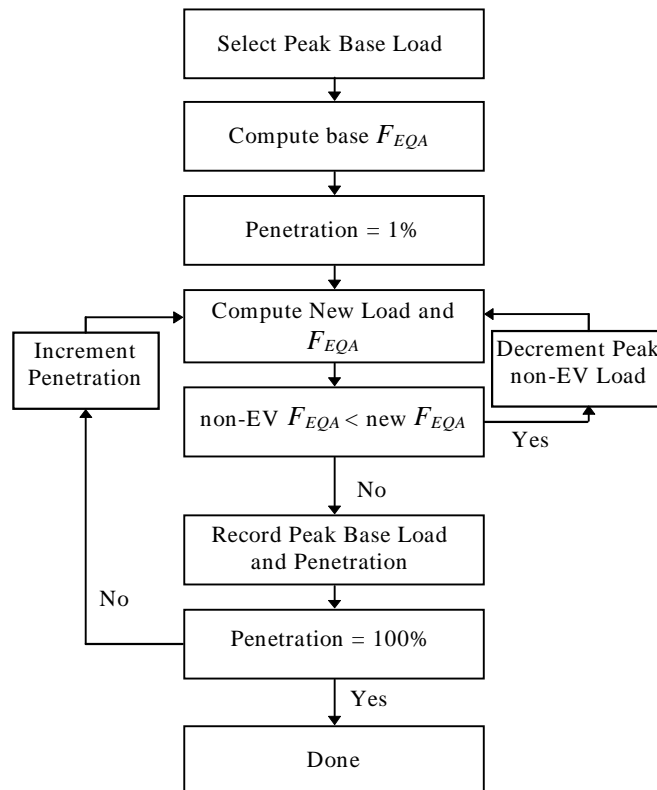
**Figure 4-6**
**Solution Process**
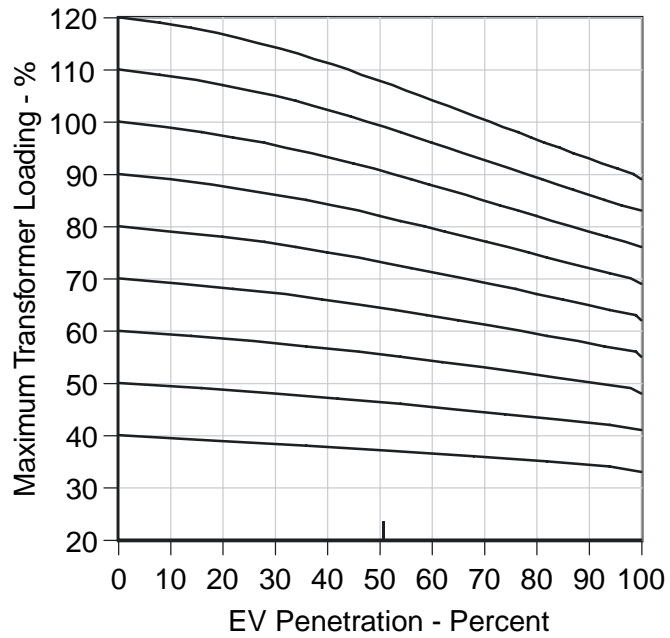
**Figure 4-7**
**Four-Hour Window, 6 p.m. Start**
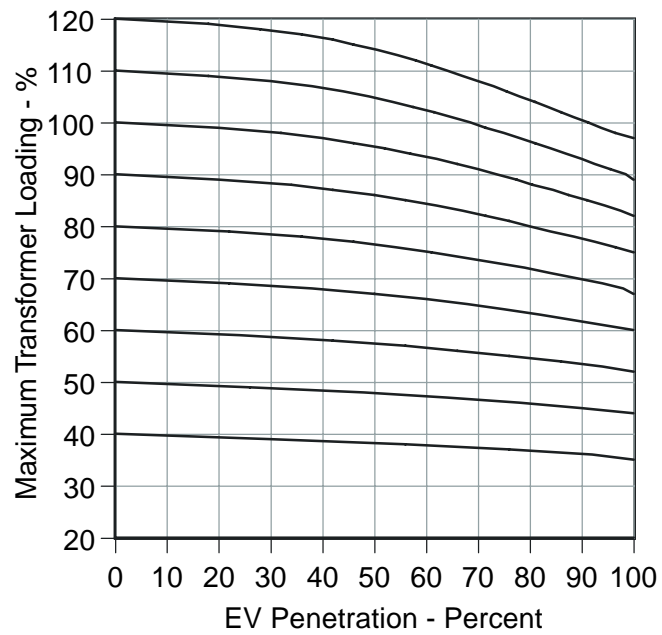


**Figure 4-8**
**Four-Hour Window, 8 p.m. Start**
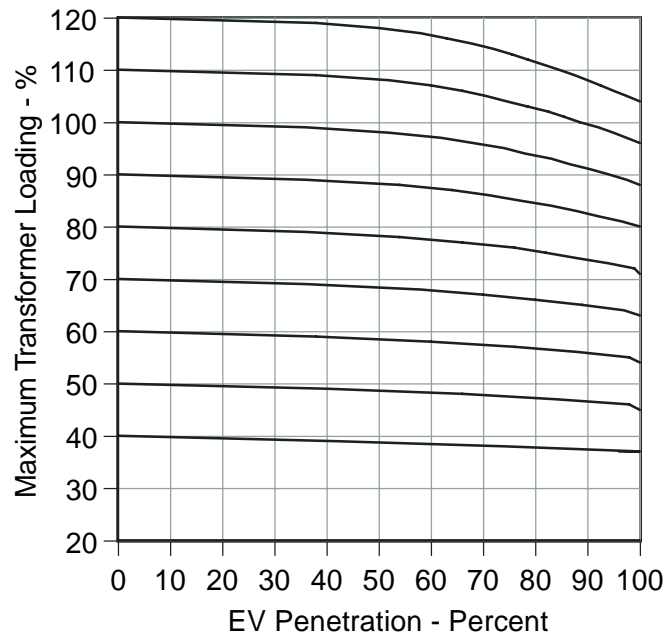
**Figure 4-9**
**Four-Hour Window, 10 p.m. Start**
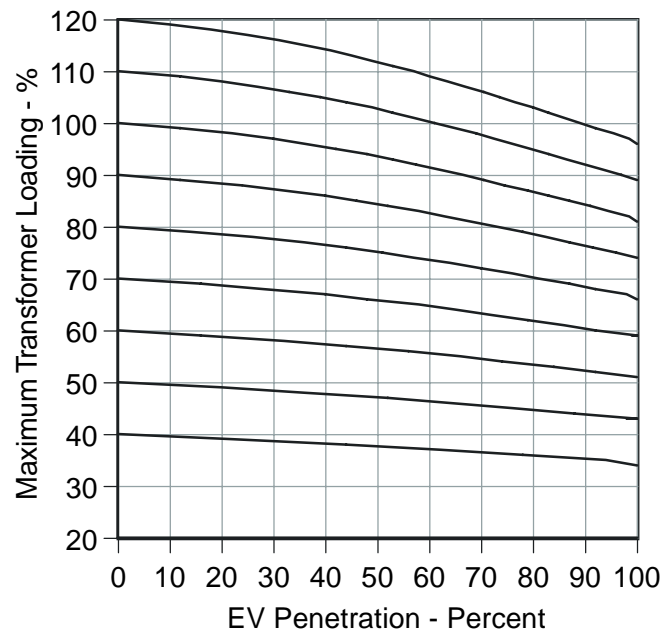


**Figure 4-10**
**Six-Hour Window, 6 p.m. Start**
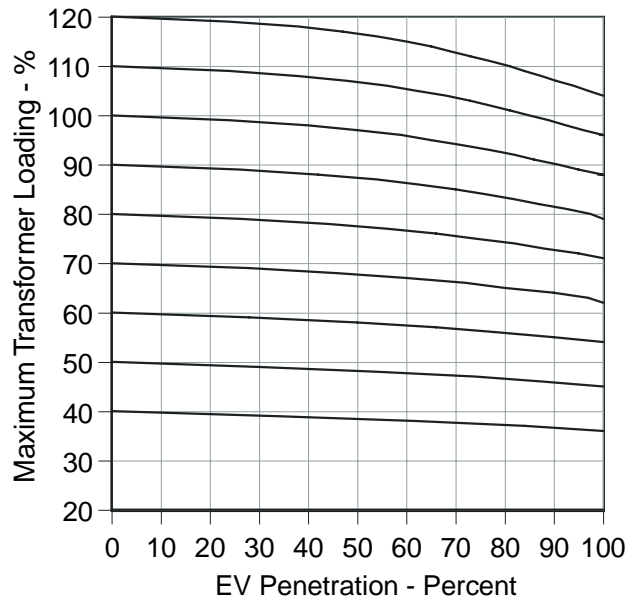
**Figure 4-11**
**Six-Hour Window, 8 p.m. Start**
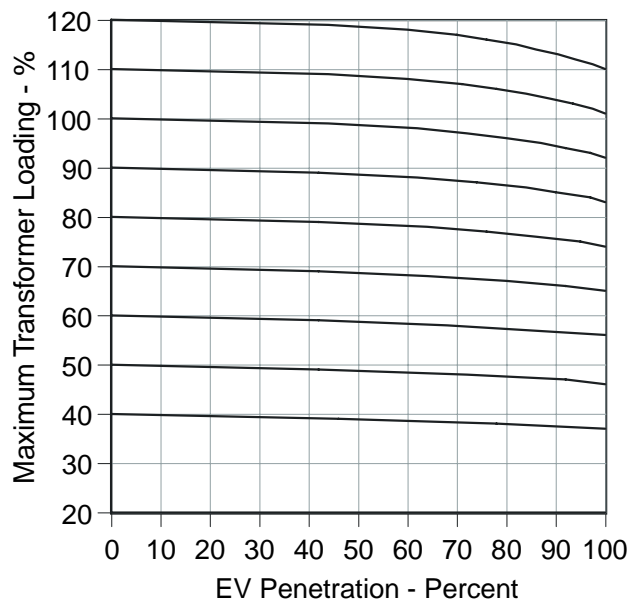


**Figure 4-12**
**Six-Hour Window, 10 p.m. Start**

Figures 4-7 to 4-12 Contours of Constant Transformer Life Expectancy for Different Charging Scenarios. (Note - Each penetration corresponds to a ratio of peak EV load relative to peak non-EV load. For the four-hour and six-hour windows at 100% penetration, these ratios are 0.62 and 0.41 respectively.)

## Summary

This chapter studies the effect of electric vehicle (EV) battery charging on a substation transformer that supplies both non-EV and EV load. The method models non-EV load using typical utility load shapes, and it models EV load so as to account for diversity introduced by varying individual charger start-times and initial battery states-of-charge. A FORTRAN implementation of the method is included as Appendix D.

Using techniques presented in [20] and [21], we present in Figures 4-7 to 4-12 contours of constant transformer life expectancy as EV loading increases for several different charging scenarios. We perform a worst-case analysis by selecting a small value for peak load per residence and by operating the transformer on a hot summer day. A larger value for peak load per residence, or a cooler day, will lessen the impact of EV charging on the transformer derating.

We show that the effect of EV charging on transformer derating is highly dependent on start-time and duration. As EV charging begins later in the day it has a less pronounced effect on the derating of the transformer since the non-EV load drops significantly as the evening progresses. This effect is promoted by the fact that the exponential relationship between insulation temperature and deterioration allows for relatively long-term additional heating at low temperatures without significant effect on transformer life expectancy. Thus, late-day EV charging has little effect on the transformer, even at high penetration levels.

Finally, this analysis includes the nonlinear effect of harmonic currents on transformer loading. The harmonic currents considered here are applicable only to the particular charger model analyzed. Variation in the harmonic content of net EV charging current can be expected due to the large number of charger topologies. Subsequent analysis of the problem neglecting harmonic currents shows the derating of the transformer to be relatively insensitive to EV harmonic currents. The three separate contours of constant life expectancy given in Figure 4-13 show the relationship between transformer derating and harmonic currents for the 6 p.m., four-hour charging scenario. The contour labeled 'Full Solution' corresponds to Figure 4-7 while the other contours are generated by first setting $P_{EC-R}$ to zero, and then all harmonic currents to zero. Figure 4-13 shows that at 100% EV penetration, harmonic currents account for only a 3% change in transformer derating.
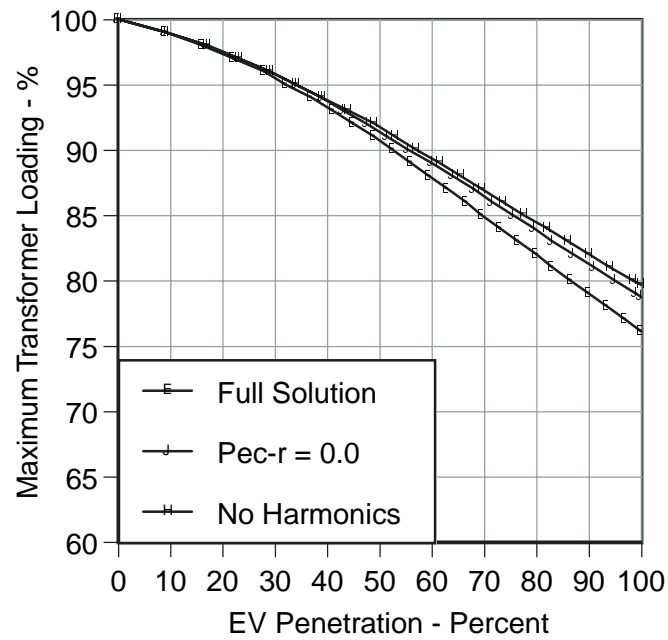
**Figure 4-13**
**Contours of Constant Life Expectancy**

# 5
# DISTRIBUTION SYSTEM HARMONIC VOLTAGES

## Introduction

The harmonic currents that EV battery charging will inject into power distribution systems not only present a threat to power distribution equipment such as transformers, but will also increase system voltage distortion levels. Thus, it is important to develop a model to characterize the possible impact of EV battery charging on distribution network harmonic voltages, and to detail the EV penetration levels that will produce critical voltage distortion.

This chapter presents a statistical method for predicting the effect that widespread EV battery charging will have on power distribution system harmonic voltage levels. The method relies on a statistical description of nonlinear load currents and commonly-available data for actual power distribution networks to determine the statistics of network harmonic voltages. Using these voltage statistics, we present the probabilities of exceeding certain specific levels of total harmonic distortion ($THD_v$). Previously, in Chapter 2, it was shown that ignoring diversity among distributed harmonic sources such as EV battery chargers leads to a significant overestimation of the harmonic problem. Thus, in order to account for diversity introduced by the uncertainty of initial battery states-of-charge (SOC) and start-times of individual chargers, we employ the statistical method we developed in Chapter 2 for predicting the net harmonic currents generated by a concentration of EV battery chargers.

Additionally, this chapter presents the results of several sample analyses of three actual power distribution networks. The results show that there is a definite threshold penetration below which EV charging has negligible impact on the number of buses whose total harmonic voltage distortion exceeds 5%.

## Formulation of the Harmonic Voltage Problem

We seek to evaluate the impact of widely distributed EV battery chargers on distribution system harmonic voltages. In order to accomplish this, we first model each EV battery charger as a harmonic current injecting load.

### Modeling Charger Load

Using the charger model and distribution for initial battery SOC presented in Chapter 2 along with a uniform distribution for start-time lasting four hours, we present in Tables E-1 and E-2 of Appendix E the statistics of the net harmonic current injections in the region where these statistics remain constant with time, i.e., the plateau region described in Chapter 2. Only

odd- harmonics have non-negligible current magnitudes. Figure 5-1 details the harmonic spectra of the mean current in percent of fundamental. Using the terminology in [9] this charger is appropriately classified as a "medium" distorting charger.

## *Modeling the Distribution System*

We rely on a combined loadflow and harmonic analysis program to evaluate and model the distribution network [22]. We connect our harmonic load in a grounded-wye configuration to permit triple harmonics to flow, and we introduce damping caused by system linear loads at PQ buses by representing them for harmonic purposes as resistive elements.
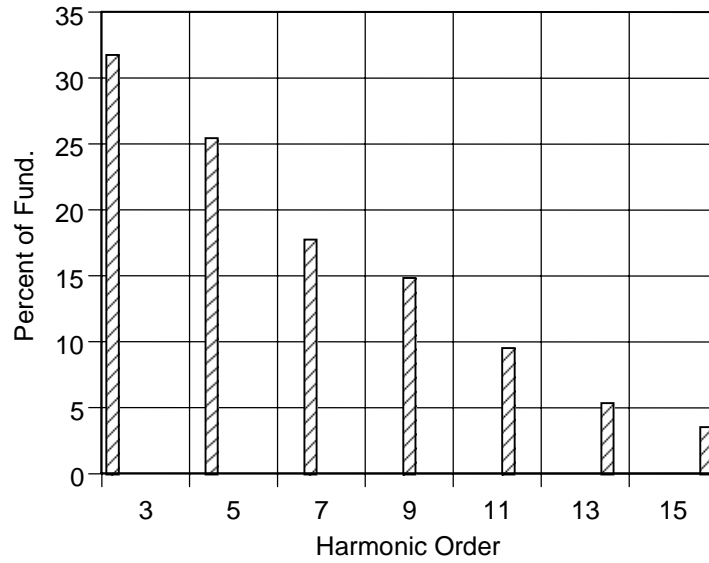


**Figure 5-1**
**Spectra of Mean Harmonic Current Injection**

We evaluate the impact of EV charging on distribution network harmonic voltages by first modeling the distribution network at the hour of interest. EV charging load is introduced at each PQ bus as a percentage of the peak summer linear load power. Though this percentage fully describes the amount of EV charging load, it is useful to parameterize this load in terms of a penetration $\pi$, i.e., the percentage of residences with an EV. We define $\Phi$ as the amount of EV load power in percent on system base,

$$\Phi = P_S \pi \frac{P_{EV}}{P_R} \frac{\rho}{100},$$
<div align="right">**Eq. 5-1**</div>

where $\rho$ is the percentage of residential load at the bus, $P_{EV}$ is the mean power of EV load in kW/charger, $P_R$ is the peak summer coincident load in kW/residence, and $P_S$ is the peak summer load in per unit on system base at the bus. Setting $P_R = 4.5$ kW, $P_{EV} = 2.22$ kW, and EV power factor = 0.9, we assign to each load bus the appropriate amount of EV load.

Harmonic injection profiles are required at each nonlinear load bus. This profile consists of the magnitude of each harmonic current in relation to the fundamental, and the corresponding phase angles with respect to local bus fundamental voltage. At each nonlinear load bus we input the mean current injection profile shown in Table E-1.

### Computing Current Statistics

Before proceeding with a statistical analysis of the system, it is necessary to describe the current injection at each bus. We define $\mathbf{I}$ as the complex-valued matrix of odd-order harmonic injection currents, row-indexed by harmonic order and column-indexed by bus number. The vector of current injections for all odd-order harmonic currents at bus $j$ is represented by $\mathbf{I_{\bullet j}}$, while the column vector of harmonic $h$ currents at all buses is represented by $\mathbf{I_{h \bullet}}$.

In subsequent analysis, we define the covariance of two random vectors $\mathbf{X}$, $\mathbf{Y}$, to be

$$\mathrm{cov}(\mathbf{X}, \mathbf{Y}) = \mathrm{E}\left[ \left( \mathbf{X} - \overline{\mathbf{X}} \right) \left( \mathbf{Y} - \overline{\mathbf{Y}} \right)^{*} \right],$$
<div align="right">**Eq. 5-2**</div>

where $\overline{\mathbf{X}}$ and $\overline{\mathbf{Y}}$ are the expectations of the random vectors $\mathbf{X}$ and $\mathbf{Y}$ respectively.

Splitting each row of the matrix $\mathbf{I}$ into two rows, the first composed of the real part and the second composed of the imaginary part, we form a real matrix having twice the row dimension as $\mathbf{I}$ which we denote as $\tilde{\mathbf{I}}$. Recognizing that harmonic current injections at each bus have a joint normal distribution [24], the current statistics at any bus $j$ are fully described by the vector of mean harmonic current injection, $\overline{\tilde{\mathbf{I}}}_{\mathbf{j}}$ and the covariance matrix of harmonic current injection at bus $j$, $\tilde{\mathbf{C}}_{\mathbf{I}}^{\mathbf{j}}$.

We proceed with computing the statistics of the random matrix $\tilde{\mathbf{I}}$ from the statistics of the EV charger concentration found in Tables E-1 and E-2. Because the statistics of harmonic injection current are initially provided in Amps/Chrgr and Amps$^2$/Chrgr, relative to the local bus fundamental voltage angle, it is first necessary to rotate them so that their phase angles are measured relative to the system swing bus, and then to rescale them to per unit. The harmonics analysis program described in the previous section generates the values of real and imaginary harmonic current injections at each load bus in pu and with respect to system swing bus. Due to our choice of mean harmonic injection profile, these currents are the mean values.

In order to correctly rotate the covariances it is necessary to account for the local voltage shift with respect to the system swing bus. Each harmonic current is advanced by the product of its harmonic order and the relative local fundamental voltage phase shift. Examining a particular bus $j$ whose relative fundamental voltage angle is represented by the unit-magnitude complex number $a + jb$, we form the diagonal matrix $\mathbf{A}$ with entries $(a + jb)h$, where $h$ is the harmonic index. The covariance matrix of harmonic currents at bus $j$ is computed from

$$\tilde{\mathbf{C}}_{\mathbf{I}}^{\mathbf{j}} = \mathrm{cov}\left( \tilde{\mathbf{H}}, \tilde{\mathbf{H}} \right),$$
<div align="right">**Eq. 5-3**</div>

where $\mathbf{H} = \mathbf{AI_{\bullet j}}$. $\tilde{\mathbf{C}}_{\mathbf{I}}^{\mathbf{j}}$ must then be scaled by the square of the mean per unit harmonic magnitude of order $h$ at bus $j$ divided by the mean harmonic magnitude of order $h$ in Amps from Table E-1.

### Computing Voltage Statistics

We seek to compute the harmonic voltage statistics at each bus. Using the harmonic analysis program we generate $\mathbf{Z_h}$, i.e., the appropriate positive, negative, or zero-sequence impedance matrix of the network for harmonic order $h$. Defining the voltage matrix $\mathbf{V}$ and the voltage vectors $\mathbf{V_{h\bullet}}$ and $\mathbf{V_{\bullet i}}$ analogously to current, we have

$$\mathbf{V_{h\bullet}} = \mathbf{Z_h I_{h\bullet}} \,.$$

**Eq. 5-4**

$\mathbf{V_{h\bullet}}$, the vector of $h$-order mean harmonic voltages is computed from (5-4). $\tilde{\mathbf{C}}_{\mathbf{V}}^{\mathbf{j}}$ denotes the covariance matrix of $\tilde{\mathbf{V}}_{\bullet \mathbf{j}}$.

### Computing Voltage Probabilities

We now embark on the study of the probability of harmonic voltage levels exceeding prescribed limits using the statistics for voltage that we derived in the previous section. The random variables describing harmonic voltage components at a single bus have a joint normal distribution, being linear combinations of the jointly normal currents. Thus, the joint probability density function of the harmonic voltages at any bus $j$ is

$$f(\hat{\mathbf{V}}) = \frac{\exp\left(-\frac{1}{2}\left(\hat{\mathbf{V}} - \overline{\tilde{\mathbf{V}}}_{\bullet \mathbf{j}}\right)\left(\tilde{\mathbf{C}}_{\mathbf{V}}^{\mathbf{j}}\right)^{-1}\left(\hat{\mathbf{V}} - \overline{\tilde{\mathbf{V}}}_{\bullet \mathbf{j}}\right)^{*}\right)}{\sqrt{(2\pi)^{N-1}\left|\tilde{\mathbf{C}}_{\mathbf{V}}^{\mathbf{j}}\right|}},$$

**Eq. 5-5**

where $N$ is the maximum harmonic order of interest, $\left(\tilde{\mathbf{C}}_{\mathbf{V}}^{\mathbf{j}}\right)^{-1}$ and $\left|\tilde{\mathbf{C}}_{\mathbf{V}}^{\mathbf{j}}\right|$ are the inverse and determinant respectively of the covariance matrix of voltage at bus $j$, and $\hat{\mathbf{V}} = \left[V_3^{\text{Re}} \quad V_3^{\text{Im}} \quad V_5^{\text{Re}} \quad V_5^{\text{Im}} \quad ... \quad V_N^{\text{Re}} \quad V_N^{\text{Im}}\right]$ is a real vector of dimension $(N-1)$.

To determine the probability that the $\text{THD}_\text{v}$ does not exceed a certain level $a$, we compute the integral

$$\Pr\left\{\left(V_3^{\text{Re}}\right)^2 + ... + \left(V_N^{\text{Im}}\right)^2 \le a^2\right\} = \int ... \int f\left(\hat{\mathbf{V}}\right) dV_3^{\text{Re}} ... dV_N^{\text{Im}} \ , \qquad\qquad \textbf{Eq. 5-6}$$

where the bounds of integration are the $(N-1)$-dimensional sphere $\left(V_3^{\text{Re}}\right)^2 + ... + \left(V_N^{\text{Im}}\right)^2 \le a^2$.
Evaluating this integral over the fourteenth-dimensional sphere corresponding to odd harmonics 3 through 15 is computationally prohibitive by standard numerical integration techniques. Instead, to evaluate this integral we rely on a Monte Carlo approach. This entails generating distinct sample vectors of the variable $\tilde{\mathbf{V}}_{\bullet\mathbf{j}}$. We note that $\mathbf{GN} + \overline{\tilde{\mathbf{V}}_{\bullet\mathbf{j}}}$ has the same distribution as $\tilde{\mathbf{V}}_{\bullet\mathbf{j}}$ where $\mathbf{G}$ is the upper left triangle matrix such that $\mathbf{GG}^{\text{T}} = \tilde{\mathbf{C}}_\mathbf{V}^\mathbf{j}$ and $\mathbf{N}$ is a vector of independent normally distributed random variables with mean zero and variance one [23]. Thus, generating samples of $\tilde{\mathbf{V}}_{\bullet\mathbf{j}}$ reduces to generating samples for $\mathbf{N}$. For each voltage sample vector computed, we determine the sum of the square of its elements and record it as a Monte Carlo trial. The integral can be evaluated satisfactorily with as few as 500 trials.

## Evaluating Specific Distribution Networks

We now embark on the study of the harmonic voltage levels of actual distribution networks using the statistics of harmonic voltages that we derived in the previous section. We have developed computer programs that accept as input the data describing any power distribution system and the harmonic current statistics similar to those presented in Tables E-1 and E-2. The programs then generate at each bus the probability distribution function (pdf) of $\text{THD}_\text{v}$ by first computing the covariance matrix $\tilde{\mathbf{C}}_\mathbf{V}^\mathbf{j}$ and the mean vector $\overline{\mathbf{V}}_{\bullet\mathbf{j}}$ at each bus $j$. With these statistics we determine the pdf of $\text{THD}_\text{v}$ by evaluating (5-6) for sufficiently many $a$.

Appendix F contains a program listing of VSTAT1.FOR. This algorithm computes the mean and covariance matrices of voltage at all buses and requires information on individual EV charger statistics, bus load levels, and the network impedance matrices. A program listing of VSTAT2.FOR, which takes the mean and covariance matrices computed by VSTAT1.FOR and evaluates (5-6) to determine the pdf of $\text{THD}_\text{v}$ at each bus in the network, is found in Appendix G.

### *Distribution System I*

We choose to study an actual power distribution system. It consists of seven feeders originating from two substation transformers that serve a suburban area in which a majority of the load is residential but which also includes industrial and commercial customers. Triple harmonic currents can flow to the substation, as the transformers are connected delta on the high side and grounded-wye on the low side. Service to the 237 load buses is provided mainly by overhead distribution lines at 12.5 kV and 25 kV. Additionally, there are 31 capacitor banks distributed

uniformly around the system for voltage support. Roughly half of these capacitor banks are switched. We begin our analysis with all fixed and switched capacitor banks on. The summer peak load is about 40 MW. The line and bus data required to model this system are found in Appendix H.

Most EV charging is expected to occur in residences during evening hours [13]. Because damping introduced by linear loads will decrease as evening progresses, we perform our study of the system during a late evening hour when we expect EV charging to have the greatest impact on distribution system harmonic voltages. Initially, we study the evening of a summer day when linear load is 75% of its daytime peak.

Figure 5-2 details the pdf of THDV at a representative bus for an EV penetration level of 50%. The plot of the pdf of third harmonic voltage is also included to show that the third harmonic of voltage is responsible for much of the voltage distortion. While the preponderance of third harmonic voltage is a function of the system and bus chosen, it is most directly a result of the strong third-harmonic current injection of the EV charger studied.

By evaluating the pdf of THDV, we can compute the probability that a specific voltage distortion level will not be exceeded. For example, Figure 5-2 indicates that THDV at the representative bus will not exceed 3.5% with a probability of 0.7. Using similar information at every bus, we proceed with our system evaluation by determining at each bus the probability that THDV will not exceed 5%. If this probability does not exceed a certain level P at some fraction of the buses, we can say, with confidence of at least P, that THDV will not exceed 5% at this fraction of buses. Similarly, we can determine the fraction of load that will be less than 5% THDV with probability of at least P.

Figures 5-3 and 5-4 give the results of this analysis as the penetration level is varied. A 50% EV penetration corresponds to an EV load that is roughly 20% as large as the linear load. It is characteristic of all the cases studied that there is very little difference between the fraction of buses and the fraction of load with THDV ≤ 5%. It is also apparent that there is a very definite threshold, around 25% penetration, where EV charging begins to have a significant impact on acceptable levels of THDV.
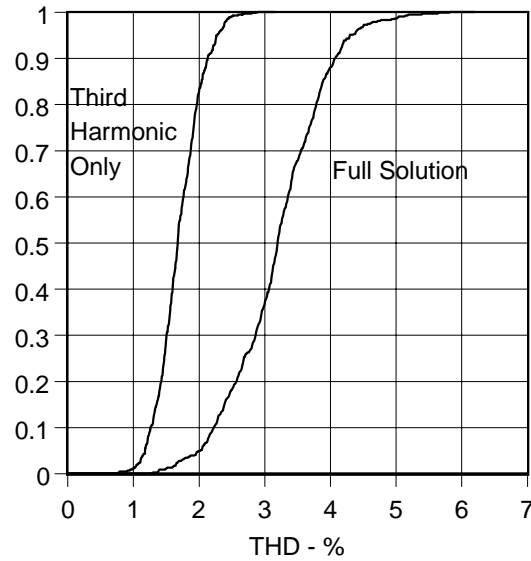
**Figure 5-2**
**Probability Distribution Function of THD$_v$ and Third Harmonic Voltage**

In order to determine the effect of seasonal variation we evaluate the system at off-peak conditions where all linear loads are at 50% of their summer peaks. This corresponds to a late evening analysis of this system in the spring or fall. Here, 50% EV penetration corresponds to an EV load that is roughly 30% as large as the linear load. Figure 5-5 relates the results of this analysis. It is apparent that the likelihood of excessive voltage distortion is greater for this case. This is largely because there is less linear load to provide damping.
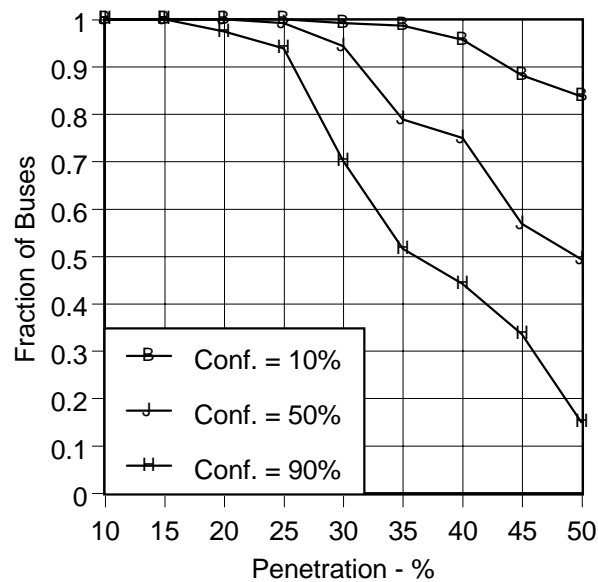


**Figure 5-3**
**Fraction of Buses with THD$_v$ ≤ 5%. Summer Case**
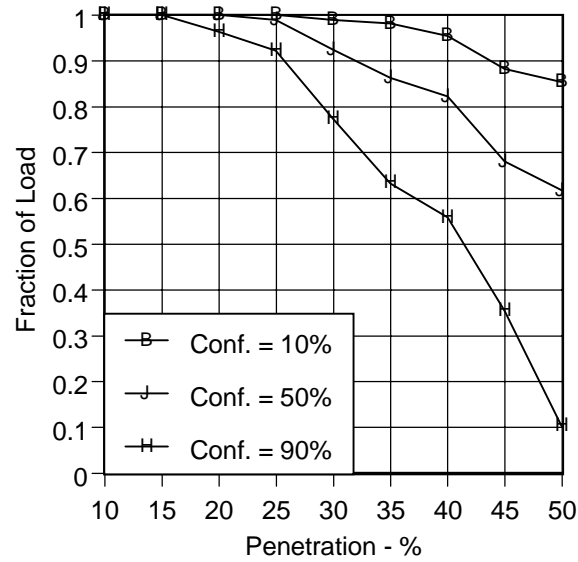
**Figure 5-4**
**Fraction of Load with THD$_v$ ≤ 5%. Summer Case**
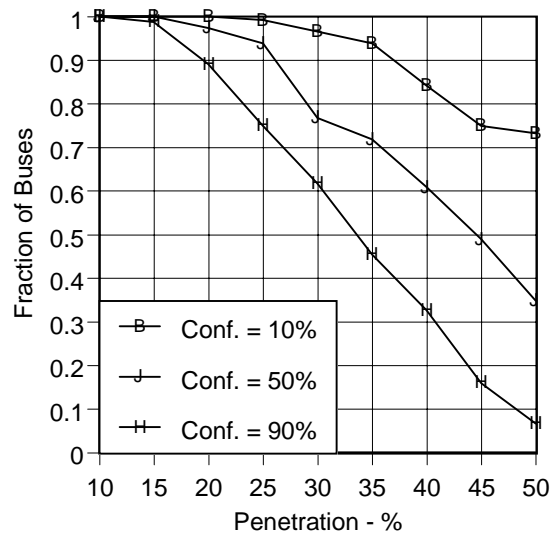
**Figure 5-5**
**Fraction of Buses with THD$_v$ ≤ 5%. Spring/Fall Case**

Additionally, we analyze the system with all capacitor banks removed. Figures 5-6 and 5-7 give the results of both a summer and a spring/fall analysis, respectively. Comparison with Figures 5-4 and 5-5 shows that the capacitor banks have little effect on EV threshold penetrations.

Using the same techniques, we have also studied the condition where the third harmonic current is totally eliminated at the charger. Penetration levels as high as 45% can be accommodated

under summer conditions without appreciable voltage distortion. The threshold penetration is about 40% for the spring/fall case. These analyses are detailed in Figures 5-8 and 5-9. Additionally, we have performed an analysis where the charger harmonic current magnitudes are rescaled while retaining the same relative spectra. The $THD_I$ of the original mean harmonic current injection is 48%. By reducing the distortion to 20%, the threshold penetration increases to 50% and 45% for the summer and spring/fall cases, respectively. Figures 5-10 and 5-11 relate to this reduced distortion evaluation.
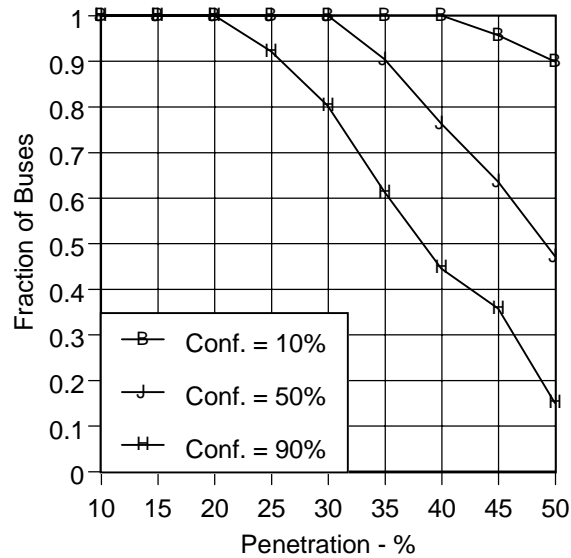


**Figure 5-6**
**Fraction of Buses with $THD_v \le 5\%$. Summer Case. No Capacitors**
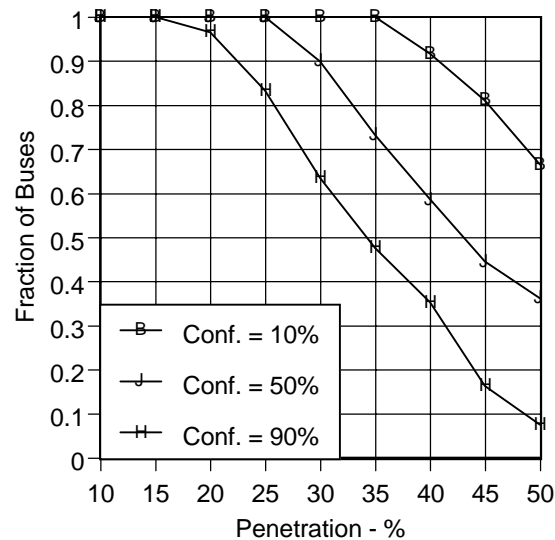


**Figure 5-7**
**Fraction of Buses with $THD_v \le 5\%$. Spring/Fall Case. No Capacitors**
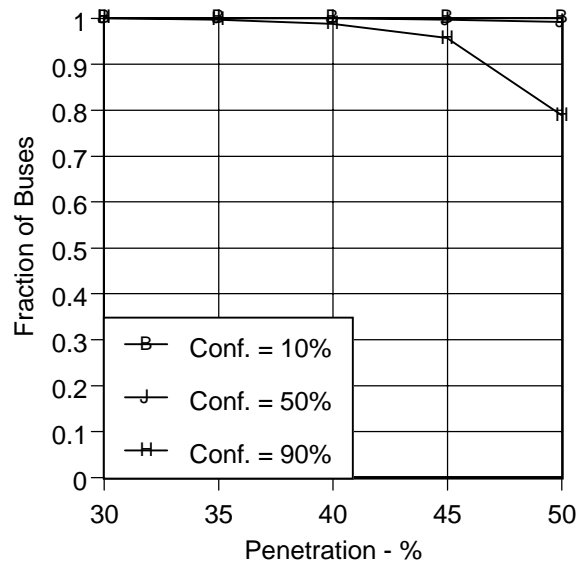
**Figure 5-8**
**Fraction of Buses with THD$_v$ ≤ 5%. Summer Case. No Third Harmonic Current**
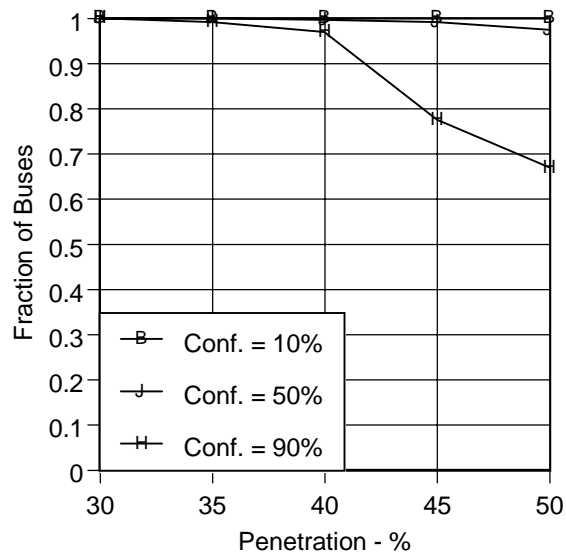


**Figure 5-9**
**Fraction of Buses with THD$_v$ ≤ 5%. Spring/Fall Case. No Third Harmonic Current**
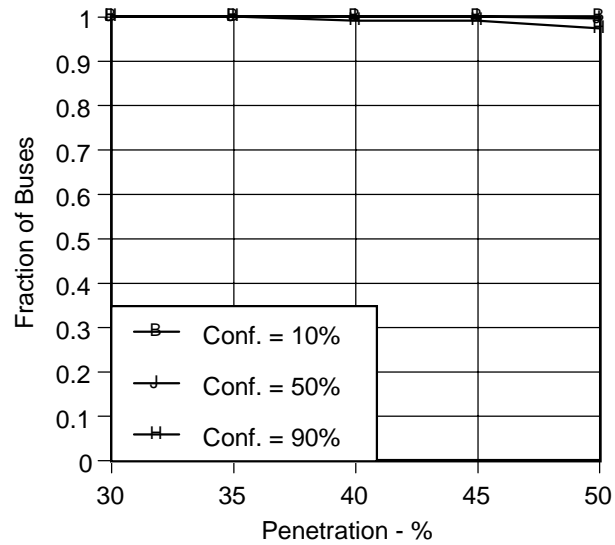
**Figure 5-10**
**Fraction of Buses with THD$_V$ ≤ 5%. Summer Case. Charger THD$_I$ = 20%**
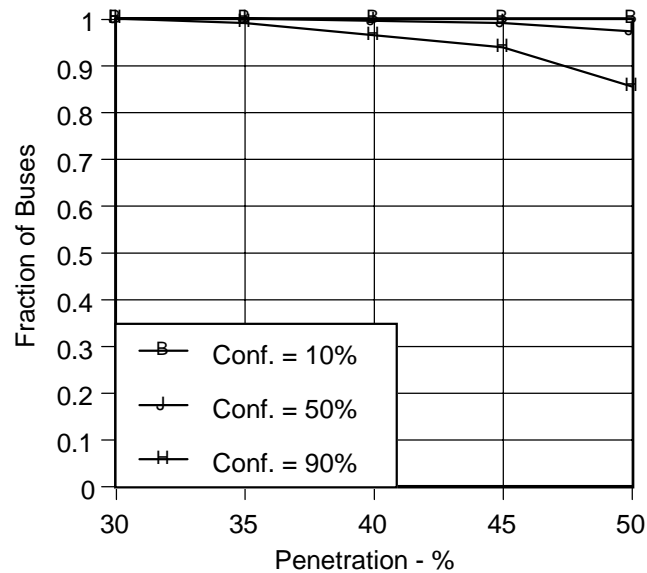


**Figure 5-11**
**Fraction of Buses with THD$_V$ ≤ 5%. Spring/Fall Case. Charger THD$_I$ = 20%**

Similar analyses of the third-harmonic-filtered and reduced distortion conditions show the threshold penetrations to be greater than 50% if the capacitors are removed from the system.

## *Distribution System II*

We choose to examine another, smaller, actual power distribution system. This system consists of a single feeder originating from one substation transformer that serves a suburban area in which a majority of the load is residential. The feeder also serves a small number of industrial and commercial customers. Triple harmonic currents can flow to the substation because the transformer is connected delta on the high side and grounded-wye on the low side. Service to the 167 three-phase load buses is provided mainly by overhead distribution lines at 12.5 kV. Additionally, there are 8 capacitor banks distributed around the system for voltage support. The summer peak load is about 10 MW. The line and bus data required to model this system are found in Appendix I.

Studying the summer and spring/fall late evening conditions described in the previous section, while including all capacitor banks, we discover that the threshold penetration of EVs exceeds 50%. Examining the condition where all capacitor banks are removed, we generate Figures 5-12 and 5-13 that describe the fraction of buses whose $THD_v$ does not exceed 5%. Removing the shunt capacitors lowers the threshold penetration significantly, indicating that the capacitor banks on this system are effectively tuned as harmonic filters. Because it is also characteristic of this system that there is very little difference between the fraction of buses and the fraction of load with $THD_v \leq 5\%$, we present information only on the fraction of buses in compliance with IEEE 519 [19].

The threshold region for this system is far more defined than that of the previous example. For the summer condition, the critical penetration is 30%. For the spring/fall condition, the threshold penetration falls to 25%. This seasonal reduction is a result of reduced damping by linear load.
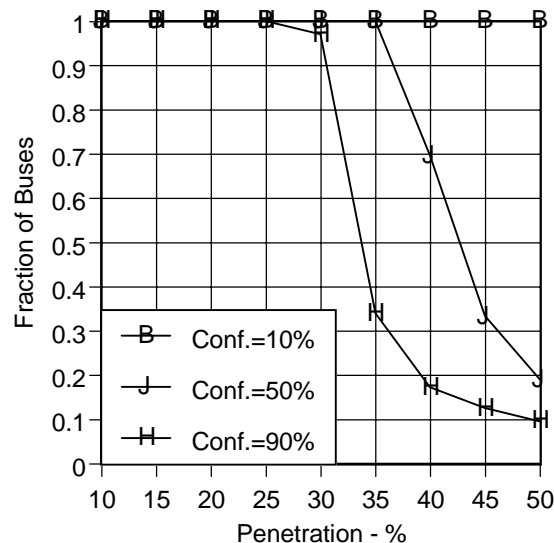


**Figure 5-12**
**Fraction of Buses with $THD_v \leq 5\%$. Summer Case. No Capacitors**
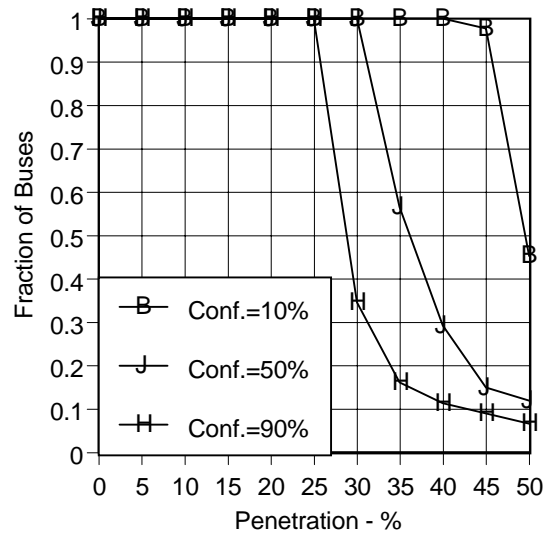
**Figure 5-13**
**Fraction of Buses with THD$_v$ ≤ 5%. Spring/Fall Case. No Capacitors**

## *Distribution System III*

We choose to evaluate a third actual power distribution system consisting of a single feeder similar to Distribution System II. Overhead 12.5 kV distribution lines provide the bulk of service to the 246 three-phase load buses. There are a total of 5 capacitor banks distributed around the system for voltage support. The summer peak load is about 7.5 MW. The line and bus data used to model this system are found in Appendix J.

Late-evening summer and spring/fall analysis with all capacitor banks on yields the results shown in Figures 5-14 and 5-15. Unlike System II, the capacitor banks do not provide substantial filtering. Like System II, the threshold region is very well defined. Figure 5-14 indicates the threshold EV penetration to be about 30% for the summer case. Figure 5-15 suggests that this penetration drops to about 25% for the spring/fall case.

Similar analysis of the distribution network without capacitor banks yields the results shown in Figures 5-16 and 5-17. Removal of the capacitor banks has little effect on the threshold EV penetrations. Rather than changing the threshold penetration, the effect of the capacitor banks is to lessen the definition of the threshold region. For example, for the summer case without capacitors the fraction of buses with THD$_v$ ≤ 5% is 70% for 35% EV penetration. This fraction of buses drops to 30% for the same case when capacitors are included.
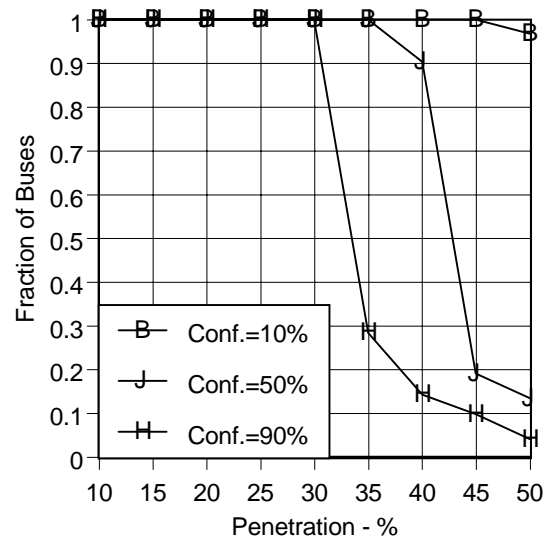
**Figure 5-14**
**Fraction of Buses with THD$_v$ ≤ 5%. Summer Case**
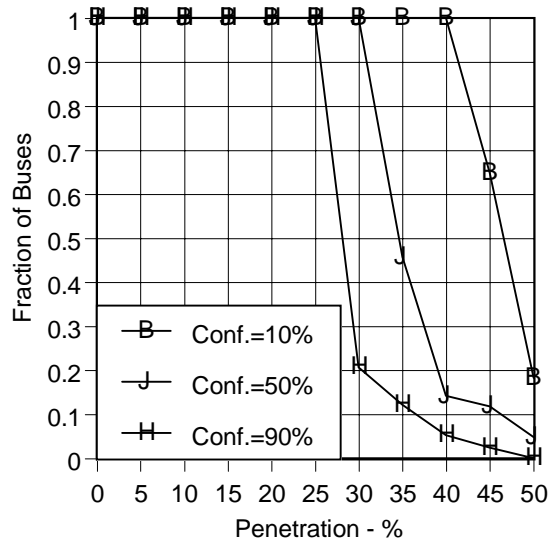


**Figure 5-15**
**Fraction of Buses with THD$_v$ ≤ 5%. Spring/Fall Case**
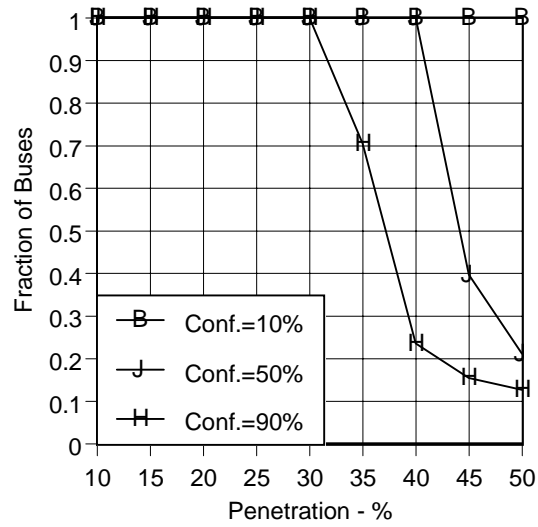
**Figure 5-16**
**Fraction of Buses with THD$_v$ ≤ 5%. Summer Case. No Capacitors**
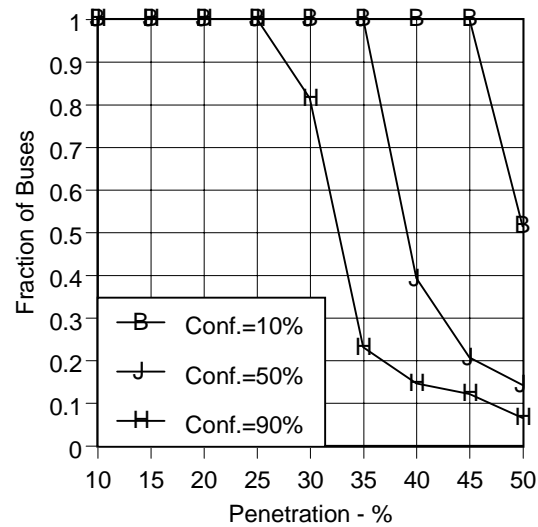


**Figure 5-17**
**Fraction of Buses with THD$_v$ ≤ 5%. Spring/Fall Case. No Capacitors**

## Summary

This chapter presents a general statistical method for predicting the harmonic voltage impact of a widely distributed harmonic producing load on a power distribution system. The method uses a statistical model for nonlinear current injections to generate the probabilities of specific total harmonic voltage distortions ($THD_V$) at any bus in the study system. FORTRAN programs that implement this method are found in Appendices F and G. We apply the method to study voltage distortion within three actual power distribution systems in the presence of widespread electric vehicle charging. We rely on the techniques presented in Chapter 2 to generate the statistics of the net harmonic currents produced by a concentration of EV chargers. Thus the statistics on voltage distortion account for variation and uncertainty in start-time and initial battery state-of-charge of the chargers.

For the specific charger studied, whose mean $THD_I$ is 48% and can thus be classified as a "medium" distorting charger [9], the analyses of several different systems show there to be a definite EV threshold penetration below which EV charging has negligible impact on the number of buses whose $THD_V$ exceeds 5%. Table 5-1 details the threshold EV penetration levels for the three distribution systems studied. The penetration values shown in Table 5-1 are those which will result in a negligible number of buses exceeding $THD_V$ of 5% with confidence at least 90%. These suggest that most existing power distribution networks will be able to accommodate the introduction of EV battery charging without violating IEEE guidelines on feeder voltage distortion [19].

**Table 5-1**
**Threshold EV Penetration Levels (%)**

| | | System | | |
|---|---|---|---|---|
| **Season** | **Capacitors** | **1** | **2** | **3** |
| Summer | on | 20 | >50 | 30 |
| Summer | off | 20 | 30 | 30 |
| Spring/Fall | on | 15 | >50 | 25 |
| Spring/Fall | off | 20 | 25 | 25 |

# *6*
# CONCLUSIONS

## Overview

The potential widespread introduction of electric vehicles (EVs) as an alternative to internal combustion vehicles presents both opportunities and challenges for power system engineers who will be required serve EV charger loads. One of the challenges associated with EV battery charging results from the potentially high harmonic currents associated with the conversion of ac power system voltages to dc battery voltages. Though most power electronic devices draw distorted currents, EV battery chargers, without deliberate and expensive design modifications, can be expected to inject especially high levels of harmonic currents because of their large power requirements. For example, where a television or computer operates around 100 W, an EV battery charger will likely operate between 3500 W and 7500 W at full power.

These large harmonic currents pose a threat to power distribution systems in a variety of ways. Harmonic currents lead to increased losses in distribution circuits and reduced life expectancy of power distribution components such as capacitors and transformers. Harmonic current injections also naturally lead to harmonic voltages on power distribution networks. These distorted voltages can affect power system loads, and specific standards have been developed to regulate voltage distortion [19].

This report develops a method to evaluate EV battery chargers as harmonic distorting loads and their possible harmonic impact on various aspects of power distribution systems. First, a statistical method for predicting the net harmonic currents injected by a large collection of EV battery chargers is developed. Next, this method is analyzed to evaluate the effect of input parameter variation on the net harmonic currents predicted by the model. Finally, the impact of EV charger harmonic currents on power distribution systems is studied by considering the effect of these currents on substation transformers and on power distribution system harmonic voltages.

Chapter 2 begins by developing a method to describe the net harmonic current injection of a large collection of EV battery chargers. The EV battery charger presents a number of challenges to those attempting to analyze its characteristics as a harmonic load. These challenges arise from the fact that unlike many harmonic current injecting loads, individual EV charger harmonic currents are not constant with time but rather vary with the state-of-charge of the battery. Additionally, there is considerable uncertainty in key variables such as start-time and initial battery state-of-charge (SOC).

Earlier studies have not considered the uncertainty in start time and initial battery SOC of an individual EV charger when attempting to evaluate the effect of EV charging on power distribution systems [9]. Thus they have likely overstated the harmonic problem of EV battery

charging. Others have considered the effect of diversity in start-time and initial battery SOC but have stopped short of developing an analytical method for accounting for these variables in the overall evaluation [11].

We develop the problem stochastically and present the statistics of the net harmonic currents for a realistic charging scenario. These statistics suggest that considering the diversity introduced by variable initial battery SOC and start-time leads to predictions of harmonic current injections that are roughly one-half those obtained by evaluating the net harmonic currents as the algebraic sum of the full power individual current injections. The analytical method relies on the Central Limit Theorem. Comparison with a similar Monte Carlo method shows the analytical method to accurately predict the net harmonic current statistics for concentrations of chargers as small in number as seven.

Subsequently, in Chapter 3, we evaluate the sensitivity of the statistics of net harmonic current injection to several key input parameters. These parameters include the statistics chosen to describe the probability density function (pdf) of miles traveled by an American commuter automobile and the length of time in which battery chargers are allowed to begin operation. Also, the power profile used to model the EV battery charger is varied in order to evaluate the effect of EV fuel-efficiency on net harmonic current injection.

We then turn our attention to the effect of EV battery charging on various aspects of power distribution networks. Chapter 4 examines the effect of EV harmonic currents on a substation transformer. The analysis begins by modeling net non-EV load with typical utility load shapes that account for industrial, commercial, and residential load variations throughout the day. EV load is modeled using results from the analytical method presented in Chapter 2. The effect of the net EV and non-EV load on the substation transformer is evaluated using ANSI/IEEE standards on transformer loading and the effects of nonlinear currents on power system devices [20-21]. A hot summer day condition is studied, and provision is made for the time variation of ambient temperature.

For specific non-EV load, EV load is introduced and the amount of transformer derating required to maintain a constant daily transformer loss-of-life with and without EV charging is computed. Varying the start-time pdf of the model presented in Chapter 2 and the time of day in which the chargers may begin operation yields several curves of transformer derating that will be useful to power system engineers. Results show that the effect of EV charging on transformer derating is highly dependent on start-time and duration. As EV charging begins later in the day, it has a less pronounced effect on the derating of the transformer. Indeed, late-day EV charging has little effect on the transformer, even at high penetration levels. Finally, it is shown that EV harmonic currents have little effect on the derating of the substation transformer. Rather, it is the increase in fundamental current that has the greatest effect on transformer derating.

Chapter 5 develops a method for predicting the harmonic voltages induced by EV battery charging on power distribution networks. The method relies on a statistical description of nonlinear load currents and commonly available data on actual power distribution networks to determine the statistics of network harmonic voltages. Thus, the technique itself can evaluate the harmonic voltage impact of any harmonic current injecting load for which the statistics of current injection are known. For the evaluation presented here, we rely on the method of Chapter 2 to provide us with the necessary current statistics.

6-2

Finally, Chapter 5 presents the results of several sample analyses of three different actual power distribution systems. The results show that there is a definite threshold penetration below which EV charging has negligible impact on the number of buses whose total harmonic voltage distortion ($THD_V$) exceeds 5%. These results suggest that most existing power distribution networks will be able to accommodate the introduction of EV battery charging without violating IEEE standards on feeder voltage distortion [19].

## Key Contributions and Possible Future Research

This report evaluates EV battery chargers as harmonic loads and considers their impact on power distribution equipment and harmonic voltages. The key contributions of this work are

1.  Developing the theoretical basis for evaluating the harmonic current injection of individual EV battery chargers under varying initial states-of-charge.

2.  Developing an analytical method for predicting the net harmonic current injection of a charger concentration that accounts for uncertainties in initial battery state-of-charge and charger start-time of individual chargers.

3.  Applying the idea of a diversity factor to EV charger harmonics to show that expected net EV harmonics are greatly reduced by considering the variation of initial battery state-of-charge and charger start-time when compared to the full power algebraic computation of net EV harmonic currents.

4.  Providing several reasonable net expected harmonic current injection spectra (magnitude and phase) from concentrations of EV chargers.

5.  Examining the effect of EV battery charging on the derating of a substation transformer, and showing that EV harmonic currents have little effect on the derating required to maintain constant transformer life-expectancy with or without EV charging.

6.  Developing a general statistical method for predicting the effect that widespread nonlinear loads will have on power distribution system harmonic voltage levels.

7.  Determining that there is a threshold penetration below which EV charging has a negligible impact on the percentage of power distribution system buses whose total harmonic voltage distortion exceeds IEEE guidelines of 5%.

There are many different EV chargers available for purchase, and there is a wide variation in their harmonic current spectra. Though the techniques presented in this report can evaluate concentrations of chargers of only one specific type, they are able to evaluate any commercially-available charger for which sufficient power and harmonic current data have been collected. There is, however, a serious lack of data regarding the currents drawn by commercially-available EV battery chargers. Though there are numerous data on the harmonic currents drawn by EV battery chargers operating at full power, there is very little information on how these harmonic currents vary during the charging cycle. Since this variation is very important in the evaluation of the net harmonic injection of a concentration of EV chargers, future EV data collection efforts should focus on measuring this effect for a variety of EV chargers.

The models presented in this work can be useful in analyzing the effect of EV battery charging not only on distribution system harmonic problems, but also on other areas of interest to power engineers. For example the predictions of net power generated by the method of Chapter 2 could be used by engineers seeking to optimally fill the off-peak valley with EV load. The relation between the pdf of start-time and expected power could be exploited to optimally set time-of-day rate structures.

It is hoped that the techniques and results presented in this report will provide power distribution system engineers a set of tools and references that will enable them to adequately prepare for the large-scale introduction of electric vehicle battery charging.

# 7
# REFERENCES

1.  J. Arrillaga, D. A. Bradley, P. S. Bodger, *Power System Harmonics*, John Wiley & Sons, New York, NY, 1985.

2.  *Power System Harmonics*, IEEE Tutorial Course Text 84EH0221-2-PWR, New York, 1981.

3.  P. G. Cummings, "Estimating the Effect of System Harmonics on Losses and Temperature Rise of Squirrel-Cage Motors," *IEEE Transactions on Industry Applications*, November/December 1986, pp. 1121-1126.

4.  D. E. Rice, "Adjustable Speed Drive and Power System Harmonics - Their Effect on Power System Components," *IEEE Transactions on Industry Applications*, IA-22(1), January/February 1986, pp. 161-177.

5.  G. C. Jain, "The Effect of Voltage Waveshpae on the Performance of a Three-phase Induction Motor," *IEEE Transactions on Power Apparatus and Systems*, vol. PAS-84, 1964, pp. 560-566.

6.  J. Douglas, "Quality of Power in the Electronics Age," EPRI Journal, vol. 10, no. 9, November 1985, pp. 6-13.

7.  M. Samotyj, "End-Use Power Quality," *EPRI Journal*, vol. 14, March 1989, pp. 40-42.

8.  L. Lamarre, "Problems with Power Quality," *EPRI Journal*, vol. 16, July/August 1991, pp. 14-23.

9.  J. K. Bohn, D. W. McMullen, P. Save, *Electric Vehicle Battery Charger Harmonics Study*, Technical Paper LM-007, Rosemead, CA, March 1995.

10. A. Mansoor, W. M. Grady, A. H. Chowdhury, M. J. Samotyj, "An Investigation of Harmonics Attenuation and Diversity Among Distributed Single-Phase Power Electronic Loads," *IEEE Trans. on PWRD*, vol. 10, no. 1, January 1995, pp. 467-473.

11. J. A. Orr, A. E. Emanuel, K. W. Oberg, "Current Harmonics Generated by a Cluster of Electric Vehicle Battery Chargers," *IEEE Trans. on PAS*, vol. 101, no. 3, March 1982, pp. 691-699.

12. R. Indrigo, C. A. Haslund, *Testing of Inductive and Conductive Electric Vehicle Chargers at PG&E*, Pacific Gas and Electric Company, Report 008.1-93.21, San Ramon, CA, October 1994.

13. *Electric Vehicle Charging Systems: Volume 2, Report of the Connector and Connecting Station Committee*, Report TR-104623-V2, Electric Power Research Institute, Palo Alto, CA, December 1994.

14. G. G. Karady, S. H. Berisha, T. Blake, R. H. Hobbs, "Power Quality Problems at Electric Vehicle's Charging Station," *Proc. of the Second Electric Transportation System Compatibility Conf.*, Long Beach, CA. September 9-15, 1995, pp. 287-292.

15. M. J. Vincent, M. A. Keyes, M. Reed, D. Sabonis, *Nationwide Personal Transportation Survey - Urban Travel Patterns*, Federal Highway Administration, Washington D.C., June 1994.

16. M. J. Riezenman, "Architecting the System," *IEEE Spectrum*, vol. 29, no. 11, November 1992, pp. 94-96.

17. C. W. Gellings, "EPRI and the Commercialization of Electric Vehicles," *Proceedings: IERE Workshop on Electric Vehicles, Advanced Batteries, and Impacts on Electric Utilities*, TR-101138, December 1992, pp. 4.7-4.17.

18. W. E. Kazibwe, T. H. Ortmeyer, M. S. A. A. Hammam, "Summation of Probabilistic Harmonic Vectors," *IEEE Trans. on PWRD*, vol. 4, no. 1, January 1989, pp. 621-626.

19. *IEEE Recommended Practices and Requirements for Harmonic Control in Power Systems*, IEEE Std. 519-1992, IEEE, New York, NY, 1993.

20. ANSI/IEEE C57.91, IEEE Guide for Loading Mineral-Oil-Immersed Transformers, 1996.

21. ANSI/IEEE C57.110, IEEE Recommended Practice for Establishing Transformer Capability When Supplying Nonsinusoidal Load Currents, 1986.

22. W. M. Grady, *PCFLO Version 5.3 User Manual*, University of Texas at Austin, Austin, TX, May 1999. (http://www.ece.utexas.edu/~grady/)

23. M. E. Johnson, *Multivariate Statistical Simulation*, John Wiley and Sons, New York, NY, 1987.

24. P. T. Staats, W. M. Grady, A. Arapostathis, R. S. Thallam, "A Statistical Method for Predicting the Net Harmonic Currents Generated by a Concentration of Electric Vehicle Battery Chargers," *IEEE Trans. on PWRD*, vol. 12, no. 3, pp. 1258-1266, July 1997.

25. P. T. Staats, W. M. Grady, A. Arapostathis, R. S. Thallam, "Sensitivity Analysis of a Statistical Method for predicting the Net Harmonic Currents Generated by a Concentration of Electric Vehicle Battery Chargers," *Conf. Proceedings of Seventh International Conference on Harmonics and Quality of Power*, October, 1996.

26. P. T. Staats, W. M. Grady, A. Arapostathis, R. S. Thallam, "A Procedure for Derating a Substation Transformer in the Presence of Widespread Electric Vehicle Battery Charging," *IEEE Trans. on PWRD*, vol. 12, no. 4, pp. 1562-1568, October 1997.

27. P. T. Staats, W. M. Grady, A. Arapostathis, R. S. Thallam, "A Statistical Analysis of the Effect of Electric Vehicle Battery Charging on Distribution System Harmonic Voltages," *IEEE Trans. on PWRD*, vol. 13, no. 2, pp. 640-646, April 1998.

28. A. Papoulis, *Probability, Random Variables and Stochastic Processes*, McGraw Hill, New York, NY, 1965.

# *A*
# APPENDIX A – COEFFICIENTS OF POLYNOMIALS RELATING EV CHARGER HARMONIC CURRENT MAGNITUDES TO OPERATING POWER

**Table A-1**
**Coefficients of Harmonic Currents. Percent of Fundamental Magnitude**
**@ 240V = $K_3P^3 + K_2P^2 + K_1P + K_0$, ($P$ in W)**

| Current | $K_3$ | $K_2$ | $K_1$ | $K_0$ |
|---|---|---|---|---|
| Fund Re. (Amps) | 0.0 | 0.0 | 4.06E-3 | 0.089 |
| Fund Im. (Amps) | 0.0 | 0.0 | -2.00E-3 | 0.1432 |
| 3rd Re. | 0.0 | 0.0 | -4.88E-3 | 43.71 |
| 3rd Im. | 2.83E-10 | -3.64E-6 | 1.48E-2 | -45.15 |
| 5th Re. | 3.15E-10 | -4.90E-6 | 2.14E-2 | -23.59 |
| 5th Im. | 1.91E-10 | -2.86E-6 | 1.97E-2 | -75.75 |
| 7th Re. | 1.81E-12 | 4.19E-7 | -6.68E-3 | 27.48 |
| 7th Im. | -3.54E-11 | 1.31E-7 | 6.73E-3 | -46.59 |
| 9th Re. | -1.45E-10 | 2.39E-6 | -1.39E-2 | 32.38 |
| 9th Im. | 5.60E-11 | -1.12E-6 | 1.05E-2 | -43.50 |
| 11th Re. | -1.01E-10 | 1.84E-6 | -1.13E-2 | 25.27 |
| 11th Im. | 8.54E-11 | -1.54E-6 | 1.10E-2 | -34.50 |
| 13th Re. | -1.50E-10 | 2.53E-6 | -1.40E-2 | 27.46 |
| 13th Im. | 2.64E-11 | -5.53E-7 | 4.66E-3 | -15.78 |
| 15th Re. | -9.88E-11 | 1.49E-6 | -7.21E-3 | 13.05 |
| 15th Im. | 4.99E-11 | -9.26E-7 | 6.04E-3 | -15.29 |

# B

## APPENDIX B – FORTRAN IMPLEMENTATION OF ANALYTICAL METHOD FOR PREDICTING NET HARMONIC CURRENT STATISTICS

```
C****************************************************************************
C        PROGRAM CHARGER.FOR
C****************************************************************************
        Real sumpwr, probm(3000), enerper(500), suminter
      Real searchm, prob, pwr(100), range, maxrange, m, enerprb(500)
      Integer maxlevel, dum ,time
      Logical done
        Real probmt(3000),meant,mean,meano,vart,var,sdt,sd,sdo
      Real w,x,y,z,ww,xx,yy,zz,ao,bo,at,bt,da,db,sum
      Real eps,delta,pi
        Real scale, pexp, pvar,  strtprb(200), pwrprb(500)
        real hexpi(26),hvari(26),cov(25),corr(25), hvarr(25),hexpr(25)
      real a,b,c,d,f
      real harm(26,150),curr(500),hcoeff(4)
      real zmin(25),zmax(25)
      real stepz(25),maxprob
      real zm(150),meanmag(26),varmag(26)
      real coefr(2),coefi(2)
        open(unit=2,file='instrt.in',status='unknown')
      open(unit=3,file='inp.in',status='unknown')
      open(unit=4,file='inpwr.in',status='unknown')
      open(unit=9,file='harmdat.in',status='unknown')
      open(unit=10,file='evar.out',status='unknown')
      open(unit=11,file='miles.out',status='unknown')
      open(unit=12,file='inpwr.out',status='unknown')
      open(unit=18,file='msg.out',status='unknown')
      open(unit=19,file='tst.out',status='unknown')

        delta = 0.01
      eps = 0.01
      pi = 3.14159265359
      maxprob = 1e-4

      Write(5,*)'Enter the maximum harmonic current of interest'
      read(5,*)maxharm
      write(5,*)'Input scan range as percentage of normal (34.2m 21.1m)'
      write(5,*)'or if you wish to input from file inpwr.in input 0'
       read(5,*)scale
      scale = scale/100
      if (scale.eq.0) then
       read(4,*)maxlevel
       do 1920 i=1,maxlevel
```

```fortran
      read(4,*)dum, enerprb(i),pwr(i)
 1920  continue
     endif
         if (scale.ne.0) then
     sumpwr = 0.0
     read(3,*)maxlevel
     do 20 i=1,maxlevel
      read(3,*)dum,pwr(i)
      sumpwr = sumpwr + pwr(i)
  20 continue
     suminter=0.0
     do 30 i=maxlevel,1,-1
      suminter=suminter+pwr(i)
      enerper(i)=1 - suminter/sumpwr
  30 continue
     endif

         read(9,*)dum,order
     read(9,*) coefr(2),coefr(1)
     read(9,*)dum,order
     write(18,*)'fund real coeffs:',coefr(2),coefr(1)
     read(9,*)coefi(2),coefi(1)
     write(18,*)'fund imag coeffs:',coefi(2),coefi(1)
     do 29 j=1,maxlevel
      harm(1,j)= pwr(j)*coefr(2)+coefr(1)
      harm(2,j)= pwr(j)*coefi(2)+coefi(1)
      curr(j)  = sqrt(harm(1,j)**2+harm(2,j)**2)
  29 continue
         do 1830 i=3,(maxharm+1)
     write(18,*)'harmonic',i
     read(9,*)dum,order
     write(18,*)'harmonic',dum,'order',order
     do 25 j=(order+1),1,-1
      read(9,*)hcoeff(j)
      write(18,*)'coeff ',j,hcoeff(j)
  25  continue
         do 26 j=1,maxlevel
     if (order.eq.1) then
      harm(i,j)=pwr(j)*hcoeff(2)+hcoeff(1)
     else if (order.eq.2) then
      harm(i,j)=pwr(j)**2*hcoeff(3) + pwr(j)*hcoeff(2) + hcoeff(1)
     else
      harm(i,j)=pwr(j)**3*hcoeff(4)+pwr(j)**2*hcoeff(3)
   1    +pwr(j)*hcoeff(2) + hcoeff(1)
     endif
     harm(i,j) = harm(i,j) / 100 * curr(j)
  26  continue
 1830 continue
     do 21 i=1,maxlevel
      pwr(i)=pwr(i)/1000
  21 continue

     write(5,*)'Input the number of chargers'
     read(5,*)ncharge
     range=75
     setmean=34.2
```

```fortran
      setsd=21.1
      maxrange = 10.0*real(range-1.0)
      maxrange = maxrange + 1
      write(10,251)'Time','expPower','varPower'
 251  format(a5,2a20,\)
      do 252 k=3,maxharm,2
       if (k.lt.10) then
        write(10,253)'expMag',k,'varMag',k
       else
        write(10,254)'expMag',k,'varMag',k
       endif
 252  continue
      write(10,503)' '

          write(5,*)'Input on-time as 5m steps (0 for 8hr default)'
      write(5,*)'or enter 999 to input from instrt.in'
      read(5,*)maxstime
      if (maxstime.lt.eps) maxstime=96
      time = maxlevel+1
      if (maxstime.ne.999) then
       do 1 i=1,maxstime
        strtprb(i) = real(1/real(maxstime))
   1   continue
      endif
      if (maxstime.eq.999) then
       read(2,*)maxstime
       do 2 i=1,maxstime
        read(2,*)dum,strtprb(i)
   2   continue
      endif
      if (scale.eq.0) then
       goto 2223
      endif
          mean = setmean * scale
      sd   = setsd   * sqrt(scale)
      write(5,*)scale
          ao = 2
      bo = 1
          run = 0
 99   continue
      sum = 0.0
      do 100 i=1,1991
      m  = real(i-1)/10 + 1
      probm(i) = log(m)/(sqrt(2*pi)*bo)*
   1         exp(-1/(2*bo**2)*(log(m)-ao)**2)
      sum = sum + probm(i)
 100  continue
      meano = 0.0
      var  = 0.0
      do 101 i=1,1991
      m = real(i-1)/10 + 1
      probm(i) = probm(i)/sum
      meano = meano + m*probm(i)
      var  = var  + m*m*probm(i)
 101  continue
      var  = var - meano**2
```

```
    sdo   = sqrt(var)
    if ((abs(meano-mean).lt.eps ).and.( abs(sdo-sd).lt.eps )) goto 110
    if (run.gt.20) goto 110
         at = ao + delta
    bt = bo
    sum = 0.0
    do 103 i=1,1991
    m  = real(i-1)/10 + 1
    probmt(i) = log(m)/(sqrt(2*pi)*bt)*
1            exp(-1/(2*bt**2)*(log(m)-at)**2)
    sum = sum + probmt(i)
103 continue
    meant = 0.0
    vart  = 0.0
    do 104 i=1,1991
    m = real(i-1)/10 + 1
    probmt(i) = probmt(i)/sum
    meant = meant + probmt(i)*m
    vart  = vart + probmt(i)*m*m
104 continue
    vart = vart - meant**2
    sdt  = sqrt(vart)
    w    = (meant - meano) / delta
    y    = (sdt -sdo) / delta
         at = ao
    bt = bo + delta
    sum=0.0
    do 105 i=1,1991
    m  = real(i-1)/10 + 1
    probmt(i) = log(m)/(sqrt(2*pi)*bt)*
1            exp(-1/(2*bt**2)*(log(m)-at)**2)
    sum = sum + probmt(i)
105 continue
    meant = 0.0
    vart  = 0.0
    do 106 i=1,1991
    m = real(i-1)/10 + 1
    probmt(i) = probmt(i)/sum
    meant = meant + probmt(i)*m
    vart  = vart + probmt(i)*m*m
106 continue
    vart = vart - meant**2
    sdt  = sqrt(vart)
    x    = (meant - meano) / delta
    z    = (sdt   - sdo) / delta
         ww = z/(w*z-x*y)
    zz = w/(w*z-x*y)
    xx = -x/(w*z-x*y)
    yy = -y/(w*z-x*y)
         run = run+1
         da = ww*(mean-meano) + xx*(sd - sdo)
    db = yy*(mean-meano) + zz*(sd - sdo)
    if (bo.lt.0.0) bo = 0.2
    if (da.gt.0.2) da = 0.2
    if (da.lt.-0.2)da =-0.2
    if (db.gt.0.2) db = 0.2
```

B-4

```fortran
      if (db.lt.-0.2)db =-0.2
      ao = ao + da
      bo = bo + db
      goto 99
 110  continue
      write(18,*)'*********** SOLUTION ***********'
      write(18,*)'a = ',ao
      write(18,*)'b = ',bo
      write(18,*)'mean = ',meano
      write(18,*)'std dev = ',sdo
      sum=0.0
      do 1112 i=1,((range-1)*10+1)
      m  = real(i-1)/10 + 1
      sum = sum + probm(i)
1112  continue
      do 112 i=1,((range-1)*10+1)
      m  = real(i-1)/10 + 1
      probm(i) = probm(i)/sum
      write(11,*)m,probm(i)
 112  continue

      m=1.0
      do 40 i=maxlevel,1,-1
      prob = 0.0
      searchm = (1.0 - enerper(i)) * (range-1.0) + 1.0
      done = .false.
      do 50 While (.not.done)
      j=(m-1)*10+1
       if (m.gt.range) then
        done = .true.
       else if (m.le.searchm) then
        prob = prob+probm(j)
        m=m+0.1
       else
        done=.true.
       endif
  50   continue
       enerprb(i)=prob
  40  continue
          sum = 0.0
      do 60 i=1,maxlevel
          sum = sum + enerprb(i)
  60  continue
  70 format(i5,f10.1,f15.8)
2223 continue
      do 4444 i=1,maxlevel
      write(18,*)i,enerprb(i),pwr(i)
4444 continue
      do 5555 i=1,maxstime
      write(18,*)i,strtprb(i)
5555 continue

      write(5,*)'Enter start and stop time, or 0, 0 for full solution'
      read(5,*)istart,istop
      if ( (istart.lt.1).or.(istop.lt.1)) then
      istart = 1
```

```
      istop = maxlevel+maxstime
      endif
      write(5,*)'ok start at time ',istart,' and stop at ',istop
      do 888 time=istart,istop
      write(5,*)'Evaluating time ',time
      do 320 i=1,maxlevel
       pwrprb(i)=0.0
 320  continue
      pexp=0.0
      pvar=0.0
      do 2222 har=3,maxharm
       hexpr(har)=0.0
       hvarr(har)=0.0
       hexpi(har)=0.0
       hvari(har)=0.0
       cov(har) =0.0
       corr(har)=0.0
       meanmag(har)=0.0
       varmag(har)=0.0
 2222 continue
      do 310 level = 1,maxlevel
       do 300 pre  = 1,level
        idum = time - level + pre
        if ((idum.le.0).or.(idum.gt.maxstime)) then
         goto 300
        else
         prob = strtprb(idum)
        endif
       pwrprb(level) = pwrprb(level) + enerprb(pre) * prob
 300  continue
 310  continue

      do 200 level=1,maxlevel
       pexp = pexp + pwrprb(level)*pwr(level)
       pvar = pvar + pwrprb(level)*pwr(level)**2
 200  continue
      pvar = pvar - pexp**2
           do 203 har=3,maxharm,2
       do 202 level=1,maxlevel
        hexpr(har)=hexpr(har)+pwrprb(level)*
     1                    harm(har,level)
        hvarr(har)=hvarr(har)+pwrprb(level)*
     1                    harm(har,level)**2
        hexpi(har)=hexpi(har)+pwrprb(level)*
     1                    harm(har+1,level)
        hvari(har)=hvari(har)+pwrprb(level)*
     1                    harm(har+1,level)**2
        cov(har) = cov(har) + pwrprb(level)*
     1              harm(har,level)*harm(har+1,level)
 202   continue
       hvarr(har)= hvarr(har) - hexpr(har)**2
       hvari(har)= hvari(har) - hexpi(har)**2
       cov(har) = cov(har) - hexpr(har)*hexpi(har)
       cov(har)  = cov(har)   * ncharge
       hvarr(har)= hvarr(har) * ncharge
       hvari(har)= hvari(har) * ncharge
```

```
     hexpr(har)= hexpr(har) * ncharge
     hexpi(har)= hexpi(har) * ncharge
     if ((hvarr(har).eq.0).or.(hvari(har).eq.0)) then
      write(18,*)'hvarr ',har,'time = ',time,'=',hvarr(har)
      write(18,*)'hvari ',har,'time = ',time,'=',hvari(har)
      write(18,*)'hexpr ',har,'time = ',time,'=',hexpr(har)
      write(18,*)'hexpi ',har,'time = ',time,'=',hexpi(har)
     else
      corr(har) = cov(har) /
    1          (sqrt(hvarr(har))*sqrt(hvari(har)))
     endif
 203  continue
 253 format(2(a19,i1),\)
 254 format(2(a18,i2),\)
1502 format(a19,i1,\)
1503 format(a18,i2,\)
1504 format(a5,a20,\)
 503 format(a1)
     cnt = 0

2500 do 1500 i=3,maxharm,2
     meanmag(i)=0
     varmag(i)=0
     a = hexpr(i)
     b = hexpi(i)
     c = hvarr(i)
     d = hvari(i)
     f = corr(i)
     if((a.eq.0).or.(b.eq.0).or.(c.eq.0).or.(d.eq.0).or.(abs(f).eq.1))
    1   then
      if ((hvarr(i).eq.0).or.(d.eq.0).or.(abs(f).eq.1)) then
       zmax(i)=0
       zmin(i)=0
       write(5,*)'zero variance - skipping - harmonic ',i
       goto 1140
      endif
      write(5,*)'alert divide by zero 1'
      write(18,*)'alert divide by zero 1'
     endif
     zg = 0.0
         zmin(i) = zfind(zg,maxprob,hvarr(i),hvari(i),
    1          hexpr(i),hexpi(i),corr(i))
     write(18,*)i,zmin(i)
     zmin(i) = max(zmin(i),0.0)
1130 zg = sqrt((a + a/abs(a)*2.5*sqrt(hvarr(i)))**2 +
    1      (b + b/abs(b)*2.5*sqrt(hvari(i)))**2)
     zmax(i) = zfind(zg,maxprob,hvarr(i),hvari(i),
    1          hexpr(i),hexpi(i),corr(i))
     write(18,*)i,zmax(i)
     if (zmax(i).lt.zmin(i)) then
      rdum = zmax(i)
      zmax(i) = zmin(i)
      zmin(i) = rdum
     endif
     zmin(i) = max(zmin(i),0.0)
         if ((i.eq.1).or.(i.eq.3)) then
```

```
        write(19,*)i,zmin(i),zmax(i)
        endif
1140  stepz(i) = (zmax(i)-zmin(i)) / 100
      zm(i)  = -stepz(i)
      if (stepz(i).ne.0) then
1111   format(a4,a15,2a12,7a15)
        do 270 j=1,100
        zm(i)=zm(i)+stepz(i)
        rdum=zprob(zm(i),hvarr(i),hvari(i),
   1         hexpr(i),hexpi(i),corr(i))
        rdum = rdum * stepz(i)
        meanmag(i)=meanmag(i)+rdum*zm(i)
        varmag(i) =varmag(i) + rdum*zm(i)**2
 111  format(i4,f15.5,2f12.9,4f15.10,3f15.5)
 270   continue
        varmag(i) = varmag(i) - meanmag(i)**2
      else
       meanmag(i)=0
       varmag(i)=0
      endif
1500 continue
1501 format(f20.5,\)
1505 format(i5,f20.5,\)
         write(10,255)time,pexp,pvar
      do 240 har=3,maxharm,2
       write(10,256)meanmag(har)/ncharge,varmag(har)/ncharge
 240  continue
      write(10,503)' '
 250 continue
 255 format(i5,2f20.5,\)
 256 format(2f20.5,\)
         write(5,*)'Evaluated - Time = ',time
 888 continue
write(18,*)'STARTPROB',strtprb
999 stop
     end
c***********************************************************************
     FUNCTION zprob(z,var1,var2,mean1,mean2,corr)

     REAL pi,std1,std2,B,C,step,th,rr,ri,eta,prob
     REAL mean1,mean2,var1,var2,corr,z,prev,now

     pi = 3.14159265359
     std1=sqrt(var1)
     std2=sqrt(var2)
     B = 1 / (std1 * std2 * 2 * pi * sqrt(1-corr**2) )
     C = - 1 / (2*(1-corr**2))
     step=2*pi/1000
         prob=0.0
     th=-step
     rr = z
     ri = 0.0
     eta = (rr - mean1)**2/var1 + (ri-mean2)**2/var2
     eta = eta - (2*corr*(rr-mean1)*(ri-mean2))/(std1*std2)
     prev = B * exp( C * eta)*z
     do 1 th=step,(2*pi),step
```

B-8

```
      rr = z * cos(th)
      ri = z * sin(th)
      eta = (rr - mean1)**2/var1 + (ri-mean2)**2/var2
      eta = eta - (2*corr*(rr-mean1)*(ri-mean2))/(std1*std2)
      now = B * exp( C * eta)*z
      prob= prob + (now + prev) / 2 * step
      prev= now
   1 continue
         zprob = prob
      END

c************************************************************************
      FUNCTION zfind(zg1,maxprob,var1,var2,exp1,exp2,corr)

      REAL zg1,zg2,z1,z2,bigstep,minstep,maxprob
      INTEGER done

      sigma = 1e-6
      minstep =0.001
      done = 0
510 if (done.lt.0.001) then
      z1 = zprob(zg1,var1,var2,exp1,exp2,corr)
      if ((z1-maxprob).lt.sigma) then
       done = 1
       goto 520
      endif
      zg2 = zg1 + minstep
      z2 = zprob(zg2,var1,var2,exp1,exp2,corr)
      if (z1.eq.z2) write(18,*)'alert divide by zero in zfind'
      bigstep = ((z1 - maxprob)*minstep) / (z1 - z2)
         zg1 = zg1 + bigstep
      endif
      goto 510
 520 zfind = zg1
         END

c************************************************************************
FUNCTION GAUSS(val,min,mean,var)

      REAL prob,mean,min,r,step,d,prev

      step = (val-min)/1000
      prob=0
      r = min
      prev =1/(2.50662827463*sqrt(var))*exp(-1*(r-mean)**2/(2*var))
      do 1 r=(min+step),val,step
       d=1/(2.50662827463*sqrt(var))*exp(-1*(r-mean)**2/(2*var))
       prob=prob + (d + prev) / 2 * step
       prev = d
   1 continue
      Gauss= prob
      END

c************************************************************************
FUNCTION CONFIDENCE(maxprob,mean,var)
```

```
    REAL prob,mean,min,var,r,step,d,prev,max,maxprob

   min = mean - 3*sqrt(var)
   max = mean + 3*sqrt(var)
   step = (max-min)/1000
   prob = 0
   r=min
   prev = 1/(2.50662827463*sqrt(var))*exp(-1*(r-mean)**2/(2*var))
   done = 0

 1 continue
   r=r+step
   d= 1/(2.50662827463*sqrt(var))*exp(-1*(r-mean)**2/(2*var))
   prob = prob + (d+prev)/2*step
   prev = d
   if (maxprob.le.prob) then
    done = 1
    confidence = r
   endif
   if (done.eq.0) goto 1
   END
```

# C
# APPENDIX C – FORTRAN IMPLEMENTATION OF MONTE CARLO METHOD FOR PREDICTING NET HARMONIC CURRENT STATISTICS

```
C*************************************************************************
C        PROGRAM CHARGEMC.FOR
C*************************************************************************
C        This program generates the statistics of harmonic current injection from a concentration C of EV battery
chargers.  It relies on Monte Carlo Trials.  Unlike the analytical method it also computes statistics on the current
THD and on the phase angle of each harmonic current.
C
C*************************************************************************


      real strtprb(150),enerprb(500),pwr(500),dummy
      real pexpect(150),pvar(150),hvar(26,150),hexpect(26,150)
      real ephase(26,150),vphase(26,150)
      real harm(26,100),curr(100),coefr(2),coefi(2),hcoeff(4)
      integer time,maxtime,maxlevel,maxstime,ncharge
      integer maxharm,probtan
      integer*2 is1,is2,is3,is4
      real eharmag(26,150)
      real vharmag(26,150)
      real comp(26,150)
      real fund(150)
      real pcomp(150),cthd(150),varthd(150),exthd(150)
      Real sumpwr, probm(3000), enerper(500), suminter
      Real searchm, prob, range, maxrange, m
      Real probmt(3000),meant,mean,meano,vart,var,sdt,sd,sdo
      Real w,x,y,z,ww,xx,yy,zz,ao,bo,at,bt,da,db,sum
      Real eps,delta,pi
      Logical done

      eps = 0.01
      delta = 0.01


      open(unit=1,file='inp.in',status='unknown')
      open(unit=2,file='instrt.in',status='unknown')
      open(unit=3,file='harmdat.in',status='unknown')
      open(unit=4,file='inpwr.in',status='unknown')
      open(unit=10,file='evar.out',status='unknown')
      open(unit=15,file='thd.out',status='unknown')
      open(unit=18,file='msg.out',status='unknown')
```

```
    pi = 3.141592654
    maxharm = 25

    probtan = 0

    write(5,*)'Input scale as percentage of normal (34.2m 21.1m)'
    write(5,*)'or if you wish to input from file inpwr.in input 0'
     read(5,*)scale

    if (scale.eq.0) then
     read(4,*)maxlevel
     do 1920 i=1,maxlevel
      read(4,*)dum, enerprb(i),pwr(i)
 1920  continue
    endif
    write(5,*)'enter the highest order harmonic.'
    read(5,*)maxharm
    read(1,*)maxlevel
    if (scale.ne.0) then
    sumpwr = 0.0
    do 10 i=1,maxlevel
     read(1,*)dum,pwr(i)
     sumpwr = sumpwr + pwr(i)
  10 continue
    endif
    write(5,*)'Input on-time as 5m steps (0 for 8hr default)'
    write(5,*)'or enter 999 to input from instrt.in'
    read(5,*)maxstime
    if (maxstime.lt.eps) maxstime=96
    time = maxlevel+1
    if (maxstime.ne.999) then
     do 1 i=1,maxstime
      strtprb(i) = real(1/real(maxstime))
   1  continue
    endif
    if (maxstime.eq.999) then
     read(2,*)maxstime
     do 2 i=1,maxstime
      read(2,*)dum,strtprb(i)
   2  continue
    endif
         do 1110 j=2,maxstime
    strtprb(j)=strtprb(j)+strtprb(j-1)
 1110 continue
         read(3,*)dum,order
    read(3,*) coefr(2),coefr(1)
    read(3,*)dum,order
    write(18,*)'fund real coeffs:',coefr(2),coefr(1)
    read(3,*)coefi(2),coefi(1)
    write(18,*)'fund imag coeffs:',coefi(2),coefi(1)
    do 29 j=1,maxlevel
     harm(1,j)= pwr(j)*coefr(2)+coefr(1)
     harm(2,j)= pwr(j)*coefi(2)+coefi(1)
     curr(j)  = sqrt(harm(1,j)**2+harm(2,j)**2)
  29 continue
         do 30 i=3,(maxharm+1)
```

```
      write(18,*)'harmonic',I
      read(3,*)dum,order
      write(18,*)'harmonic',dum,'order',order
      do 25 j=(order+1),1,-1
       read(3,*)hcoeff(j)
       write(18,*)'coeff ',j,hcoeff(j)
  25  continue
         do 26 j=1,maxlevel
      if (order.eq.1) then
       harm(i,j)=pwr(j)*hcoeff(2)+hcoeff(1)
      else if (order.eq.2) then
       harm(i,j)=pwr(j)**2*hcoeff(3) + pwr(j)*hcoeff(2) + hcoeff(1)
      else
       harm(i,j)=pwr(j)**3*hcoeff(4)+pwr(j)**2*hcoeff(3)
   1    +pwr(j)*hcoeff(2) + hcoeff(1)
      endif
      harm(i,j) = harm(i,j) / 100 * curr(j)
  26  continue
  30 continue
         write(15,298)'time','exthd','varthd'
 298 format(a5,2a20)
 299 format(i5,2f20.5)
      write(10,292)'time','epower','varpower'
 292 format(a5,a20,a20,\)
      do 293 k=1,maxharm,2
       if (k.lt.10) then
        write(10,294)'exmag',k,'varmag',k,'exphase',k,'vphase',k
       else
        write(10,1294)'exmag',k,'varmag',k,'exphase',k,'vphase',k
       endif
 293 continue
 294 format(4(a19,i1),\)
1294 format(4(a18,i2),\)
      write(10,775)' '
         if (scale.ne.0) then
      suminter=0.0
      do 1130 i=maxlevel,1,-1
       suminter=suminter+pwr(i)
       enerper(i)=1 - suminter/sumpwr
1130 continue
      range=75
      setmean=34.2
      setsd=21.1
      maxrange = 10.0*real(range-1.0)
      maxrange = maxrange + 1
      endif
         do 31 j=1,maxlevel
      pwr(j)=pwr(j)/1000
  31 continue
         write(5,*)'How many chargers?'
      read(5,*) ncharge
      write(5,*)'How many trials?'
      read(5,*)numtry
      scale = scale / 100
         if (scale.eq.0) goto 2223
         mean = setmean * scale
```

```
     sd   = setsd   * sqrt(scale)
     write(5,*)'processing scale = ',scale
         ao = 2
   bo = 1
         run = 0
 99 continue
   sum = 0.0
   do 100 i=1,1991
   m  = real(i-1)/10 + 1
   probm(i) = log(m)/(sqrt(2*pi)*bo)*
 1          exp(-1/(2*bo**2)*(log(m)-ao)**2)
   sum = sum + probm(i)
 100 continue
   meano = 0.0
   var  = 0.0
   do 101 i=1,1991
   m = real(i-1)/10 + 1
   probm(i) = probm(i)/sum
   meano = meano + m*probm(i)
   var  = var  + m*m*probm(i)
 101 continue
   var  = var - meano**2
   sdo  = sqrt(var)

         if ((abs(meano-mean).lt.eps ).and.( abs(sdo-sd).lt.eps )) goto 110
   if (run.gt.20) goto 110
         at = ao + delta
   bt = bo
   sum = 0.0
   do 103 i=1,1991
   m  = real(i-1)/10 + 1
   probmt(i) = log(m)/(sqrt(2*pi)*bt)*
 1          exp(-1/(2*bt**2)*(log(m)-at)**2)
   sum = sum + probmt(i)
 103 continue
   meant = 0.0
   vart  = 0.0
   do 104 i=1,1991
   m = real(i-1)/10 + 1
   probmt(i) = probmt(i)/sum
   meant = meant + probmt(i)*m
   vart  = vart + probmt(i)*m*m
 104 continue
   vart = vart - meant**2
   sdt  = sqrt(vart)
   w    = (meant - meano) / delta
   y    = (sdt -sdo) / delta
         at = ao
   bt = bo + delta
   sum=0.0
   do 105 i=1,1991
   m  = real(i-1)/10 + 1
   probmt(i) = log(m)/(sqrt(2*pi)*bt)*
 1          exp(-1/(2*bt**2)*(log(m)-at)**2)
   sum = sum + probmt(i)
 105 continue
```

C-4

```
    meant = 0.0
    vart  = 0.0
    do 106 i=1,1991
     m = real(i-1)/10 + 1
     probmt(i) = probmt(i)/sum
     meant = meant + probmt(i)*m
     vart  = vart + probmt(i)*m*m
106 continue
    vart = vart - meant**2
    sdt  = sqrt(vart)
    x    = (meant - meano) / delta
    z    = (sdt   - sdo) / delta
         ww = z/(w*z-x*y)
    zz = w/(w*z-x*y)
    xx = -x/(w*z-x*y)
    yy = -y/(w*z-x*y)
    run = run+1
         da = ww*(mean-meano) + xx*(sd - sdo)
    db = yy*(mean-meano) + zz*(sd - sdo)
    if (bo.lt.0.0) bo = 0.2
    if (da.gt.0.2) da = 0.2
    if (da.lt.-0.2)da =-0.2
    if (db.gt.0.2) db = 0.2
    if (db.lt.-0.2)db =-0.2
    ao = ao + da
    bo = bo + db
    goto 99
110 continue
    write(18,*)'*********** SOLUTION **********'
    write(18,*)'a = ',ao
    write(18,*)'b = ',bo
    write(18,*)'mean = ',meano
    write(18,*)'std dev = ',sdo
    sum=0.0
    do 1112 i=1,((range-1)*10+1)
     m  = real(i-1)/10 + 1
     sum = sum + probm(i)
1112 continue
    do 112 i=1,((range-1)*10+1)
     m  = real(i-1)/10 + 1
     probm(i) = probm(i)/sum
112 continue
         m=1.0
    do 40 i=maxlevel,1,-1
     prob = 0.0
     searchm = (1.0 - enerper(i)) * (range-1.0) + 1.0
     done = .false.
     do 50 While (.not.done)
     j=(m-1)*10+1
      if (m.gt.range) then
       done = .true.
      else if (m.le.searchm) then
       prob = prob+probm(j)
       m=m+0.1
      else
       done=.true.
```

```
        endif
  50  continue
     enerprb(i)=prob
  40 continue
    sum = 0.0
    do 60 i=1,maxlevel
    sum = sum + enerprb(i)
  60 continue
    write(18,*)'Probability Sum = ',sum
  70 format(i5,f10.1,f15.8)
2223 continue
    do 1100 j=2,maxlevel
     enerprb(j)=enerprb(j)+enerprb(j-1)
 1100 continue
        write(5,*)'Running Trials'
        snapct = 0
        call gettim(is1,is2,is3,is4)
    call seed(is4)
    pr1=10
    rd1 = real(numtry)
    icnt=0
        do 200 itry=1,numtry
    if (icnt.le.(itry*100/numtry)) then
     write(5,*)icnt,'%'
     icnt=icnt+10
     endif
    rd2 = real(itry)
    if (rd2/rd1.gt.pr1) then
     write(5,2000)pr1,'%'
     pr1=pr1+10
     endif
 2000 format(T1)
do 800 k=1,(maxstime+maxlevel)
     cthd(k) = 0.0
     pcomp(k)= 0.0
     do 810 i=1,(maxharm+1)
     comp(i,k)=0.0
  810   continue
  800   continue
    do 801 i=1,(maxstime+maxlevel)
    fund(i)=0.0
  801  continue
tround=0
    do 230 chrgnum=1,ncharge
    call random(st)
    do 201 j=1,maxstime
     if (strtprb(j).ge.st) then
      stime=j
      goto 202
     endif
  201   continue
  202   continue
    call random(st)
    do 203 j=1,maxlevel
     if (enerprb(j).ge.st) then
      stpower=j
```

C-6

```
          goto 204
          endif
 203   continue
 204   continue
      do 210 ipower=stpower,maxlevel
       itime=(ipower-stpower)+stime
             pexpect(itime)=pexpect(itime) + pwr(ipower)
       pcomp(itime)=pcomp(itime)+pwr(ipower)
       do 220 i=1,maxharm,2
        hexpect(i,itime)=  hexpect(i,itime) + harm(i,ipower)
        hexpect(i+1,itime)=hexpect(i+1,itime)+harm(i+1,ipower)
        comp(i,itime)=comp(i,itime)+harm(i,ipower)
        comp(i+1,itime)=comp(i+1,itime)+harm(i+1,ipower)
 220     continue
1210 format(12f15.5)
1211 format(12a15)
 210   continue
 230   continue
do 888 i=1,(maxstime+maxlevel)
      pvar(i)=pvar(i)+pcomp(i)**2
      j=1
      do 830 k=1,maxharm,2
      j=j+1
      dummy = sqrt(comp(k,i)**2+comp(k+1,i)**2)
      hvar(k,i)=hvar(k,i)+comp(k,i)**2
      hvar(k+1,i)=hvar(k+1,i)+comp(k+1,i)**2
      vharmag(k,i)=vharmag(k,i)+dummy**2
      eharmag(k,i)=eharmag(k,i)+dummy
      if (k.ne.1) cthd(i) = cthd(i) + dummy**2
      if ( (comp(k,i).ne.0.0).or.(comp(k+1,i).ne.0.0) ) then
       if ((i.eq.70).and.(k.eq.1)) probtan = probtan+1
       dummy=atan2(comp(k+1,i),comp(k,i))
       dummy=dummy*180/pi
       ephase(k,i)=ephase(k,i)+dummy
       vphase(k,i)=vphase(k,i)+dummy**2
      endif
 830   continue
      dummy = sqrt(comp(1,i)**2+comp(2,i)**2)
      if(dummy.ne.0.0) then
       exthd(i) = exthd(i) + sqrt(cthd(i))/dummy
       varthd(i)= varthd(i)+ cthd(i)/dummy**2
      endif
 888  continue
200 continue
          write(5,*)'Trials completed.  Evaluating'
4001 format(a5,8a20)
    do 889 itime=1,(maxstime+maxlevel)
     pexpect(itime)=pexpect(itime)/rd1
     pvar(itime)=pvar(itime)/rd1
     exthd(itime)=exthd(itime)/rd1*100
     varthd(itime)=varthd(itime)/rd1
     do 410 i=1,maxharm,2
      eharmag(i,itime)=eharmag(i,itime)/rd1
      vharmag(i,itime)=vharmag(i,itime)/rd1
      ephase(i,itime)=ephase(i,itime)/rd1
      vphase(i,itime)=vphase(i,itime)/rd1
```

```
      hexpect(i,itime)=hexpect(i,itime)/rd1
      hexpect(i+1,itime)=hexpect(i+1,itime)/rd1
      hvar(i+1,itime)=hvar(i+1,itime)/rd1
      hvar(i,itime)=hvar(i,itime)/rd1
 410  continue
 889 continue
4000 format(i5,8f20.5)
do 890 j=1,(maxstime+maxlevel)
        pvar(j)=pvar(j)-pexpect(j)**2
     varthd(j)=(varthd(j)-exthd(j)**2)*10000
     do 245 k=1,maxharm,2
      hvar(k,j)=hvar(k,j)-hexpect(k,j)**2
      hvar(k+1,j)=hvar(k+1,j)-hexpect(k+1,j)**2
      vharmag(k,j)=vharmag(k,j)-eharmag(k,j)**2
      vphase(k,j)=vphase(k,j)-ephase(k,j)**2
 245   continue
 890 continue
        write(5,*)'Outputting to EVAR.OUT'
    write(18,*)'Outputting the expectation and variance data'
        do 891 itime=1,(maxstime+maxlevel)
     write(15,299)itime,exthd(itime),varthd(itime)
     write(10,296)itime,pexpect(itime)/ncharge,pvar(itime)/ncharge
     do 295 k=1,maxharm,2
      write(10,291)eharmag(k,itime)/ncharge,vharmag(k,itime)/ncharge,
    1 ephase(k,itime),vphase(k,itime)
 295  continue
     write(10,775)' '
 891 continue
 296 format(i5,2f20.5,\)
 291 format(4f20.5,\)
 775 format(a1)
      stop
      end
```

# D
## APPENDIX D – FORTRAN IMPLEMENTATION OF METHOD FOR DERATING A SUBSTATION TRANSFORMER

```
C***********************************************************************
c PROGRAM HEAT.FOR
C***********************************************************************
C    This program will accept as input a 24 hour load curve,
C    and a fixed harmonic distorting load and compute the transformer
C    hot spot temperature over the period.  From this it computes the
C    aging acceleration factor and varies penetration of ev load
C    to maintain this constant.
C    It generates a series of EV penetration / derating curves for various peak non-EV loading

        Real dtTOR,dtHR,R,taur,rm,rn
    Real tH(4,500),dtTO,dtTOU,dTTOi,tau
    Real dtH,dtHU,dtHi,rK,tA(400)
    Real harm(15,200),harm1(15,200),Sbas(400),Srated,Sev(400)
    real pchg(400),pfchg,pfb(400)
    real rknh,rkh,rktot(400),sineb,sinec
    real resmult,preload,pbas
    real max,multi

    Character approx*1,chardum*1
    Logical finish

    open(unit=1,file='intrans.in',status='unknown')
    open(unit=2,file='basload.in',status='unknown')
    open(unit=3,file='input.out',status='unknown')
    open(unit=4,file='chgload.in',status='unknown')
    open(unit=9,file='resload.out',status='unknown')
    open(unit=7,file='penet.out',status='unknown')
    open(unit=8,file='totload.out',status='unknown')
    open(unit=14,file='chgload.out',status='unknown')
    open(unit=10,file='heat.out',status='unknown')
    open(unit=11,file='test.out',status='unknown')
    open(unit=13,file='k.out',status='unknown')
    open(unit=15,file='temp.in',status='unknown')
        open(unit=21,file='penet1.out',status='unknown')
    open(unit=22,file='penet2.out',status='unknown')
    open(unit=23,file='penet3.out',status='unknown')
    open(unit=24,file='penet4.out',status='unknown')
    open(unit=25,file='penet5.out',status='unknown')
    open(unit=26,file='penet6.out',status='unknown')
    open(unit=27,file='penet7.out',status='unknown')
    open(unit=28,file='penet8.out',status='unknown')
    open(unit=29,file='penet9.out',status='unknown')
```

```
        rmaxloss = 0.0133


            1 format(a1)
            read(4,*)numlevel
        read(4,*)num,maxharm,pfchg
        do 20 i=1,num
         read(4,6)idum,Pchg(i)
         write(14,2)i,Pchg(i)
         do 21 j=3,maxharm,2
          read(4,7)harm1(j,i)
          write(14,3)harm1(j,i)
          harm1(j,i)=harm1(j,i)/3
    21  continue
          write(14,1)' '
          read(4,1)chardum
    20 continue
     2 format(i3,f14.7,\)
     3 format(f16.7,\)
     6 format(i3,f14.7,\)
     7 format(f16.7,\)


            fin = 3
        end=24


        read(2,*)peakres
            do 10 i=1,(24*numlevel),numlevel
        read(2,*)idum,Pbas,pfb(i)
        read(15,*)idum,tA(i)
        tA(i) = 1.0/1.8*(ta(i)-32.0)
            Sbas(i) = Pbas/pfb(i)
    10 continue
        Sbas(24*numlevel+1)=Sbas(1)
        pfb(24*numlevel+1)=pfb(1)
        tA(24*numlevel+1)=tA(1)
        do 11 i=1,(24*numlevel),numlevel
         diffb = Sbas(i+numlevel) - Sbas(i)
         difpfb= pfb(i+numlevel)-pfb(i)
         difft = tA(i+numlevel)-tA(i)
         write(9,5)i,Sbas(i),pfb(i),ta(i)
         write(9,1)' '
         do 12 j=1,numlevel-1
          Sbas(i+j)=Sbas(i)+diffb*j/numlevel
          pfb(i+j)=pfb(i)+difpfb*j/numlevel
          tA(i+j)=tA(i)+difft*j/numlevel
          write(9,5)i+j,Sbas(i+j),pfb(i+j),tA(i+j)
          write(9,1)' '
    12  continue
    11 continue
     5 format(i6,3f10.4,\)

c    Data is set in 'intrans.in' as follows:
c    Pecr       Eddy current losses in %
c    dtTOR      Top oil rise over ambient at rated load.
c    dtHR       Hottest spot conductor rise over top-oil temp at rated load
c    R          Ratio of load loss at rated load to no load loss.
```

D-2

```
c    tauR    Oil Thermal time constant for rated load.
c    rN      exponent used to compute Top-oil temp rise.
c    rM      exponent used to compute variation of hot-spot temp. rise
c    tauw    exponent used to compute variation in winding hot spot..

     read(1,*)pecr
     write(3,*)'Pecr ',pecr
     read(1,*) dtTOR
     write(3,*) 'dtTOR',dtTOR
     read(1,*) dtHR
     write(3,*) 'dtHR',dtHR
     read(1,*) R
     write(3,*) 'R',R
     read(1,*) tauR
     write(3,*) 'tauR',tauR
     read(1,*) rN
     write(3,*) 'rN',rN
     read(1,*) rM
     write(3,*) 'rM',rM
     read(1,*) tauw
     write(3,*) 'tauw',tauw
         write(5,*)'Amount of residential load in %'
     read(5,*)resmult
     resmult = resmult/100
     write(5,*)'At what time index does EV charging begin?'
     read(5,*)evbegin
         loop=0
     rpenet =  0.0
         write(5,*)'Maximum designed load level in percent'
     read(5,*)rmaxld
     write(5,*)'Minimum designed load level in percent'
     read(5,*)rminld
     write(5,*)'Step between Min and Max Load Levels'
     read(5,*)rstepld
         ip = 20
     do 9987 rhitmax = rmaxld,rminld,-rstepld
         ip = ip + 1
     loop = 0
     rpenet = 0.0
     load = rhitmax + 1
     finish = .false.
     do 9876 while (.not.finish)
         load = load - 1.0
     write(5,*)'Computing for non-EV max load level in percent - ',load
     loop = loop+1
     preload = real(load)/100
     write(5,*)'Load level ',preload
     rmax = Sbas(1)
     do 14 i=1,(24*numlevel)
      if (Sbas(i).gt.rmax) rmax=Sbas(i)
  14 continue
     multi = preload / rmax
     do 15 i=1,(24*numlevel)
      Sbas(i) = Sbas(i) * multi
      write(8,*)i,Sbas(i),pfb(i)
  15 continue
```

```
      600 continue
   write(11,*)' '
   write(11,*)'New iteration'
   write(11,*)'Trying penetration ',rpenet
   write(5,*)'Trying penetration ',rpenet
      rmaxres = preload * resmult * rpenet
      do 50 i=1,num
  Sev(i) = (Pchg(i)/pfchg * rmaxres)/(peakres)
  do 51 j=3,maxharm,2
   harm(j,i) = harm1(j,i) * (0.240) / (peakres) * rmaxres
      51  continue
  50 continue
      do 120 i=1,(evbegin-1)
  rktot(i) = Sbas(i)
      120 continue
      sinec = sin(acos(pfchg))
  do 121 i=evbegin,(evbegin+num-1)
  j = i-evbegin + 1
  sineb = sin( acos(pfb(i)) )
  r1knh = (Sev(j)*pfchg + Sbas(i)*pfb(i))
  r2knh = (Sev(j)*sinec + Sbas(i)*sineb)
  rknh  = sqrt(r1knh**2+r2knh**2)
  pf1   = cos(atan(r2knh/r1knh))
  rms2  = (rknh/3)**2
  rms2w = rms2
  a260  = rms2
  do 122 k=3,maxharm,2
   rms2  = rms2 + harm(k,j)**2
   rms2w = rms2w+ harm(k,j)**2 * k**2
 122  continue
   rms2w = rms2w * pecr
   rkh = sqrt( (rms2 + rms2w)/((1+pecr)*a260) )
   rktot(i) = rkh * rknh
121 continue
      do 123 i=(evbegin+num-1),numlevel*end
  rktot(i) = Sbas(i)
      123 continue
      ibegin = numlevel*24
  iend   = numlevel*18
  rK = 0.0
  do 30 i=ibegin,iend,-1
  rK = rK + rktot(i)
 30 continue
  rK = rK / (ibegin-iend)
      dtTOi = dtTOR * ((rK**2*R+1)/(R+1))**rN

  dtHi = dtHR*rk**(2*rM)
      dtTOi = 0.0
  dtHi  = 0.0
      do 110 ipass = 1,fin
  do 100 i = 1, numlevel*end
  if ((ipass.ne.1).or.(i.ne.1)) then
  dtHi = dtH
  dtTOi = dtTO
  endif
```

D-4

```
   rK = rktot(i)

   dtTOU = dtTOR* ((rK**2*R+1)/(R+1))**rN
        if (dtTOU.ne.dtTOi) then
   tau = tauR*( (dtTOU - dtTOi)/dtTOR )
   tau = tau /( (dtTOU/dtTOR)**1/rN - (dtTOi/dtTOR)**1/rN )
   else
    tau = tauR
   endif
        dtTO = (dtTOU - dtTOi)*(1-exp(-1/(tau*real(numlevel))))+dtTOi
        dtHU = dtHR*rK**(2*rM)
        dtH  = (dtHU-dtHi)*(1-exp(-1/(tauw*real(numlevel))))+dtHi
        tH(ipass,i) = tA(i) + dtTO + dtH
100 continue
110 continue

        rnum = real(numlevel)
   Feqa = 0.0
   rdiv = 0.0
   do 500 i=1,numlevel*end
    Faa   = exp(15000/383 - 15000/(tH(3,i)+273))
    Feqa  = Feqa + Faa
500 continue
   Feqa = Feqa / real(numlevel*end)
        if (loop.eq.1) then
    if (load.lt.31) then
     finish = .true.
     goto 9876
    endif
    Feqstat=Feqa
    eps = Feqstat / 100
    write(11,*)'Feq static',feqstat
        write(7,*)preload*100,'   0.0'
    write(ip,*)preload*100,'   0.0'
    else if ((Feqa.lt.Feqstat+eps).and.(Feqa.gt.Feqstat-eps)) then
    pass = 0
    write(7,*)load,rpenet,feqa
    write(ip,*)load,rpenet,feqa
    else if ((Feqa.lt.Feqstat).and.(pass.lt.1)) then
     rpeneto= rpenet
     rpenet = rpenet + 0.02
     write(11,*)'Going to try ',rpenet
     write(11,*)'Feqa ',feqa
     if (rpenet.gt.1.0) then
     finish = .true.
      goto 9876
     else
      goto 600
     endif
    else if (Feqa.gt.Feqstat) then
     pass=1
     rpenet2= rpeneto
     rpeneto= rpenet
     rpenet = rpenet - abs((rpenet-rpenet2)/2)
     write(11,*)'Going to try ',rpenet
     write(11,*)'Feqa ',feqa
```

```fortran
      if (rpenet.gt.1.0) then
       finish = .true.
       goto 9876
      else
       goto 600
      endif
    else if ((Feqa.lt.Feqstat).and.(pass.ge.1)) then
      rpenet2= rpeneto
      rpeneto= rpenet
      rpenet = rpenet + abs((rpenet-rpenet2)/2)
      write(11,*)'Going to try ',rpenet
      write(11,*)'Feqa ',feqa
      if (rpenet.gt.1.0) then
       finish = .true.
       goto 9876
      else
       goto 600
      endif
    endif
9876 continue
9987 continue
9999 stop

      end
```

# E

## APPENDIX E – STATISTICS OF HARMONIC CURRENTS GENERATED BY A CONCENTRATION OF EV BATTERY CHARGERS

**Table E-1**
**Mean Values of Harmonic Current Components of EV Charger Concentration - A/Charger**

| 3 Re. | 3 Im. | 5 Re. | 5 Im. | 7 Re. | 7 Im. | 9 Re. |
|-------|-------|-------|-------|-------|-------|-------|
| 1.32 | -1.66 | -0.06 | -1.7 | 0.47 | -1.08 | 0.41 |

| 9 Im. | 11 Re. | 11 Im. | 13 Re. | 13 Im. | 15 Re. | 15 Im. |
|-------|--------|--------|--------|--------|--------|--------|
| -0.90 | 0.25 | -0.59 | 0.24 | -0.26 | 0.13 | -0.20 |

**Table E-2**
**Values of Covariances Between Harmonic Current Components of EV Charger Concentration - $A^2$/Charger**

| Curr. | 3 Real | 3 Imag. | 5 Real | 5 Imag. | 7 Real | 7 Imag. | 9 Real |
|-------|--------|---------|--------|---------|--------|---------|--------|
| 3 Re. | 2.94 | -3.53 | 0.04 | -3.78 | 1.01 | -2.42 | 0.87 |
| 3 Im. | -3.53 | 5.67 | 0.62 | 4.40 | -1.02 | 2.55 | -0.96 |
| 5 Re. | 0.04 | 0.62 | 0.36 | -0.10 | 0.07 | -0.17 | 0.02 |
| 5 Im. | -3.78 | 4.40 | 0.10 | 4.88 | -1.32 | 3.15 | -1.13 |
| 7 Re. | 1.01 | -1.02 | 0.07 | -1.32 | 0.39 | -0.89 | 0.32 |
| 7 Im. | -2.43 | 2.55 | -0.18 | 3.15 | -0.90 | 2.09 | -0.74 |
| 9 Re. | 0.87 | -0.96 | 0.02 | -1.13 | 0.32 | -0.74 | 0.27 |
| 9 Im. | -1.99 | 2.22 | -0.08 | 2.58 | -0.72 | 1.69 | -0.60 |
| 11 Re. | 0.51 | -0.54 | 0.01 | -0.68 | 0.20 | -0.45 | 0.17 |
| 11 Im. | -1.28 | 1.440 | -0.05 | 1.66 | -0.46 | 1.09 | -0.70 |
| 13 Re. | 0.482 | -0.57 | -0.02 | -0.63 | 0.18 | -0.41 | 0.16 |
| 13 Im. | -0.56 | 0.57 | -0.04 | 0.73 | -0.21 | 0.49 | -0.18 |
| 15 Re. | 0.25 | -0.36 | -0.02 | -0.36 | 0.09 | -0.22 | 0.09 |
| 15 Im. | -0.41 | 0.46 | -0.01 | 0.53 | -0.16 | 0.36 | -0.13 |

**Table E-2**
**Values of Covariances Between Harmonic Current Components of EV Charger**
**Concentration - A²/Charger (Continued)**

| Curr. | 9 Imag. | 11 Real | 11 Imag. | 13 Real | 13 Imag. | 15 Real | 15 Imag. |
|---|---|---|---|---|---|---|---|
| 3 Re. | 1.99 | 0.51 | -1.28 | 0.48 | -0.56 | 0.28 | -0.41 |
| 3 Im. | 2.22 | -0.54 | 1.40 | -0.57 | 0.57 | -0.36 | 0.46 |
| 5 Re. | -0.08 | 0.01 | -0.05 | -0.02 | -0.04 | -0.02 | -0.01 |
| 5 Im. | 2.58 | -0.68 | 1.66 | -0.63 | 0.74 | -0.36 | 0.54 |
| 7 Re. | -0.72 | 0.20 | -0.17 | 0.18 | -0.21 | 0.09 | -0.16 |
| 7 Im. | 1.70 | -0.15 | 1.09 | -0.41 | 0.49 | -0.22 | 0.36 |
| 9 Re. | -0.61 | 0.17 | -0.40 | 0-16 | -0.18 | 0.08 | -0.13 |
| 9 Im. | 1.37 | -0.37 | 0.89 | -0.34 | 0.40 | -0.19 | 0.29 |
| 11 Re. | -0.37 | 0.11 | -0.24 | 0.10 | -0.11 | 0.05 | -0.08 |
| 11 Im. | 0.89 | -0.24 | 0.57 | -0.22 | 0.56 | -0.12 | 0.19 |
| 13 Re. | -0.34 | 0.10 | -0.22 | 0.10 | -0.10 | 0.05 | -0.08 |
| 13 Im. | 0.39 | -0.11 | 0.26 | -0.10 | 0.12 | -0.05 | 0.08 |
| 15 Re. | -0.19 | 0.05 | -0.12 | 0.05 | -0.05 | 0.03 | -0.04 |
| 15 Im. | 0.30 | -0.08 | 0.19 | -0.78 | 0.09 | -0.04 | 0.06 |

# F
## APPENDIX F – FORTRAN IMPLEMENTATION OF A METHOD TO COMPUTE STATISTICS OF NETWORK HARMONIC VOLTAGES - I

```
C***********************************************************************
c    PROGRAM VOLTAGE STATISTICS 1
C***********************************************************************
c
c    This computes the means, variances and covariances(between real and imaginary
c    of all harmonics) of voltage at every bus.

        Outputs are of a form to be read by the program Voltage Statistics 2.
c***********************************************************************
      real evmean(16),evvar(16),evcov(16,16),evmag(16),evang(16)
      real vmag(500),vangle(500),pumagi(500),pureali(500)
      real puimagi(500),rcovm(500,14,14)
      real amean(500,14),avar(500,14),acov(500,14)
      real csvlt,snvlt,scale(500)
      real voltm(500,16),voltvr(500),voltvi(500),voltcv(500)
      real zmat(14,500,500)
      real vcovm(500,14,14)
      integer iusebus(500),imaxhrm,intbus(10000)
      character first
      Logical done

      open(unit=1,file='vsoln',status='unknown')
      open(unit=2,file='evar',status='unknown')
      open(unit=3,file='echo.out',status='unknown')
      open(unit=4,file='vector.out',status='unknown')
      open(unit=7,file='voltstat.out',status='unknown')
      open(unit=8,file='zbus.out',status='unknown')
      open(unit=9,file='cov.out',status='unknown')
          open(unit=15,file='covmat.out',status='unknown')
      open(unit=16,file='meanmat.out',status='unknown')

      degtorad = 0.01745329252
      radtodeg = 57.2957795132
      pi = 4*datan(1.0)
  5 format(a1)
      ievmxhm = 15
      iminhrm = 3
      imaxhrm = 15
          write(3,*)'Maximum harmonic of interest',imaxhrm
      write(3,*)' '
      write(3,*)'EV info'
```

```fortran
      write(3,8)'Harmonic order', 'Mean (A)', 'Variance (A^2)',
     1       'Covariance (A^2)','Mag (A)','Angle (A)'
      do 10 i=3,ievmxhm,2
       read(2,*)idum,evmean(i),evvar(i),evcov(i,i+1)
       read(2,*)idum,evmean(i+1),evvar(i+1)
       evmag(i)=sqrt(evmean(i)**2+evmean(i+1)**2)
       evang(i)=atan2(evmean(i+1),evmean(i))
       write(3,9)i, evmean(i),evvar(i),evcov(i,i+1)
       write(3,9)i+1,evmean(i+1),evvar(i+1)
   10 continue
    8 format(a16,a10,a16,a18,a8,a11)
    9 format(i16,f10.4,f16.4,f18.4,f8.4,f11.4)
      do 12 i=3,ievmxhm+1
       do 11 j=3,ievmxhm+1
        read(2,13)evcov(i,j)
        write(3,13)evcov(i,j)
   11  continue
       read(2,5)first
       write(3,5)' '
   12 continue
   13 format(f12.5,\)
   18 format(2a10,4a12)
      done = .false.
      inumbus = 0
      write(3,*)' '
      write(3,*)' '
      write(3,*)'Fundamental Voltage and Current Information'
      write(3,18)'Int bus','User bus','Vmag','Vangle','Imag','Iangle'
      do 19 i=1,4
       read(1,5)first
   19 continue
      do 20 while (.not.(done))
       read(1,21)i
       if (i.gt.1) then
        done =.true.
        backspace(unit=1)
       else
        inumbus=inumbus+1
        read(1,22)iusebus(inumbus)
        intbus(iusebus(inumbus))=inumbus
        read(1,*)vmag(inumbus),vangle(inumbus),
     1        pumagi(inumbus),rdum
        write(3,23)inumbus,iusebus(inumbus),vmag(inumbus),
     1          vangle(inumbus),pumagi(inumbus),rdum
        vangle(inumbus)=degtorad*vangle(inumbus)
       endif
   20 continue
   21 format(i6,\)
   22 format(i6,\)
   23 format(2i10,4f12.5)

c**************************************************************************
c*    START THE BIG LOOP THAT WILL DETERMINE THE VOLTAGE STATISTICS      *
c**************************************************************************
      write(3,5)' '
      write(3,5)' '
```

```
      write(3,*)'Harmonic Voltage and Current Information from Vsoln'
      write(3,5)' '
      write(3,30)'Harmonic','Intbus','Usr Bus','Vmag','Vang',
     1       'Cur mag','Cur ang'
30 format(3a10,4a12)
31 format(3i10,4f12.5)
      write(5,*)'Computing currents'

      do 1000 iharm=iminhrm,imaxhrm,2
      write(5,*)'Harmonic = ',iharm
       ih = iharm - 2
       csev = cos(evang(iharm))
       snev = sin(evang(iharm))
           write(4,41)'Harm.','Bus','MeanR','MeanI','VarR','VarI','Cov',
     1       'Angle'
       do 40 j=1,inumbus
        read(1,*)i,k,rdum1,rdum2,pumagi(j),rdum3
        write(3,31)i,j,iusebus(j),rdum1,rdum2,pumagi(j),rdum3
        pureali(j) = - pumagi(j)*csev
        puimagi(j) = - pumagi(j)*snev
        angvolt = iharm*vangle(j)
        csvlt    = cos(angvolt)
        snvlt    = sin(angvolt)
        scale(j)    = pumagi(j)**2 / evmag(iharm)**2
        rvarr    = evvar(iharm)*scale(j)
        rvari    = evvar(iharm+1)*scale(j)
        rcov     = evcov(iharm,iharm+1)+evmean(iharm)*evmean(iharm+1)
        rcov     = rcov*scale(j)-pureali(j)*puimagi(j)
           amean(j,ih) = csvlt*pureali(j) - snvlt*puimagi(j)
        amean(j,ih+1) = csvlt*puimagi(j) + snvlt*pureali(j)
        avar(j,ih)= csvlt**2*rvarr + snvlt**2*rvari - 2*csvlt*snvlt*rcov
        avar(j,ih+1)=csvlt**2*rvari+ snvlt**2*rvarr + 2*csvlt*snvlt*rcov
        acov(j,ih)= (csvlt**2-snvlt**2)*rcov + csvlt*snvlt*(rvarr-rvari)
           if (amean(j,ih).ne.0.0) then
        write(4,42)iharm,j,amean(j,ih),amean(j,ih+1),avar(j,ih)
     1      ,avar(j,ih+1),acov(j,ih),atan2(amean(j,ih+1),amean(j,ih))
        else
        write(4,42)iharm,j,amean(j,ih),amean(j,ih+1),avar(j,ih),
     1  avar(j,ih+1),acov(j,ih),angvolt
        endif
           do 33 k=3,imaxhrm,2
         ik = k - 2
         snvlt2=sin(k*vangle(j))
         csvlt2=cos(k*vangle(j))
           rcovm(j,ih,ik) = csvlt*csvlt2*evcov(iharm,k) - csvlt*snvlt2
     1 *evcov(iharm,k+1) - snvlt*csvlt2*evcov(iharm+1,k) + snvlt*
     2 snvlt2*evcov(iharm+1,k+1)
           rcovm(j,ih,ik+1) = csvlt*csvlt2*evcov(iharm,k+1) + csvlt*
     1 snvlt2*evcov(iharm,k) - snvlt*csvlt2*evcov(iharm+1,k+1) -
     2 snvlt*snvlt2*evcov(iharm+1,k)

         rcovm(j,ih+1,ik) = csvlt*csvlt2*evcov(iharm+1,k) - csvlt*
     1 snvlt2*evcov(iharm+1,k+1) + snvlt*csvlt2*evcov(iharm,k) -
     2 snvlt*snvlt2*evcov(iharm,k+1)

         rcovm(j,ih+1,ik+1) = csvlt*csvlt2*evcov(iharm+1,k+1) + csvlt
```

```
    1    *snvlt2*evcov(iharm+1,k) + snvlt*csvlt2*evcov(iharm,k+1) +
    2    snvlt*snvlt2*evcov(iharm,k)

      rcovm(j,ih,ik)   = rcovm(j,ih,ik)    * scale(j)
      rcovm(j,ih,ik+1) = rcovm(j,ih,ik+1)  * scale(j)
      rcovm(j,ih+1,ik) = rcovm(j,ih+1,ik)  * scale(j)
      rcovm(j,ih+1,ik+1)= rcovm(j,ih+1,ik+1)* scale(j)
   33  continue
   40  continue
   41  format(a7,a5,6a10)
   42  format(i7,i5,5f10.5,f10.2)


c************************************************************************
c    COMPUTE THE VOLTAGE STATISTICS BY MULTIPLYING THE Z-MATRIX
c    VECTOR BY THE CURRENT VECTOR
c************************************************************************
        write(7,62)'Harm.','Bus','Mag','MeanR','VarR','MeanI','VarI','Cov'
        write(5,*)'Reading Zmatrix information'
    if (iharm.eq.3) then
     open(unit=6,file='zbus.3',status='unknown')
    else if (iharm.eq.5) then
     open(unit=6,file='zbus.5',status='unknown')
    else if (iharm.eq.7) then
     open(unit=6,file='zbus.7',status='unknown')
    else if (iharm.eq.9) then
     open(unit=6,file='zbus.9',status='unknown')
    else if (iharm.eq.11) then
     open(unit=6,file='zbus.11',status='unknown')
    else if (iharm.eq.13) then
     open(unit=6,file='zbus.13',status='unknown')
    else
     open(unit=6,file='zbus.15',status='unknown')
    endif
    do 4 i=1,5
     read(6,5)first
   4 continue
        do 51 i=1,inumbus
    do 50 j=1,inumbus
     read(6,*)rdum,ir,ic,zmag,zphase
     zmag = zmag / 100
     zphase = zphase * degtorad
     zmat(ih,intbus(ir),intbus(ic)) = zmag*cos(zphase)
     zmat(ih+1,intbus(ir),intbus(ic)) = zmag*sin(zphase)
   50  continue
   51  continue
    close(unit=6)

    do 70 i=1,inumbus
     voltm(i,ih) = 0.0
     voltm(i,ih+1)=0.0
     voltvr(i) = 0.0
     voltvi(i) = 0.0
     voltcv(i) = 0.0
     do 60 j=1,inumbus
      voltm(i,ih) = voltm(i,ih)+ zmat(ih,i,j)*amean(j,ih)
    1          - zmat(ih+1,i,j) * amean(j,ih+1)
```

```
      voltvr(i) = voltvr(i) + zmat(ih,i,j)**2*avar(j,ih)
     1      +zmat(ih+1,i,j)**2*avar(j,ih+1) - 2*zmat(ih,i,j)
     2      *zmat(ih+1,i,j)*acov(j,ih)

      voltm(i,ih+1)=voltm(i,ih+1)+ zmat(ih,i,j)*amean(j,ih+1) +
     1        zmat(ih+1,i,j)*amean(j,ih)

      voltvi(i) = voltvi(i) + zmat(ih,i,j)**2*avar(j,ih+1)
     1      +zmat(ih+1,i,j)**2*avar(j,ih) + 2*zmat(ih,i,j)
     2      *zmat(ih+1,i,j)*acov(j,ih)

      voltcv(i) = voltcv(i) + (zmat(ih,i,j)**2-zmat(ih+1,i,j)**2)
     1        *acov(j,ih) + zmat(ih,i,j)*zmat(ih+1,i,j)
     2        *(avar(j,ih)-avar(j,ih+1))

  60  continue
        if (i.eq.5) then
      write(9,*)iharm,voltvr(i),voltvi(i),voltcv(i)
       endif
          write(7,61)iharm,i,sqrt(voltm(i,ih)**2+voltm(i,ih+1)**2),
     1  voltm(i,ih),voltvr(i),voltm(i,ih+1),voltvi(i),voltcv(i)
  61 format(i7,i5,6f12.5)
  62 format(a7,a5,a10,5a12)
  63 format(4f10.5)
  70 continue
1000 continue
          write(5,*)'Computing Covariance matrix.'
    do 140 ibus = 1,inumbus
     do 130 iharm1=3,imaxhrm,2
      ih1 = iharm1-2
      do 120 iharm2=3,imaxhrm,2
       ih2 = iharm2 - 2
       do 110 j=1,inumbus
       ra = zmat(ih1,ibus,j)
       rb = zmat(ih1+1,ibus,j)
       rc = zmat(ih2,ibus,j)
       rd = zmat(ih2+1,ibus,j)
       vcovm(ibus,ih1,ih2) = vcovm(ibus,ih1,ih2)
     1      + ra*rc*rcovm(j,ih1,ih2) - ra*rd*rcovm(j,ih1,ih2+1)
     2      - rb*rc*rcovm(j,ih1+1,ih2) + rb*rd*rcovm(j,ih1+1,ih2+1)

       vcovm(ibus,ih1+1,ih2+1) = vcovm(ibus,ih1+1,ih2+1)
     1      + ra*rc*rcovm(j,ih1+1,ih2+1) + rb*rc*rcovm(j,ih1,ih2+1)
     2      + ra*rd*rcovm(j,ih1+1,ih2) + rb*rd*rcovm(j,ih1,ih2)

       vcovm(ibus,ih1+1,ih2) = vcovm(ibus,ih1+1,ih2)
     1      + ra*rc*rcovm(j,ih1+1,ih2) - ra*rd*rcovm(j,ih1+1,ih2+1)
     2      + rb*rc*rcovm(j,ih1,ih2) - rb*rd*rcovm(j,ih1,ih2+1)

       vcovm(ibus,ih1,ih2+1) = vcovm(ibus,ih1,ih2+1)
     1      + ra*rc*rcovm(j,ih1,ih2+1) + ra*rd*rcovm(j,ih1,ih2)
     2      - rb*rc*rcovm(j,ih1+1,ih2+1) - rb*rd*rcovm(j,ih1+1,ih2)

 110    continue
 120    continue
```

```
 130  continue
 140 continue
         do 150 j=3,imaxhrm,2
    ij = j - 2
    write(9,*)vcovm(5,ij,ij),vcovm(5,ij+1,ij+1),vcovm(5,ij,ij+1)
 150 continue
         write(15,*)inumbus
   write(15,*)imaxhrm
   do 500 i=1,inumbus
    do 510 j=1,imaxhrm-1
     do 520 k=1,imaxhrm-1
      write(15,522)vcovm(i,j,k)
 520   continue
     write(15,523)' '
 510  continue
 500 continue
 522 format(f20.10,\)
 523 format(a1)
         do 550 i=1,inumbus
    do 560 j=1,imaxhrm-1
     write(16,*)voltm(i,j)
 560  continue
 550 continue
         stop
   end
```

# G
## APPENDIX G – FORTRAN IMPLEMENTATION OF A METHOD TO COMPUTE STATISTICS OF NETWORK HARMONIC VOLTAGES - II

```
C******************************************************************************
C PROGRAM VOLTAGE STATISTICS 2
C******************************************************************************
c THIS PROGRAM WILL COMPUTE THE PROBABILITIES OF SUM
C SQUARED VOLTAGES AT PARTICULAR BUSES USING A MONTE CARLO
C EVALUATION OF THE VOLTAGE STATISTICS.  IT REQUIRES THE VOLTAGE
C STATISTICS CONTAINED IN COVMAT.OUT AND MEANMAT.OUT THAT ARE
C GENERATED BY THE PROGRAM IN APPENDIX F
C******************************************************************************

C Outputs of interest are found in '519.out'.  This file contains one line
C        fraction of buses with THD of voltage below 5% with confidence 10%,
C        fraction of load with THD of voltage below 5% with confidence 10%,
C        ' of buses ' ' with confidence 50%,
C        ' of load ' ' with confidence 50%,
C        ' of buses ' ' with confidence 90%,
C        ' of load ' ' with confidence 90%,


C******************************************************************************

      character first
      real voltm(500,16),num(3),numl(3)
      real vcovm(500,14,14),max(3),rload(500),HITW(3,500),hit(3,500)
      integer ispace,hits(500,500)
      REAL*8 mat(14,14),cmat(14,14),pi,N01(14),Norm(14),rstep,SSV
      REAL*8 sum,step(500),val(500,3),rs(3)
          Logical done

          open(unit=1,file='vsoln.out',status='unknown')
      open(unit=2,file='covtest',status='unknown')
      open(unit=15,file='covmat.out',status='unknown')
      open(unit=16,file='meanmat.out',status='unknown')
      open(unit=17,file='thd.out',status='unknown')
      open(unit=20,file='test.out',status='unknown')
      open(unit=21,file='ten.out',status='unknown')
      open(unit=22,file='fifty.out',status='unknown')
      open(unit=23,file='ninety.out',status='unknown')
      open(unit=24,file='519.out',access='append',status='unknown')

      degtorad = 0.01745329252
      radtodeg = 57.2957795132
      pi = 4*datan(1.0)
```

```
   eps = 0.000001
   read(15,*)inumbus
    read(15,*)imaxhrm
    do 500 i=1,inumbus
     do 510 j=1,imaxhrm-1
      do 520 k=1,imaxhrm-1
       read(15,522)vcovm(i,j,k)
 520   continue
      read(15,523)first
 510  continue
 500 continue
 522 format(f20.10,\)
 523 format(a1)
    do 524 j=1,inumbus
     write(2,*)j,vcovm(j,1,1)
 524 continue
         do 501 i=1,4
    read(1,2)first
 501 continue
    do 502 i=1,inumbus
     read(1,*)dum1,dum2,dum3,dum4,rload(i)
 502 continue
  2 format(a1)
        skip = 0
    do 550 i=1,inumbus
     flag = 0
     do 560 j=1,imaxhrm-1
      read(16,*)voltm(i,j)
      if (abs(voltm(i,j)).lt.eps) flag = 1
 560  continue
     if (flag.eq.1) skip = skip + 1
 550 continue
    inumbus = inumbus - skip
    write(5,*)inumbus

    n = 14
    itrials = 5
         write(5,*)inumbus
         iminhrm = 3
         imxh=15
    imxh=imxh-1

C***********************************************************************
c    COMPUTE THE PROBABILITY THAT AT A SPECIFIC BUS THE SUM SQUARED
C    DISTORTION IS BELOW A SPECIFIC LEVEL RA.
C***********************************************************************
         ii = 16
    rtry = real(itrials*100.0)
    call gettim(ihr,imin,isec,ihnd)
    do 5000 ibus = 1,inumbus
     write(5,*)'Evaluating bus ',ibus
         call seed(-1)
     ii = ii + 1
         do 210 j=1,n
      do 200 k=1,n
       mat(j,k) = vcovm(ibus,j,k)
```

```
 200  continue
 210  continue
      call cholesk(n,mat,cmat)
      SSV = 0.0
      do 211 j=(iminhrm-2),imxh
       SSV = SSV + voltm(ibus,j)**2
 211  continue
      SSV = sqrt(SSV)
      if (SSV.lt.eps) write(5,*)'ERROR IMMINENT - MEAN SSV = 0.0'
      rstep = SSV/250
      do 212 j=1,500
       HITS(ibus,j) = 0
 212  continue

         do 300 inumber=1,itrials
      do 310 in = 1,100
c    generate a set of N(0,1) random numbers
      do 220 j=1,n
       N01(j) = RANDN()
 220  continue
      SSV = 0.0
c    multiply by the varied covariance matrix
      do 230 j=1,n
       sum = 0.0
       do 240 k=1,j
        sum = sum + cmat(j,k)*N01(k)
 240   continue
       NORM(j)=sum + voltm(ibus,j)
 230  continue
      do 231 j=(iminhrm-2),imxh
       SSV = SSV + NORM(j)**2
 231  continue
         SSV = Sqrt(SSV)
      ispace = SSV / rstep
      ispace = ispace + 1
      if (ispace.gt.500) ispace = 500
      HITS(ibus,ispace) = HITS(ibus,ispace) + 1
 310  continue
 300  continue
         step(ibus)=rstep
         do 2000 j = 2,500
      hits(ibus,j) = hits(ibus,j)+hits(ibus,j-1)
      if(ibus.eq.5) write(20,*)rstep*real(j),hits(ibus,j)
2000  continue
5000 continue
      write(5,*)'DONE WITH TRIALS.  -  EVALUATING RESULTS'
         tenp    = rtry*(0.10)
      fiftyp  = rtry*(0.50)
      ninetyp = rtry*(0.90)
      write(5,*)tenp,fiftyp,ninetyp
      do 2100 ibus=1,inumbus
      write(5,*)'ibus = ',ibus
       done = .false.
       j=1
       do 2200 while (.not.done)
       j = j+1
```

```
      if (hits(ibus,j).lt.tenp) then
       val(ibus,1)=j
      else if (hits(ibus,j).lt.fiftyp) then
       val(ibus,2)=j
      else if (hits(ibus,j).lt.ninetyp) then
       val(ibus,3)=j
      else
       done = .true.
      endif
2200 continue
2100 continue
          do 2300 ibus=1,inumbus
     do 2301 i = 1,3
      val(ibus,i) = val(ibus,i)*step(ibus)
      if (val(ibus,i).le.(5.0)) then
       num(i) = num(i) + 1
       numl(i) = numl(i) +rload(ibus)
      endif
2301  continue
2300 continue

          max(1) = val(1,1)
     max(2) = val(1,2)
     max(3) = val(1,3)
     do 2310 ibus=2,inumbus
      do 2311 i = 1,3
       if (val(ibus,i).gt.max(i)) max(i) = val(ibus,i)
2311  continue
2310 continue
          do i=1,3
     rs(i) = max(i) / 500
     if (abs(rs(i)).lt.eps) write(5,*)'ERROR IMMINENT - MAX=0 LINE224'
     end do

          totload = 0.0
     do 2320 ibus=1,inumbus
      totload = totload + rload(ibus)
      do 2321 i=1,3
       idum = int(val(ibus,i) / rs(i))
       hit(i,idum) = hit(i,idum)+1
       hitw(i,idum)= hitw(i,idum)+rload(ibus)
2321 continue
2320 continue

     if (totload.lt.eps) write(5,*)'ERROR IMMINENT-TOTLOAD=0 LINE238'
     do 2400 i=1,3
      do 2401 j=1,500
       hitw(i,j) = hitw(i,j) / totload
       hit(i,j) = hit(i,j) / real(inumbus)
2401 continue
2400 continue
          do 2331 i=1,3
     iwr = 20+i
     do 2330 idum=2,500
      hit(i,idum)=hit(i,idum)+hit(i,idum-1)
      hitw(i,idum)=hitw(i,idum)+hitw(i,idum-1)
```

G-4

```
      write(iwr,*)real(idum*rs(i)),hit(i,idum),hitw(i,idum)
2330  continue
2331  continue
         num(1)=num(1)/real(inumbus)
   num(2)=num(2)/real(inumbus)
   num(3)=num(3)/real(inumbus)
   numl(1)=numl(1)/totload
   numl(2)=numl(2)/totload
   numl(3)=numl(3)/totload
   write(5,*)'The percentages of buses and load'
   write(5,*)'that meet 519 with probability at least'
   write(5,*)'90% ',num(1)
   write(5,*)'50% ',num(2)
   write(5,*)'10% ',num(3)
   write(24,981)num(1),numl(1),num(2),numl(2),num(3),numl(3)
 981 format(6f10.5)
9999 continue
         call gettim(i2hr,i2min,i2sec,i2hnd)
   i2hr  = i2hr*60*60 + i2min * 60 + i2sec
   ihr = ihr*60*60 +imin*60 +isec
   i2hr  = i2hr - ihr
   write(5,*)'the evaluation took ',i2hr,' seconds'
   stop
   end


c(*****************************************************************)

   SUBROUTINE Cholesk(i,m,cm)

   real*8 m(14,14),cm(14,14)
   integer i

   integer j,k,im,ip
   real sum

   eps = 0.0000001
   cm(1,1) = sqrt(m(1,1))
   do 110 j=1,i
    sum = 0.0
    do 80 ip=1,j-1
     sum = sum + cm(j,ip)**2
  80  continue
    cm(j,j) = m(j,j) - sum
    if (cm(j,j).lt.0.0) then
     cm(j,j) = 0.0
     goto 110
    else
     cm(j,j) = sqrt(cm(j,j))
    endif
    if ( cm(j,j).lt.eps) then
     write(5,*)'CHOLESK DIVIDE BY ZERO'
     goto 110
    endif
        do 100 k = j+1,i
        sum = 0.0
    do 90 im = 1,j-1
```

```
         sum = sum + cm(j,im)*cm(k,im)
  90  continue
          cm(k,j) = ( m(j,k) - sum ) / cm(j,j)
 100  continue
 110 continue

    return
    end


c(*************************************************************************)


    FUNCTION RANDN()
C  The function RANDN() returns a normally distributed pseudo-random
C  number with zero mean and unit variance.  Calls are made to a
C  function subprogram RANDU() which must return independent random
C  numbers uniform in the interval (0,1).
C
C  The algorithm uses the ratio of uniforms method of A.J. Kinderman
C  and J.F. Monahan augmented with quadratic bounding curves.
C
    DATA S,T,A,B / 0.449871, -0.386595, 0.19600, 0.25472/
    DATA R1,R2/ 0.27597, 0.27846/
C
C  Generate P = (u,v) uniform in rectangle enclosing acceptance region
 50     continue
    Call RANDOM(U)
    if (u.eq.0.0) write(5,*)'Generated uniform random number of 0.0'
    Call RANDOM(V)
    V = 1.7156 * (V - 0.5)
C  Evaluate the quadratic form
    X  = U - S
    Y  = ABS(V) - T
    Q  = X**2 + Y*(A*Y - B*X)
C  Accept P if inside inner ellipse
    IF (Q .LT. R1) GOTO 100
C  Reject P if outside outer ellipse
    IF (Q .GT. R2) GOTO 50
C  Reject P if outside acceptance region
    IF (V**2 .GT. -4.0*ALOG(U)*U**2) GOTO 50
C  Return ratio of P's coordinates as the normal deviate
 100    RANDN = V/U
    RETURN
    END
```

# *H*
# APPENDIX H – BUS AND LINE DATA FOR POWER DISTRIBUTION NETWORK I

**Table H-1**
**Bus Data for Power Distribution Network I**

| Bus Number | Bus Type | P Load (%) | Q Load (%) | Bus Voltage (%) | Shunt Load (%) |
|---|---|---|---|---|---|
| 1001 | 3 | 0.00 | 0.00 | 0 | 0.00 |
| 1002 | 3 | 0.00 | 0.00 | 0 | 0.00 |
| 1003 | 3 | 0.00 | 0.00 | 0 | 0.00 |
| 1004 | 3 | 0.00 | 0.00 | 0 | 0.00 |
| 1005 | 1 | | | 105 | |
| 1 | 3 | 0.00 | 0.00 | | 0.00 |
| 2 | 3 | 0.00 | 0.00 | | 0.00 |
| 3 | 3 | 2.34 | 1.45 | | 0.00 |
| 4 | 3 | 0.85 | 0.53 | | 0.00 |
| 5 | 3 | 1.49 | 0.92 | | 0.00 |
| 6 | 3 | 1.28 | 0.79 | | 0.00 |
| 7 | 3 | 1.28 | 0.79 | | 0.00 |
| 8 | 3 | 0.00 | 0.00 | | 0.00 |
| 9 | 3 | 0.00 | 0.00 | | 0.00 |
| 10 | 3 | 2.13 | 1.32 | | -6.00 |
| 11 | 3 | 2.13 | 1.32 | | 0.00 |
| 12 | 3 | 0.00 | 0.00 | | 0.00 |
| 13 | 3 | 0.43 | 0.26 | | -6.00 |
| 14 | 3 | 3.40 | 2.11 | | 0.00 |
| 15 | 3 | 1.83 | 1.13 | | 0.00 |
| 16 | 3 | 2.34 | 1.45 | | 0.00 |
| 17 | 3 | 0.72 | 0.45 | | 0.00 |
| 18 | 3 | 0.21 | 0.13 | | 0.00 |
| 19 | 3 | 2.98 | 1.84 | | -6.00 |
| 20 | 3 | 0.00 | 0.00 | | 0.00 |
| 21 | 3 | 0.00 | 0.00 | | 0.00 |
| 22 | 3 | 0.00 | 0.00 | | 0.00 |
| 23 | 3 | 0.43 | 0.26 | | 0.00 |
| 24 | 3 | 1.28 | 0.79 | | -9.00 |
| 25 | 3 | 0.85 | 0.53 | | 0.00 |

**Table H-1**
**Bus Data for Power Distribution Network I (Continued)**

| Bus Number | Bus Type | P Load (%) | Q Load (%) | Bus Voltage (%) | Shunt Load (%) |
|---|---|---|---|---|---|
| 26 | 3 | 1.70 | 1.05 | | 0.00 |
| 27 | 3 | 1.28 | 0.79 | | 0.00 |
| 28 | 3 | 4.25 | 2.63 | | 0.00 |
| 29 | 3 | 3.83 | 2.37 | | 0.00 |
| 30 | 3 | 0.00 | 0.00 | | 0.00 |
| 31 | 3 | 0.00 | 0.00 | | 0.00 |
| 32 | 3 | 0.00 | 0.00 | | 0.00 |
| 33 | 3 | 0.00 | 0.00 | | 0.00 |
| 34 | 3 | 0.00 | 0.00 | | 0.00 |
| 35 | 3 | 0.00 | 0.00 | | 0.00 |
| 36 | 3 | 0.00 | 0.00 | | 0.00 |
| 37 | 3 | 0.00 | 0.00 | | 0.00 |
| 38 | 3 | 0.00 | 0.00 | | 0.00 |
| 39 | 3 | 0.09 | 0.05 | | 0.00 |
| 40 | 3 | 0.09 | 0.05 | | 0.00 |
| 50 | 3 | 0.00 | 0.00 | | 0.00 |
| 51 | 3 | 0.43 | 0.26 | | 0.00 |
| 52 | 3 | 0.43 | 0.26 | | -6.00 |
| 53 | 3 | 8.50 | 5.27 | | 0.00 |
| 54 | 3 | 8.50 | 5.27 | | 0.00 |
| 55 | 3 | 0.85 | 0.53 | | 0.00 |
| 56 | 3 | 0.85 | 0.53 | | 0.00 |
| 57 | 3 | 0.00 | 0.00 | | 0.00 |
| 58 | 3 | 0.43 | 0.26 | | 0.00 |
| 59 | 3 | 2.55 | 1.58 | | 0.00 |
| 60 | 3 | 0.43 | 0.26 | | 0.00 |
| 61 | 3 | 7.65 | 4.74 | | 0.00 |
| 62 | 3 | 3.83 | 2.37 | | 0.00 |
| 63 | 3 | 2.13 | 1.32 | | 0.00 |
| 64 | 3 | 1.28 | 0.79 | | 0.00 |
| 65 | 3 | 2.13 | 1.32 | | -6.00 |
| 66 | 3 | 0.85 | 0.53 | | 0.00 |
| 67 | 3 | 1.70 | 1.05 | | 0.00 |
| 68 | 3 | 1.70 | 1.05 | | 0.00 |
| 69 | 3 | 1.06 | 0.66 | | 0.00 |
| 70 | 3 | 1.06 | 0.66 | | 0.00 |
| 71 | 3 | 0.85 | 0.53 | | 0.00 |
| 72 | 3 | 0.64 | 0.40 | | 0.00 |
| 73 | 3 | 0.64 | 0.40 | | 0.00 |

**Table H-1**
**Bus Data for Power Distribution Network I (Continued)**

| Bus Number | Bus Type | P Load (%) | Q Load (%) | Bus Voltage (%) | Shunt Load (%) |
|---|---|---|---|---|---|
| 74 | 3 | 2.55 | 1.58 | | 0.00 |
| 75 | 3 | 1.70 | 1.05 | | 0.00 |
| 76 | 3 | 2.13 | 1.32 | | -6.00 |
| 77 | 3 | 2.13 | 1.32 | | 0.00 |
| 78 | 3 | 4.25 | 2.63 | | 0.00 |
| 79 | 3 | 3.83 | 2.37 | | 0.00 |
| 80 | 3 | 1.28 | 0.79 | | 0.00 |
| 81 | 3 | 0.85 | 0.53 | | 0.00 |
| 100 | 3 | 0.30 | 0.18 | | -6.00 |
| 101 | 3 | 3.27 | 2.03 | | 0.00 |
| 102 | 3 | 5.10 | 3.16 | | -6.00 |
| 103 | 3 | 3.40 | 2.11 | | 0.00 |
| 104 | 3 | 3.83 | 2.37 | | 0.00 |
| 105 | 3 | 2.55 | 1.58 | | 0.00 |
| 106 | 3 | 0.85 | 0.53 | | 0.00 |
| 107 | 3 | 0.85 | 0.53 | | 0.00 |
| 108 | 3 | 1.70 | 1.05 | | 0.00 |
| 109 | 3 | 0.00 | 0.00 | | 0.00 |
| 110 | 3 | 0.00 | 0.00 | | 0.00 |
| 111 | 3 | 4.25 | 2.63 | | -6.00 |
| 112 | 3 | 3.40 | 2.11 | | 0.00 |
| 113 | 3 | 3.83 | 2.37 | | -6.00 |
| 114 | 3 | 6.38 | 3.95 | | -6.00 |
| 115 | 3 | 7.82 | 4.85 | | 0.00 |
| 116 | 3 | 2.55 | 1.58 | | 0.00 |
| 117 | 3 | 1.87 | 1.16 | | 0.00 |
| 118 | 3 | 0.00 | 0.00 | | 0.00 |
| 119 | 3 | 1.28 | 0.79 | | 0.00 |
| 120 | 3 | 1.28 | 0.79 | | 0.00 |
| 121 | 3 | 0.00 | 0.00 | | -6.00 |
| 122 | 3 | 0.09 | 0.05 | | 0.00 |
| 123 | 3 | 4.76 | 2.95 | | 0.00 |
| 124 | 3 | 1.45 | 0.90 | | -6.00 |
| 125 | 3 | 0.72 | 0.45 | | 0.00 |
| 126 | 3 | 4.00 | 2.48 | | 0.00 |
| 127 | 3 | 0.04 | 0.03 | | 0.00 |
| 128 | 3 | 1.11 | 0.68 | | 0.00 |
| 129 | 3 | 2.38 | 1.48 | | -6.00 |
| 130 | 3 | 2.13 | 1.32 | | 0.00 |

**Table H-1**
**Bus Data for Power Distribution Network I (Continued)**

| Bus Number | Bus Type | P Load (%) | Q Load (%) | Bus Voltage (%) | Shunt Load (%) |
|---|---|---|---|---|---|
| 131 | 3 | 0.85 | 0.53 | | 0.00 |
| 132 | 3 | 0.64 | 0.40 | | 0.00 |
| 133 | 3 | 0.64 | 0.40 | | 0.00 |
| 134 | 3 | 0.00 | 0.00 | | 0.00 |
| 135 | 3 | 0.00 | 0.00 | | 0.00 |
| 136 | 3 | 0.00 | 0.00 | | 0.00 |
| 150 | 3 | 0.00 | 0.00 | | 0.00 |
| 151 | 3 | 0.43 | 0.26 | | 0.00 |
| 152 | 3 | 0.43 | 0.26 | | 0.00 |
| 153 | 3 | 12.62 | 7.82 | | 0.00 |
| 154 | 3 | 16.87 | 10.46 | | 0.00 |
| 155 | 3 | 5.95 | 3.69 | | -6.00 |
| 156 | 3 | 1.70 | 1.05 | | 0.00 |
| 157 | 3 | 1.28 | 0.79 | | 0.00 |
| 158 | 3 | 0.85 | 0.53 | | 0.00 |
| 159 | 3 | 0.43 | 0.26 | | 0.00 |
| 160 | 3 | 3.40 | 2.11 | | 0.00 |
| 161 | 3 | 5.10 | 3.16 | | -3.00 |
| 162 | 3 | 2.55 | 1.58 | | 0.00 |
| 163 | 3 | 0.00 | 0.00 | | 0.00 |
| 164 | 3 | 0.00 | 0.00 | | 0.00 |
| 165 | 3 | 0.00 | 0.00 | | 0.00 |
| 166 | 3 | 0.00 | 0.00 | | 0.00 |
| 167 | 3 | 0.00 | 0.00 | | 0.00 |
| 168 | 3 | 0.00 | 0.00 | | 0.00 |
| 169 | 3 | 0.00 | 0.00 | | 0.00 |
| 170 | 3 | 0.00 | 0.00 | | 0.00 |
| 171 | 3 | 0.00 | 0.00 | | 0.00 |
| 172 | 3 | 0.00 | 0.00 | | 0.00 |
| 173 | 3 | 4.68 | 2.90 | | 0.00 |
| 174 | 3 | 4.25 | 2.63 | | -9.00 |
| 175 | 3 | 2.55 | 1.58 | | 0.00 |
| 176 | 3 | 4.25 | 2.63 | | 0.00 |
| 177 | 3 | 2.13 | 1.32 | | 0.00 |
| 200 | 3 | 0.55 | 0.34 | | 0.00 |
| 201 | 3 | 3.53 | 2.19 | | 0.00 |
| 202 | 3 | 2.98 | 1.84 | | 0.00 |
| 203 | 3 | 0.85 | 0.53 | | 0.00 |
| 204 | 3 | 0.85 | 0.53 | | 0.00 |

**Table H-1**
**Bus Data for Power Distribution Network I (Continued)**

| Bus Number | Bus Type | P Load (%) | Q Load (%) | Bus Voltage (%) | Shunt Load (%) |
|---|---|---|---|---|---|
| 205 | 3 | 2.13 | 1.32 | | 0.00 |
| 206 | 3 | 1.28 | 0.79 | | 0.00 |
| 207 | 3 | 0.85 | 0.53 | | 0.00 |
| 208 | 3 | 0.34 | 0.21 | | -6.00 |
| 209 | 3 | 0.34 | 0.21 | | -6.00 |
| 210 | 3 | 0.00 | 0.00 | | 0.00 |
| 211 | 3 | 0.00 | 0.00 | | 0.00 |
| 212 | 3 | 0.00 | 0.00 | | 0.00 |
| 213 | 3 | 0.43 | 0.26 | | 0.00 |
| 214 | 3 | 1.28 | 0.79 | | 0.00 |
| 215 | 3 | 0.43 | 0.26 | | 0.00 |
| 216 | 3 | 0.43 | 0.26 | | 0.00 |
| 217 | 3 | 0.00 | 0.00 | | 0.00 |
| 218 | 3 | 0.00 | 0.00 | | 0.00 |
| 219 | 3 | 0.00 | 0.00 | | -6.00 |
| 220 | 3 | 3.40 | 2.11 | | 0.00 |
| 221 | 3 | 0.00 | 0.00 | | -6.00 |
| 222 | 3 | 1.49 | 0.92 | | 0.00 |
| 223 | 3 | 0.64 | 0.40 | | 0.00 |
| 224 | 3 | 0.21 | 0.13 | | 0.00 |
| 225 | 3 | 0.43 | 0.26 | | 0.00 |
| 226 | 3 | 1.91 | 1.19 | | 0.00 |
| 227 | 3 | 0.43 | 0.26 | | 0.00 |
| 228 | 3 | 0.00 | 0.00 | | 0.00 |
| 229 | 3 | 0.85 | 0.53 | | 0.00 |
| 230 | 3 | 0.85 | 0.53 | | 0.00 |
| 231 | 3 | 4.68 | 2.90 | | 0.00 |
| 232 | 3 | 1.28 | 0.79 | | 0.00 |
| 233 | 3 | 2.13 | 1.32 | | 0.00 |
| 234 | 3 | 2.13 | 1.32 | | 0.00 |
| 250 | 3 | 0.00 | 0.00 | | 0.00 |
| 251 | 3 | 0.21 | 0.13 | | 0.00 |
| 252 | 3 | 0.00 | 0.00 | | 0.00 |
| 253 | 3 | 0.85 | 0.53 | | 0.00 |
| 254 | 3 | 0.60 | 0.37 | | 0.00 |
| 255 | 3 | 0.04 | 0.03 | | -9.00 |
| 256 | 3 | 1.06 | 0.66 | | 0.00 |
| 257 | 3 | 5.53 | 3.42 | | 0.00 |
| 258 | 3 | 1.06 | 0.66 | | -9.00 |
| 259 | 3 | 0.85 | 0.53 | | 0.00 |
| 260 | 3 | 1.28 | 0.79 | | 0.00 |
| 261 | 3 | 0.47 | 0.29 | | 0.00 |

**Table H-1**
**Bus Data for Power Distribution Network I (Continued)**

| Bus Number | Bus Type | P Load (%) | Q Load (%) | Bus Voltage (%) | Shunt Load (%) |
|---|---|---|---|---|---|
| 262 | 3 | 0.81 | 0.50 | | 0.00 |
| 263 | 3 | 9.35 | 5.79 | | 0.00 |
| 264 | 3 | 8.50 | 5.27 | | 0.00 |
| 265 | 3 | 0.21 | 0.13 | | 0.00 |
| 266 | 3 | 3.36 | 2.08 | | 0.00 |
| 267 | 3 | 2.13 | 1.32 | | 0.00 |
| 268 | 3 | 1.06 | 0.66 | | 0.00 |
| 269 | 3 | 0.04 | 0.03 | | 0.00 |
| 270 | 3 | 0.85 | 0.53 | | 0.00 |
| 271 | 3 | 0.85 | 0.53 | | 0.00 |
| 272 | 3 | 0.00 | 0.00 | | -9.00 |
| 273 | 3 | 6.80 | 4.21 | | 0.00 |
| 274 | 3 | 6.80 | 4.21 | | 0.00 |
| 300 | 3 | 0.00 | 0.00 | | 0.00 |
| 301 | 3 | 0.00 | 0.00 | | -4.50 |
| 302 | 3 | 0.00 | 0.00 | | 0.00 |
| 303 | 3 | 0.55 | 0.34 | | -9.00 |
| 304 | 3 | 9.48 | 5.87 | | 0.00 |
| 305 | 3 | 8.50 | 5.27 | | 0.00 |
| 306 | 3 | 5.10 | 3.16 | | 0.00 |
| 307 | 3 | 3.19 | 1.98 | | 0.00 |
| 308 | 3 | 2.13 | 1.32 | | 0.00 |
| 309 | 3 | 1.28 | 0.79 | | 0.00 |
| 310 | 3 | 0.64 | 0.40 | | 0.00 |
| 311 | 3 | 5.10 | 3.16 | | 0.00 |
| 312 | 3 | 2.55 | 1.58 | | 0.00 |
| 313 | 3 | 0.43 | 0.26 | | -9.00 |
| 314 | 3 | 0.00 | 0.00 | | 0.00 |
| 315 | 3 | 4.68 | 2.90 | | 0.00 |
| 316 | 3 | 0.85 | 0.53 | | 0.00 |
| 317 | 3 | 0.00 | 0.00 | | 0.00 |
| 318 | 3 | 0.00 | 0.00 | | 0.00 |
| 319 | 3 | 1.70 | 1.05 | | 0.00 |
| 320 | 3 | 1.06 | 0.66 | | 0.00 |
| 321 | 3 | 5.31 | 3.29 | | -12.00 |
| 322 | 3 | 4.68 | 2.90 | | -6.00 |
| 323 | 3 | 0.00 | 0.00 | | 0.00 |
| 324 | 3 | 4.25 | 2.63 | | 0.00 |
| 325 | 3 | 8.08 | 5.00 | | 0.00 |
| 326 | 3 | 0.85 | 0.53 | | 0.00 |
| 327 | 3 | 3.40 | 2.11 | | -6.00 |
| 328 | 3 | 1.28 | 0.79 | | 0.00 |
| 329 | 3 | 0.85 | 0.53 | | 0.00 |

**Table H-2**
**Line Data for Power Distribution Network I. Note: There is a 30 Degree Phase Shift between Buses 1003 and 1 and Buses 1004 and 150**

| From Bus | To Bus | R (+) (%) | X (+) (%) | Line Charg. (+) (%) | R (0) (%) | X (0) (%) |
|---|---|---|---|---|---|---|
| 1001 | 1003 | 0.1019 | 0.5938 | 12 | 0.4606 | 1.9093 |
| 1002 | 1003 | 0.0338 | 0.2388 | 6 | 0.2018 | 0.7627 |
| 1003 | 1004 | 0.0189 | 0.1296 | 3 | 0.092 | 0.4567 |
| 1004 | 1005 | 0.0516 | 0.3587 | 6 | 0.2748 | 1.2112 |
| 1003 | 1 | 0.354 | 6.92 | 0 | 0.354 | 20.36 |
| 1004 | 150 | 0.121 | 3.844 | 0 | 0.121 | 3.844 |
| 1 | 50 | 0.449 | 1.254 | 0.0037 | 1.053 | 6.429 |
| 50 | 51 | 0.783 | 2.186 | 0.0064 | 1.835 | 11.204 |
| 51 | 52 | 0.68 | 2.001 | 0.0053 | 1.594 | 9.515 |
| 52 | 53 | 0.128 | 0.378 | 0.001 | 0.301 | 1.795 |
| 53 | 54 | 0.916 | 0.661 | 0.0194 | 1.149 | 2.661 |
| 53 | 55 | 0.308 | 0.906 | 0.0024 | 0.722 | 4.308 |
| 55 | 56 | 4.482 | 1.476 | 0.0023 | 4.983 | 5.587 |
| 55 | 57 | 0.411 | 1.147 | 0.0034 | 0.963 | 5.878 |
| 57 | 58 | 0.358 | 0.442 | 0.001 | 0.531 | 1.923 |
| 58 | 59 | 0.95 | 0.712 | 0.0012 | 1.192 | 2.697 |
| 59 | 60 | 2.009 | 0.661 | 0.001 | 2.234 | 2.504 |
| 59 | 61 | 5.292 | 3.969 | 0.0067 | 6.639 | 15.026 |
| 61 | 62 | 2.164 | 0.712 | 0.0011 | 2.406 | 2.697 |
| 61 | 63 | 4.206 | 3.155 | 0.0053 | 5.277 | 11.944 |
| 57 | 64 | 0.141 | 0.394 | 0.0012 | 0.331 | 2.02 |
| 64 | 65 | 0.372 | 1.095 | 0.0029 | 0.872 | 5.206 |
| 65 | 66 | 0.385 | 1.133 | 0.003 | 0.902 | 5.386 |
| 66 | 67 | 0.038 | 0.113 | 0.0003 | 0.09 | 0.539 |
| 67 | 68 | 0.244 | 0.717 | 0.0019 | 0.572 | 3.411 |
| 67 | 69 | 0.128 | 0.378 | 0.001 | 0.301 | 1.795 |
| 69 | 70 | 0.141 | 0.415 | 0.0011 | 0.331 | 1.975 |
| 70 | 71 | 1.085 | 0.814 | 0.0014 | 1.362 | 3.082 |
| 70 | 72 | 0.077 | 0.227 | 0.0006 | 0.18 | 1.077 |
| 72 | 73 | 1.546 | 0.509 | 0.0008 | 1.718 | 1.926 |
| 69 | 74 | 0.334 | 0.982 | 0.0026 | 0.782 | 4.668 |
| 74 | 75 | 1.236 | 0.407 | 0.0006 | 1.375 | 1.541 |
| 74 | 76 | 0.064 | 0.189 | 0.0005 | 0.15 | 0.898 |
| 76 | 77 | 0.308 | 0.906 | 0.0024 | 0.722 | 4.308 |
| 77 | 78 | 0.064 | 0.189 | 0.0005 | 0.15 | 0.898 |
| 78 | 79 | 5.41 | 1.781 | 0.0028 | 6.014 | 6.742 |
| 78 | 80 | 0.205 | 0.604 | 0.0016 | 0.481 | 2.872 |
| 80 | 81 | 0.205 | 0.573 | 0.0017 | 0.481 | 2.939 |

**Table H-2**
**Line Data for Power Distribution Network I. Note: There is a 30 Degree Phase Shift between Buses 1003 and 1 and Buses 1004 and 150 (Continued)**

| From Bus | To Bus | R (+) | X (+) | Line Charg. (+) | R (0) | X (0) |
|---|---|---|---|---|---|---|
| | | (%) | (%) | (%) | (%) | (%) |
| 1 | 100 | 0.103 | 0.302 | 0.0008 | 0.241 | 1.436 |
| 100 | 101 | 1.373 | 4.04 | 0.0106 | 3.219 | 19.209 |
| 101 | 102 | 0.411 | 1.147 | 0.0034 | 0.963 | 5.878 |
| 102 | 103 | 0.654 | 1.828 | 0.0053 | 1.534 | 9.368 |
| 103 | 104 | 0.513 | 1.434 | 0.0042 | 1.203 | 7.347 |
| 104 | 105 | 0.783 | 2.186 | 0.0064 | 1.835 | 11.204 |
| 105 | 106 | 8.192 | 2.697 | 0.0044 | 9.108 | 10.43 |
| 105 | 107 | 0.269 | 0.753 | 0.0022 | 0.632 | 3.857 |
| 104 | 108 | 1.27 | 3.738 | 0.0098 | 2.978 | 17.772 |
| 108 | 109 | 1.236 | 0.407 | 0.0006 | 1.375 | 1.541 |
| 109 | 110 | 1.236 | 0.407 | 0.0102 | 1.375 | 1.541 |
| 108 | 111 | 0.385 | 1.133 | 0.003 | 0.902 | 5.386 |
| 111 | 112 | 0.924 | 2.719 | 0.0071 | 2.166 | 12.925 |
| 104 | 113 | 0.475 | 1.326 | 0.0039 | 1.113 | 6.796 |
| 113 | 114 | 1.027 | 2.867 | 0.0084 | 2.406 | 14.694 |
| 114 | 115 | 1.027 | 2.867 | 0.0084 | 2.406 | 14.694 |
| 115 | 116 | 4.173 | 1.374 | 0.0021 | 4.64 | 5.201 |
| 115 | 117 | 0.385 | 1.075 | 0.0031 | 0.902 | 5.51 |
| 117 | 118 | 0.064 | 0.189 | 0.0005 | 0.15 | 0.898 |
| 118 | 119 | 0.064 | 0.189 | 0.0005 | 0.15 | 0.898 |
| 119 | 120 | 0.616 | 1.812 | 0.0048 | 1.444 | 8.617 |
| 119 | 121 | 4.884 | 3.663 | 0.0062 | 6.129 | 13.87 |
| 121 | 122 | 0.746 | 0.56 | 0.0009 | 0.936 | 2.119 |
| 122 | 123 | 0.757 | 2.115 | 0.0062 | 1.775 | 10.837 |
| 123 | 124 | 0.103 | 0.287 | 0.0008 | 0.241 | 1.469 |
| 124 | 125 | 0.282 | 0.788 | 0.0023 | 0.662 | 4.041 |
| 123 | 126 | 5.834 | 4.211 | 0.0077 | 7.32 | 16.952 |
| 126 | 127 | 0.34 | 0.077 | 0.0072 | 0.645 | 0.137 |
| 122 | 128 | 1.628 | 1.221 | 0.0021 | 2.043 | 4.623 |
| 128 | 129 | 4.884 | 3.663 | 0.0062 | 6.129 | 13.87 |
| 129 | 130 | 0.746 | 0.56 | 0.0009 | 0.936 | 2.119 |
| 130 | 131 | 0.885 | 2.473 | 0.0072 | 2.076 | 12.674 |
| 130 | 132 | 0.204 | 0.153 | 0.0003 | 0.255 | 0.578 |
| 132 | 133 | 2.374 | 1.714 | 0.0031 | 2.979 | 6.899 |
| 132 | 134 | 1.967 | 1.476 | 0.0025 | 2.468 | 5.587 |
| 134 | 135 | 0.513 | 1.434 | 0.0042 | 1.203 | 7.347 |
| 135 | 136 | 0.081 | 0.112 | 0.0318 | 0.482 | 0.137 |
| 1 | 2 | 0.372 | 1.039 | 0.003 | 0.872 | 5.327 |

**Table H-2**
**Line Data for Power Distribution Network I. Note: There is a 30 Degree Phase Shift between Buses 1003 and 1 and Buses 1004 and 150 (Continued)**

| From Bus | To Bus | R (+) | X (+) | Line Charg. (+) | R (0) | X (0) |
|---|---|---|---|---|---|---|
| | | (%) | (%) | (%) | (%) | (%) |
| 2 | 3 | 0.95 | 0.685 | 0.0013 | 1.192 | 2.76 |
| 3 | 4 | 1.832 | 1.322 | 0.0024 | 2.298 | 5.322 |
| 3 | 5 | 2.849 | 2.056 | 0.0038 | 3.575 | 8.279 |
| 2 | 6 | 0.077 | 0.215 | 0.0006 | 0.18 | 1.102 |
| 6 | 7 | 0.539 | 1.505 | 0.0044 | 1.263 | 7.715 |
| 7 | 8 | 0.128 | 0.358 | 0.001 | 0.301 | 1.837 |
| 7 | 9 | 0.244 | 0.681 | 0.002 | 0.572 | 3.49 |
| 9 | 10 | 0.141 | 0.394 | 0.0012 | 0.331 | 2.02 |
| 10 | 11 | 0.642 | 1.792 | 0.0052 | 1.504 | 9.184 |
| 11 | 12 | 0.308 | 0.906 | 0.0024 | 0.722 | 4.308 |
| 12 | 13 | 0.128 | 0.358 | 0.001 | 0.301 | 1.837 |
| 13 | 14 | 0.334 | 0.932 | 0.0027 | 0.782 | 4.776 |
| 14 | 15 | 1.085 | 0.783 | 0.0014 | 1.362 | 3.154 |
| 15 | 16 | 1.628 | 1.175 | 0.0022 | 2.043 | 4.731 |
| 16 | 17 | 16.074 | 5.292 | 0.0083 | 17.871 | 20.035 |
| 17 | 18 | 7.598 | 5.699 | 0.0096 | 9.533 | 21.576 |
| 14 | 19 | 0.539 | 1.505 | 0.0044 | 1.263 | 7.715 |
| 19 | 20 | 0.064 | 0.179 | 0.0005 | 0.15 | 0.918 |
| 20 | 21 | 0.244 | 0.681 | 0.002 | 0.572 | 3.49 |
| 20 | 22 | 1.151 | 9.314 | 0.0053 | 1.983 | 16.41 |
| 22 | 23 | 0.133 | 0.574 | 0.0295 | 0.423 | 3.05 |
| 23 | 24 | 0.061 | 0.179 | 0.0075 | 0.143 | 0.853 |
| 24 | 25 | 0.093 | 0.274 | 0.0115 | 0.218 | 1.302 |
| 25 | 26 | 0.042 | 0.123 | 0.0052 | 0.098 | 0.583 |
| 26 | 27 | 20.556 | 6.767 | 0.0106 | 22.855 | 25.621 |
| 26 | 28 | 0.026 | 0.076 | 0.0032 | 0.06 | 0.359 |
| 28 | 29 | 0.305 | 0.229 | 0.0062 | 0.383 | 0.867 |
| 29 | 30 | 0.034 | 0.025 | 0.0007 | 0.043 | 0.096 |
| 28 | 31 | 0.045 | 0.132 | 0.0056 | 0.105 | 0.628 |
| 31 | 32 | 0.026 | 0.076 | 0.0032 | 0.06 | 0.359 |
| 31 | 33 | 0.509 | 0.382 | 0.0103 | 0.638 | 1.445 |
| 33 | 34 | 0.309 | 0.102 | 0.0025 | 0.344 | 0.385 |
| 33 | 35 | 0.187 | 0.14 | 0.0038 | 0.234 | 0.53 |
| 35 | 36 | 0.594 | 0.445 | 0.012 | 0.745 | 1.686 |
| 35 | 37 | 0.563 | 0.271 | 0.0076 | 0.658 | 1.084 |
| 35 | 38 | 0.644 | 0.483 | 0.013 | 0.809 | 1.83 |
| 38 | 39 | 2.164 | 0.712 | 0.0187 | 2.406 | 2.755 |
| 39 | 40 | 0.386 | 0.127 | 0.0033 | 0.43 | 0.492 |

**Table H-2**
**Line Data for Power Distribution Network I. Note: There is a 30 Degree Phase Shift between Buses 1003 and 1 and Buses 1004 and 150 (Continued)**

| From Bus | To Bus | R (+) | X (+) | Line Charg. (+) | R (0) | X (0) |
|---|---|---|---|---|---|---|
| | | (%) | (%) | (%) | (%) | (%) |
| 150 | 151 | 0.01 | 0.014 | 0.0636 | 0.06 | 0.017 |
| 151 | 152 | 0.286 | 1.233 | 0.0634 | 0.91 | 6.555 |
| 152 | 153 | 0.045 | 0.055 | 0.0019 | 0.066 | 0.24 |
| 153 | 154 | 0.024 | 0.034 | 0.0095 | 0.144 | 0.041 |
| 154 | 155 | 1.289 | 0.967 | 0.0016 | 1.617 | 3.66 |
| 155 | 156 | 2.171 | 1.628 | 0.0027 | 2.724 | 6.164 |
| 154 | 157 | 0.407 | 0.305 | 0.0005 | 0.511 | 1.156 |
| 157 | 158 | 0.543 | 0.407 | 0.0007 | 0.681 | 1.541 |
| 158 | 159 | 0.746 | 0.56 | 0.0009 | 0.936 | 2.119 |
| 157 | 160 | 1.289 | 0.967 | 0.0016 | 1.617 | 3.66 |
| 160 | 161 | 2.307 | 1.73 | 0.0029 | 2.894 | 6.55 |
| 161 | 162 | 1.085 | 0.814 | 0.0014 | 1.362 | 3.082 |
| 152 | 163 | 0.016 | 0.068 | 0.0035 | 0.051 | 0.364 |
| 163 | 164 | 0.111 | 0.479 | 0.0247 | 0.354 | 2.549 |
| 164 | 165 | 0.865 | 0.649 | 0.0175 | 1.085 | 2.456 |
| 164 | 166 | 0.032 | 0.137 | 0.007 | 0.101 | 0.728 |
| 166 | 167 | 0.136 | 0.102 | 0.0027 | 0.17 | 0.385 |
| 167 | 168 | 1.221 | 0.916 | 0.0247 | 1.532 | 3.468 |
| 166 | 169 | 0.016 | 0.068 | 0.0035 | 0.051 | 0.364 |
| 169 | 170 | 0.205 | 0.099 | 0.0028 | 0.239 | 0.394 |
| 170 | 171 | 0.356 | 0.267 | 0.0072 | 0.447 | 1.011 |
| 169 | 172 | 0.105 | 0.454 | 0.0234 | 0.335 | 2.413 |
| 172 | 173 | 0.073 | 0.317 | 0.0163 | 0.234 | 1.684 |
| 173 | 174 | 0.061 | 0.179 | 0.0075 | 0.143 | 0.853 |
| 173 | 175 | 0.042 | 0.123 | 0.0052 | 0.098 | 0.583 |
| 175 | 176 | 0.642 | 1.792 | 0.0839 | 1.504 | 9.184 |
| 176 | 177 | 0.678 | 0.49 | 0.0144 | 0.851 | 1.971 |
| 150 | 300 | 0.032 | 0.045 | 0.2036 | 0.193 | 0.055 |
| 300 | 301 | 0.051 | 0.143 | 0.0067 | 0.12 | 0.735 |
| 301 | 302 | 0.058 | 0.161 | 0.0075 | 0.135 | 0.827 |
| 302 | 303 | 0.026 | 0.076 | 0.0032 | 0.06 | 0.359 |
| 303 | 304 | 0.173 | 0.51 | 0.0214 | 0.406 | 2.424 |
| 304 | 305 | 2.171 | 1.567 | 0.046 | 2.724 | 6.308 |
| 304 | 306 | 0.138 | 0.406 | 0.0171 | 0.323 | 1.93 |
| 306 | 307 | 0.164 | 0.481 | 0.0202 | 0.384 | 2.289 |
| 307 | 308 | 0.109 | 0.305 | 0.0143 | 0.256 | 1.561 |
| 308 | 309 | 0.441 | 0.318 | 0.0093 | 0.553 | 1.281 |
| 308 | 310 | 0.077 | 0.215 | 0.0101 | 0.18 | 1.102 |

**Table H-2**
**Line Data for Power Distribution Network I. Note: There is a 30 Degree Phase Shift between Buses 1003 and 1 and Buses 1004 and 150 (Continued)**

| From Bus | To Bus | R (+) | X (+) | Line Charg. (+) | R (0) | X (0) |
|---|---|---|---|---|---|---|
| | | (%) | (%) | (%) | (%) | (%) |
| 307 | 311 | 0.215 | 0.632 | 0.0266 | 0.504 | 3.007 |
| 311 | 312 | 0.814 | 0.588 | 0.0172 | 1.021 | 2.365 |
| 311 | 313 | 0.051 | 0.151 | 0.0064 | 0.12 | 0.718 |
| 313 | 314 | 0.077 | 0.227 | 0.0095 | 0.18 | 1.077 |
| 306 | 315 | 1.434 | 1.856 | 0.0582 | 2.125 | 7.526 |
| 315 | 316 | 3.443 | 2.582 | 0.0696 | 4.32 | 9.776 |
| 316 | 317 | 0.746 | 0.56 | 0.0009 | 0.936 | 2.119 |
| 317 | 318 | 0.339 | 0.254 | 0.0004 | 0.426 | 0.963 |
| 318 | 319 | 0.204 | 0.153 | 0.0003 | 0.255 | 0.578 |
| 319 | 320 | 3.46 | 2.595 | 0.0044 | 4.341 | 9.825 |
| 319 | 321 | 1.832 | 1.374 | 0.0023 | 2.298 | 5.201 |
| 321 | 322 | 12.143 | 9.108 | 0.0153 | 15.236 | 34.483 |
| 322 | 323 | 0.407 | 0.305 | 0.0005 | 0.511 | 1.156 |
| 317 | 324 | 0.339 | 0.254 | 0.0004 | 0.426 | 0.963 |
| 324 | 325 | 3.256 | 2.442 | 0.0041 | 4.086 | 9.247 |
| 325 | 326 | 5.719 | 1.883 | 0.0029 | 6.358 | 7.128 |
| 325 | 327 | 5.631 | 4.223 | 0.0071 | 7.065 | 15.989 |
| 327 | 328 | 0.882 | 0.661 | 0.0011 | 1.107 | 2.504 |
| 328 | 329 | 2.009 | 0.661 | 0.001 | 2.234 | 2.504 |
| 150 | 250 | 0.032 | 0.045 | 0.2036 | 0.193 | 0.055 |
| 250 | 251 | 0.077 | 0.215 | 0.0101 | 0.18 | 1.102 |
| 251 | 252 | 0.032 | 0.09 | 0.0042 | 0.075 | 0.459 |
| 251 | 253 | 0.026 | 0.072 | 0.0034 | 0.06 | 0.367 |
| 253 | 254 | 0.618 | 0.204 | 0.0053 | 0.687 | 0.787 |
| 253 | 255 | 0.083 | 0.233 | 0.0109 | 0.196 | 1.194 |
| 255 | 256 | 0.061 | 0.17 | 0.008 | 0.143 | 0.872 |
| 256 | 257 | 0.927 | 0.305 | 0.0076 | 1.031 | 1.156 |
| 256 | 258 | 0.122 | 0.34 | 0.0159 | 0.286 | 1.745 |
| 258 | 259 | 0.042 | 0.116 | 0.0055 | 0.098 | 0.597 |
| 259 | 260 | 0.01 | 0.027 | 0.0013 | 0.023 | 0.138 |
| 260 | 261 | 0.136 | 0.098 | 0.0029 | 0.17 | 0.394 |
| 260 | 262 | 0.116 | 0.151 | 0.0047 | 0.173 | 0.612 |
| 259 | 263 | 0.067 | 0.198 | 0.0083 | 0.158 | 0.942 |
| 263 | 264 | 0.282 | 0.831 | 0.0349 | 0.662 | 3.949 |
| 263 | 265 | 0.016 | 0.047 | 0.002 | 0.038 | 0.224 |
| 265 | 266 | 0.233 | 0.302 | 0.0095 | 0.345 | 1.223 |
| 266 | 267 | 0.814 | 0.611 | 0.0165 | 1.021 | 2.312 |
| 266 | 268 | 0.116 | 0.151 | 0.0047 | 0.173 | 0.612 |

**Table H-2**
**Line Data for Power Distribution Network I. Note: There is a 30 Degree Phase Shift between Buses 1003 and 1 and Buses 1004 and 150 (Continued)**

| From Bus | To Bus | R (+) (%) | X (+) (%) | Line Charg. (+) (%) | R (0) (%) | X (0) (%) |
|---|---|---|---|---|---|---|
| 268 | 269 | 0.128 | 0.358 | 0.0168 | 0.301 | 1.837 |
| 265 | 270 | 0.01 | 0.027 | 0.0013 | 0.023 | 0.138 |
| 270 | 271 | 0.116 | 0.151 | 0.0047 | 0.173 | 0.612 |
| 270 | 272 | 0.087 | 0.242 | 0.0113 | 0.203 | 1.24 |
| 272 | 273 | 0.071 | 0.197 | 0.0092 | 0.165 | 1.01 |
| 273 | 274 | 0.334 | 0.932 | 0.0436 | 0.782 | 4.776 |
| 150 | 200 | 0.032 | 0.045 | 0.2036 | 0.193 | 0.055 |
| 200 | 201 | 0.308 | 0.86 | 0.0025 | 0.722 | 4.408 |
| 201 | 202 | 3.709 | 1.221 | 0.0019 | 4.124 | 4.623 |
| 201 | 203 | 1.236 | 0.407 | 0.0006 | 1.375 | 1.541 |
| 203 | 204 | 2.473 | 0.814 | 0.0013 | 2.749 | 3.082 |
| 203 | 205 | 0.773 | 0.254 | 0.0004 | 0.859 | 0.963 |
| 205 | 206 | 3.4 | 1.119 | 0.0017 | 3.78 | 4.238 |
| 205 | 207 | 1.546 | 0.509 | 0.0008 | 1.718 | 1.926 |
| 200 | 208 | 0.308 | 0.86 | 0.0025 | 0.722 | 4.408 |
| 208 | 209 | 6.173 | 4.63 | 0.0078 | 7.746 | 17.53 |
| 209 | 210 | 0.95 | 0.712 | 0.0012 | 1.192 | 2.697 |
| 210 | 211 | 3.596 | 2.697 | 0.0045 | 4.511 | 10.21 |
| 210 | 212 | 0.543 | 0.407 | 0.0007 | 0.681 | 1.541 |
| 212 | 213 | 0.95 | 0.712 | 0.0012 | 1.192 | 2.697 |
| 213 | 214 | 1.832 | 1.374 | 0.0023 | 2.298 | 5.201 |
| 214 | 215 | 4.173 | 1.374 | 0.0021 | 4.64 | 5.201 |
| 214 | 216 | 1.085 | 0.814 | 0.0014 | 1.362 | 3.082 |
| 216 | 217 | 0.95 | 0.712 | 0.0012 | 1.192 | 2.697 |
| 217 | 218 | 0.287 | 0.353 | 0.0008 | 0.425 | 1.539 |
| 218 | 219 | 0.407 | 0.305 | 0.0005 | 0.511 | 1.156 |
| 219 | 220 | 0.678 | 0.509 | 0.0009 | 0.851 | 1.926 |
| 220 | 221 | 0.543 | 0.407 | 0.0007 | 0.681 | 1.541 |
| 221 | 222 | 0.678 | 0.509 | 0.0009 | 0.851 | 1.926 |
| 222 | 223 | 0.287 | 0.353 | 0.0008 | 0.425 | 1.539 |
| 223 | 224 | 1.7 | 0.56 | 0.0009 | 1.89 | 2.119 |
| 223 | 225 | 2.578 | 1.933 | 0.0033 | 3.235 | 7.32 |
| 222 | 226 | 8.655 | 2.849 | 0.0047 | 9.623 | 11.021 |
| 226 | 227 | 9.119 | 3.002 | 0.0049 | 10.139 | 11.611 |
| 226 | 228 | 0.464 | 0.153 | 0.0003 | 0.516 | 0.59 |
| 228 | 229 | 0.287 | 0.353 | 0.0008 | 0.425 | 1.539 |
| 229 | 230 | 4.173 | 1.374 | 0.0021 | 4.64 | 5.201 |
| 220 | 231 | 3.935 | 2.84 | 0.0052 | 4.937 | 11.433 |
| 231 | 232 | 2.51 | 1.883 | 0.0032 | 3.149 | 7.128 |
| 231 | 233 | 2.51 | 1.883 | 0.0032 | 3.149 | 7.128 |
| 233 | 234 | 0.087 | 0.242 | 0.0113 | 0.203 | 1.24 |

# I

# APPENDIX I – BUS AND LINE DATA FOR POWER DISTRIBUTION NETWORK II

**Table I-1**
**Bus Data for Power Distribution Network II**

| Bus Number | Bus Type | P Load (%) | Q Load (%) | Bus Voltage (%) | Shunt Load (%) |
|---|---|---|---|---|---|
| 2 | 3 | 0 | 0 | | 0 |
| 3 | 3 | 0 | 0 | | -12 |
| 4 | 3 | 0 | 0 | | 0 |
| 5 | 3 | 2.816 | 1.437 | | 0 |
| 7 | 3 | 2.792 | 1.377 | | 0 |
| 9 | 3 | 0 | 0 | | 0 |
| 10 | 3 | 2.379 | 1.163 | | 0 |
| 11 | 3 | 0 | 0 | | -12 |
| 15 | 3 | 0 | 0 | | 0 |
| 12 | 3 | 0 | 0 | | 0 |
| 13 | 3 | 0.708 | 0.361 | | 0 |
| 14 | 3 | 0.03 | 0.017 | | 0 |
| 16 | 3 | 0 | 0 | | 0 |
| 17 | 3 | 0.906 | 0.462 | | 0 |
| 18 | 3 | 0 | 0 | | 0 |
| 19 | 3 | 0 | 0 | | 0 |
| 20 | 3 | 2.224 | 1.136 | | 0 |
| 21 | 3 | 1.465 | 0.748 | | 0 |
| 22 | 3 | 0 | 0 | | 0 |
| 23 | 3 | 2.062 | 1.053 | | 0 |
| 24 | 3 | 0.089 | 0.045 | | 0 |
| 25 | 3 | 0 | 0 | | 0 |
| 26 | 3 | 0.33 | 0.168 | | 0 |
| 418 | 3 | 5.639 | 2.879 | | 0 |
| 27 | 3 | 0.487 | 0.248 | | 0 |
| 28 | 3 | 0.099 | 0.051 | | 0 |
| 29 | 3 | 0.33 | 0.168 | | 0 |
| 30 | 3 | 0 | 0 | | 0 |
| 31 | 3 | 0.398 | 0.203 | | 0 |
| 414 | 3 | 0 | 0 | | 0 |

**Table I-1**
**Bus Data for Power Distribution Network II (Continued)**

| Bus Number | Bus Type | P Load (%) | Q Load (%) | Bus Voltage (%) | Shunt Load (%) |
|---|---|---|---|---|---|
| 32 | 3 | 0 | 0 | | -12 |
| 33 | 3 | 0 | 0 | | 0 |
| 34 | 3 | 0 | 0 | | 0 |
| 394 | 3 | 0 | 0 | | 0 |
| 35 | 3 | 0.026 | 0.015 | | 0 |
| 36 | 3 | 0 | 0 | | 0 |
| 37 | 3 | 0 | 0 | | 0 |
| 38 | 3 | 0 | 0 | | 0 |
| 57 | 3 | 0 | 0 | | 0 |
| 39 | 3 | 0 | 0 | | 0 |
| 40 | 3 | 2.616 | 1.337 | | 0 |
| 41 | 3 | 0 | 0 | | -6 |
| 42 | 3 | 0.126 | 0.064 | | 0 |
| 43 | 3 | 0.68 | 0.347 | | 0 |
| 58 | 3 | 0.387 | 0.198 | | 0 |
| 59 | 3 | 0.366 | 0.187 | | 0 |
| 60 | 3 | 10.309 | 5.264 | | 0 |
| 61 | 3 | 0.586 | 0.299 | | 0 |
| 62 | 3 | 0.478 | 0.244 | | 0 |
| 63 | 3 | 0 | 0 | | 0 |
| 64 | 3 | 0.471 | 0.24 | | 0 |
| 344 | 3 | 0 | 0 | | 0 |
| 65 | 3 | 0.089 | 0.045 | | 0 |
| 66 | 3 | 0.199 | 0.102 | | 0 |
| 67 | 3 | 0.377 | 0.192 | | 0 |
| 68 | 3 | 1.02 | 0.521 | | 0 |
| 69 | 3 | 0 | 0 | | 0 |
| 70 | 3 | 0 | 0 | | 0 |
| 71 | 3 | 0.403 | 0.206 | | 0 |
| 267 | 3 | 0 | 0 | | 0 |
| 72 | 3 | 0 | 0 | | 0 |
| 73 | 3 | 0.324 | 0.166 | | 0 |
| 74 | 3 | 1.162 | 0.592 | | 0 |
| 75 | 3 | 1.125 | 0.574 | | 0 |
| 76 | 3 | 0.638 | 0.326 | | 0 |
| 77 | 3 | 0 | 0 | | -12 |
| 78 | 3 | 0 | 0 | | 0 |
| 79 | 3 | 0.57 | 0.291 | | 0 |
| 128 | 3 | 0 | 0 | | 0 |

**Table I-1**
**Bus Data for Power Distribution Network II (Continued)**

| Bus Number | Bus Type | P Load (%) | Q Load (%) | Bus Voltage (%) | Shunt Load (%) |
|---|---|---|---|---|---|
| 80 | 3 | 0.633 | 0.323 | | 0 |
| 81 | 3 | 0.586 | 0.299 | | 0 |
| 82 | 3 | 0.743 | 0.379 | | 0 |
| 83 | 3 | 0 | 0 | | 0 |
| 84 | 3 | 0.492 | 0.251 | | 0 |
| 85 | 3 | 0 | 0 | | 0 |
| 86 | 3 | 0.701 | 0.358 | | 0 |
| 87 | 3 | 0.717 | 0.383 | | 0 |
| 88 | 3 | 0 | 0 | | 0 |
| 89 | 3 | 0.519 | 0.292 | | 0 |
| 90 | 3 | 0.523 | 0.265 | | 0 |
| 91 | 3 | 0 | 0 | | 0 |
| 92 | 3 | 0.246 | 0.126 | | 0 |
| 122 | 3 | 1.341 | 0.767 | | 0 |
| 93 | 3 | 3.453 | 1.769 | | 0 |
| 94 | 3 | 0 | 0 | | -12 |
| 95 | 3 | 0 | 0 | | 0 |
| 96 | 3 | 0 | 0 | | 0 |
| 102 | 3 | 0.436 | 0.189 | | 0 |
| 97 | 3 | 0.097 | 0.056 | | 0 |
| 98 | 3 | 0.681 | 0.381 | | 0 |
| 103 | 3 | 0.171 | 0.096 | | 0 |
| 104 | 3 | 0.204 | 0.117 | | 0 |
| 129 | 3 | 0 | 0 | | 0 |
| 130 | 3 | 0 | 0 | | 0 |
| 131 | 3 | 0.586 | 0.299 | | 0 |
| 132 | 3 | 0 | 0 | | 0 |
| 133 | 3 | 0 | 0 | | 0 |
| 134 | 3 | 0 | 0 | | 0 |
| 135 | 3 | 0 | 0 | | 0 |
| 136 | 3 | 0 | 0 | | 0 |
| 137 | 3 | 0 | 0 | | 0 |
| 138 | 3 | 0 | 0 | | 0 |
| 139 | 3 | 0 | 0 | | 0 |
| 140 | 3 | 0 | 0 | | 0 |
| 247 | 3 | 0.4 | 0.206 | | 0 |
| 141 | 3 | 0 | 0 | | 0 |
| 246 | 3 | 0.674 | 0.385 | | 0 |
| 142 | 3 | 0.612 | 0.278 | | 0 |

**Table I-1**
**Bus Data for Power Distribution Network II (Continued)**

| Bus Number | Bus Type | P Load (%) | Q Load (%) | Bus Voltage (%) | Shunt Load (%) |
|---|---|---|---|---|---|
| 143 | 3 | 0 | 0 | | 0 |
| 144 | 3 | 0 | 0 | | 0 |
| 145 | 3 | 0.62 | 0.328 | | 0 |
| 146 | 3 | 0.172 | 0.089 | | 0 |
| 147 | 3 | 0.202 | 0.098 | | 0 |
| 148 | 3 | 0.214 | 0.11 | | 0 |
| 149 | 3 | 0.058 | 0.029 | | 0 |
| 150 | 3 | 0.089 | 0.045 | | 0 |
| 151 | 3 | 0.079 | 0.04 | | 0 |
| 152 | 3 | 2.375 | 1.213 | | 0 |
| 153 | 3 | 0 | 0 | | 0 |
| 177 | 3 | 0.492 | 0.251 | | 0 |
| 154 | 3 | 0 | 0 | | 0 |
| 155 | 3 | 0 | 0 | | 0 |
| 156 | 3 | 0.553 | 0.286 | | 0 |
| 157 | 3 | 2.786 | 1.423 | | 0 |
| 158 | 3 | 4.015 | 2.052 | | 0 |
| 178 | 3 | 0.188 | 0.096 | | 0 |
| 179 | 3 | 0 | 0 | | 0 |
| 180 | 3 | 0.277 | 0.142 | | 0 |
| 181 | 3 | 1.182 | 0.605 | | 0 |
| 182 | 3 | 4.97 | 2.552 | | 0 |
| 183 | 3 | 0 | 0 | | 0 |
| 184 | 3 | 0 | 0 | | 0 |
| 185 | 3 | 0.136 | 0.07 | | 0 |
| 186 | 3 | 0.335 | 0.171 | | 0 |
| 187 | 3 | 0.193 | 0.099 | | 0 |
| 188 | 3 | 0.374 | 0.192 | | 0 |
| 189 | 3 | 2.522 | 1.287 | | 0 |
| 190 | 3 | 0 | 0 | | 0 |
| 195 | 3 | 0.471 | 0.24 | | 0 |
| 191 | 3 | 0 | 0 | | 0 |
| 192 | 3 | 0 | 0 | | 0 |
| 194 | 3 | 0.131 | 0.067 | | 0 |
| 196 | 3 | 0 | 0 | | 0 |
| 197 | 3 | 0.55 | 0.28 | | 0 |
| 268 | 3 | 0 | 0 | | 0 |
| 269 | 3 | 3.482 | 1.777 | | 0 |
| 270 | 3 | 0 | 0 | | 0 |

**Table I-1**
**Bus Data for Power Distribution Network II (Continued)**

| Bus Number | Bus Type | P Load (%) | Q Load (%) | Bus Voltage (%) | Shunt Load (%) |
|---|---|---|---|---|---|
| 271 | 3 | 1.141 | 0.582 | | 0 |
| 272 | 3 | 0 | 0 | | 0 |
| 273 | 3 | 0.869 | 0.443 | | 0 |
| 274 | 3 | 0.152 | 0.077 | | 0 |
| 275 | 3 | 1.585 | 0.809 | | 0 |
| 276 | 3 | 0 | 0 | | 0 |
| 277 | 3 | 0.183 | 0.094 | | 0 |
| 278 | 3 | 0.131 | 0.067 | | 0 |
| 279 | 3 | 0 | 0 | | -12 |
| 280 | 3 | 2.651 | 1.354 | | 0 |
| 281 | 3 | 1.272 | 0.649 | | 0 |
| 282 | 3 | 0.513 | 0.261 | | 0 |
| 283 | 3 | 0 | 0 | | 0 |
| 284 | 3 | 0 | 0 | | 0 |
| 285 | 3 | 1.171 | 0.598 | | 0 |
| 345 | 3 | 0 | 0 | | -12 |
| 346 | 3 | 2.251 | 1.148 | | 0 |
| 395 | 3 | 1.496 | 0.754 | | 0 |
| 396 | 3 | 1.283 | 0.64 | | 0 |
| 415 | 3 | 0.409 | 0.209 | | 0 |
| 1000 | 1 | | | 105 | |
| 1 | 3 | 0 | 0 | 0 | 0 |

**Table I-2**
**Line Data for Power Distribution System II.  Note:  There is a 30 Degree Phase Shift between Buses 1000 and 1**

| From Bus | To Bus | R (+) (%) | X (+) (%) | Line Charg. (+) (%) | R (0) (%) | X (0) (%) |
|---|---|---|---|---|---|---|
| 1000 | 1 | 0.203 | 5.266 | 0 | 0.579 | 14.905 |
| 1 | 2 | 0.017 | 0.021 | 0 | 0.052 | 0.014 |
| 2 | 3 | 0.143 | 0.66 | 0 | 0.907 | 2.592 |
| 3 | 4 | 0.016 | 0.073 | 0 | 0.101 | 0.288 |
| 4 | 5 | 0.064 | 0.293 | 0 | 0.403 | 1.152 |
| 5 | 7 | 0.048 | 0.22 | 0 | 0.302 | 0.864 |
| 7 | 9 | 0.064 | 0.293 | 0 | 0.403 | 1.152 |
| 9 | 10 | 0.216 | 0.03 | 0 | 0.44 | 0.019 |
| 9 | 11 | 0.032 | 0.147 | 0 | 0.202 | 0.576 |
| 9 | 15 | 0.056 | 0.257 | 0 | 0.353 | 1.008 |
| 11 | 12 | 0.032 | 0.147 | 0 | 0.202 | 0.576 |
| 12 | 13 | 0.216 | 0.03 | 0 | 0.44 | 0.019 |
| 12 | 14 | 0.016 | 0.073 | 0 | 0.101 | 0.288 |
| 15 | 16 | 0.019 | 0.088 | 0 | 0.121 | 0.346 |
| 16 | 17 | 0.081 | 0.374 | 0 | 0.514 | 1.469 |
| 17 | 18 | 0.057 | 0.264 | 0 | 0.363 | 1.037 |
| 18 | 19 | 0.054 | 0.249 | 0 | 0.343 | 0.979 |
| 19 | 20 | 0.046 | 0.213 | 0 | 0.292 | 0.835 |
| 20 | 21 | 0.045 | 0.205 | 0 | 0.282 | 0.806 |
| 21 | 22 | 0.024 | 0.11 | 0 | 0.151 | 0.432 |
| 22 | 23 | 0.022 | 0.103 | 0 | 0.141 | 0.403 |
| 23 | 24 | 0.059 | 0.271 | 0 | 0.373 | 1.066 |
| 24 | 25 | 0.01 | 0.044 | 0 | 0.06 | 0.173 |
| 25 | 26 | 0.027 | 0.125 | 0 | 0.171 | 0.49 |
| 25 | 418 | 0.477 | 0.164 | 0 | 0.606 | 0.538 |
| 26 | 27 | 0.067 | 0.308 | 0 | 0.423 | 1.21 |
| 27 | 28 | 0.046 | 0.213 | 0 | 0.292 | 0.835 |
| 28 | 29 | 0.035 | 0.161 | 0 | 0.222 | 0.634 |
| 29 | 30 | 0.03 | 0.139 | 0 | 0.191 | 0.547 |
| 30 | 31 | 0.04 | 0.183 | 0 | 0.252 | 0.72 |
| 30 | 414 | 0.033 | 0.154 | 0 | 0.212 | 0.605 |
| 31 | 32 | 0.03 | 0.139 | 0 | 0.191 | 0.547 |
| 32 | 33 | 0.022 | 0.103 | 0 | 0.141 | 0.403 |
| 33 | 34 | 0.033 | 0.154 | 0 | 0.212 | 0.605 |
| 33 | 394 | 0.087 | 0.03 | 0 | 0.098 | 0.116 |
| 34 | 35 | 0.006 | 0.029 | 0 | 0.04 | 0.115 |
| 35 | 36 | 0.019 | 0.088 | 0 | 0.121 | 0.346 |
| 36 | 37 | 0.01 | 0.044 | 0 | 0.06 | 0.173 |

**Table I-2**
**Line Data for Power Distribution System II. Note: There is a 30 Degree Phase Shift**
**between Buses 1000 and 1 (Continued)**

| From Bus | To Bus | R (+) (%) | X (+) (%) | Line Charg. (+) (%) | R (0) (%) | X (0) (%) |
|---|---|---|---|---|---|---|
| 37 | 38 | 0.158 | 0.216 | 0 | 0.344 | 0.694 |
| 37 | 57 | 0.016 | 0.046 | 0 | 0.064 | 0.171 |
| 38 | 39 | 0.11 | 0.15 | 0 | 0.239 | 0.483 |
| 39 | 40 | 0.219 | 0.301 | 0 | 0.479 | 0.966 |
| 40 | 41 | 0.302 | 0.413 | 0 | 0.658 | 1.328 |
| 41 | 42 | 0.123 | 0.169 | 0 | 0.269 | 0.543 |
| 42 | 43 | 0.151 | 0.207 | 0 | 0.329 | 0.664 |
| 57 | 58 | 0.042 | 0.123 | 0 | 0.171 | 0.455 |
| 58 | 59 | 0.081 | 0.237 | 0 | 0.332 | 0.881 |
| 59 | 60 | 0.039 | 0.115 | 0 | 0.161 | 0.426 |
| 60 | 61 | 0.036 | 0.107 | 0 | 0.15 | 0.398 |
| 61 | 62 | 0.076 | 0.222 | 0 | 0.311 | 0.825 |
| 62 | 63 | 0.031 | 0.092 | 0 | 0.128 | 0.341 |
| 63 | 64 | 0.049 | 0.146 | 0 | 0.203 | 0.54 |
| 63 | 344 | 0.179 | 0.062 | 0 | 0.227 | 0.202 |
| 64 | 65 | 0.065 | 0.192 | 0 | 0.268 | 0.711 |
| 65 | 66 | 0.023 | 0.069 | 0 | 0.096 | 0.256 |
| 66 | 67 | 0.047 | 0.138 | 0 | 0.193 | 0.512 |
| 67 | 68 | 0.096 | 0.283 | 0 | 0.396 | 1.052 |
| 68 | 69 | 0.042 | 0.123 | 0 | 0.171 | 0.455 |
| 69 | 70 | 0.052 | 0.153 | 0 | 0.214 | 0.569 |
| 70 | 71 | 0.013 | 0.038 | 0 | 0.054 | 0.142 |
| 70 | 267 | 0.008 | 0.023 | 0 | 0.032 | 0.085 |
| 71 | 72 | 0.062 | 0.085 | 0 | 0.135 | 0.272 |
| 72 | 73 | 0.082 | 0.113 | 0 | 0.179 | 0.362 |
| 73 | 74 | 0.096 | 0.132 | 0 | 0.209 | 0.422 |
| 74 | 75 | 0.165 | 0.225 | 0 | 0.359 | 0.724 |
| 75 | 76 | 0.24 | 0.329 | 0 | 0.524 | 1.056 |
| 76 | 77 | 0.144 | 0.197 | 0 | 0.314 | 0.634 |
| 77 | 78 | 0.082 | 0.113 | 0 | 0.179 | 0.362 |
| 78 | 79 | 0.027 | 0.038 | 0 | 0.06 | 0.121 |
| 78 | 128 | 0.047 | 0.067 | 0 | 0.115 | 0.239 |
| 79 | 80 | 0.329 | 0.451 | 0 | 0.718 | 1.448 |
| 80 | 81 | 0.199 | 0.272 | 0 | 0.434 | 0.875 |
| 81 | 82 | 0.329 | 0.451 | 0 | 0.718 | 1.448 |
| 82 | 83 | 0.062 | 0.085 | 0 | 0.135 | 0.272 |
| 83 | 84 | 0.261 | 0.357 | 0 | 0.568 | 1.147 |
| 84 | 85 | 0.192 | 0.263 | 0 | 0.419 | 0.845 |

**Table I-2**
**Line Data for Power Distribution System II.  Note:  There is a 30 Degree Phase Shift**
**between Buses 1000 and 1 (Continued)**

| From Bus | To Bus | R (+) | X (+) | Line Charg. (+) | R (0) | X (0) |
|---|---|---|---|---|---|---|
| | | (%) | (%) | (%) | (%) | (%) |
| 85 | 86 | 0.089 | 0.122 | 0 | 0.194 | 0.392 |
| 86 | 87 | 0.069 | 0.094 | 0 | 0.15 | 0.302 |
| 87 | 88 | 0.089 | 0.031 | 0 | 0.114 | 0.101 |
| 88 | 89 | 0.447 | 0.154 | 0 | 0.568 | 0.504 |
| 89 | 90 | 0.536 | 0.185 | 0 | 0.682 | 0.605 |
| 90 | 91 | 0.536 | 0.185 | 0 | 0.682 | 0.605 |
| 91 | 92 | 0.596 | 0.205 | 0 | 0.758 | 0.673 |
| 91 | 122 | 0.447 | 0.154 | 0 | 0.568 | 0.504 |
| 92 | 93 | 0.507 | 0.175 | 0 | 0.644 | 0.572 |
| 93 | 94 | 0.358 | 0.123 | 0 | 0.455 | 0.404 |
| 94 | 95 | 0.387 | 0.134 | 0 | 0.493 | 0.437 |
| 95 | 96 | 0.417 | 0.144 | 0 | 0.531 | 0.471 |
| 95 | 102 | 0.477 | 0.164 | 0 | 0.606 | 0.538 |
| 96 | 97 | 0.119 | 0.041 | 0 | 0.152 | 0.135 |
| 97 | 98 | 0.834 | 0.288 | 0 | 1.061 | 0.942 |
| 102 | 103 | 0.209 | 0.072 | 0 | 0.265 | 0.235 |
| 103 | 104 | 0.089 | 0.031 | 0 | 0.114 | 0.101 |
| 128 | 129 | 0.071 | 0.101 | 0 | 0.173 | 0.359 |
| 129 | 130 | 0.077 | 0.109 | 0 | 0.187 | 0.388 |
| 130 | 131 | 0.071 | 0.101 | 0 | 0.173 | 0.359 |
| 131 | 132 | 0.071 | 0.101 | 0 | 0.173 | 0.359 |
| 132 | 133 | 0.071 | 0.101 | 0 | 0.173 | 0.359 |
| 133 | 134 | 0.029 | 0.042 | 0 | 0.072 | 0.149 |
| 134 | 135 | 0.047 | 0.067 | 0 | 0.115 | 0.239 |
| 135 | 136 | 0.041 | 0.059 | 0 | 0.101 | 0.209 |
| 136 | 137 | 0.024 | 0.034 | 0 | 0.058 | 0.12 |
| 137 | 138 | 0.065 | 0.093 | 0 | 0.158 | 0.329 |
| 138 | 139 | 0.041 | 0.059 | 0 | 0.101 | 0.209 |
| 139 | 140 | 0.041 | 0.056 | 0 | 0.09 | 0.181 |
| 139 | 247 | 0.144 | 0.197 | 0 | 0.314 | 0.634 |
| 140 | 141 | 0.11 | 0.15 | 0 | 0.239 | 0.483 |
| 140 | 246 | 0.052 | 0.012 | 0 | 0.097 | 0.019 |
| 141 | 142 | 0.075 | 0.103 | 0 | 0.165 | 0.332 |
| 142 | 143 | 0.048 | 0.066 | 0 | 0.105 | 0.211 |
| 143 | 144 | 0.069 | 0.094 | 0 | 0.15 | 0.302 |
| 144 | 145 | 0.021 | 0.028 | 0 | 0.045 | 0.091 |
| 145 | 146 | 0.021 | 0.028 | 0 | 0.045 | 0.091 |
| 146 | 147 | 0.034 | 0.047 | 0 | 0.075 | 0.151 |

**Table I-2**
**Line Data for Power Distribution System II.  Note:  There is a 30 Degree Phase Shift between Buses 1000 and 1 (Continued)**

| From Bus | To Bus | R (+) | X (+) | Line Charg. (+) | R (0) | X (0) |
|---|---|---|---|---|---|---|
| | | (%) | (%) | (%) | (%) | (%) |
| 147 | 148 | 0.055 | 0.075 | 0 | 0.12 | 0.241 |
| 148 | 149 | 0.158 | 0.216 | 0 | 0.344 | 0.694 |
| 149 | 150 | 0.075 | 0.103 | 0 | 0.165 | 0.332 |
| 150 | 151 | 0.062 | 0.085 | 0 | 0.135 | 0.272 |
| 151 | 152 | 0.075 | 0.103 | 0 | 0.165 | 0.332 |
| 152 | 153 | 0.387 | 0.134 | 0 | 0.493 | 0.437 |
| 152 | 177 | 0.165 | 0.225 | 0 | 0.359 | 0.724 |
| 153 | 154 | 0.149 | 0.051 | 0 | 0.189 | 0.168 |
| 154 | 155 | 1.132 | 0.39 | 0 | 1.44 | 1.278 |
| 155 | 156 | 0.804 | 0.277 | 0 | 1.023 | 0.908 |
| 156 | 157 | 0.298 | 0.103 | 0 | 0.379 | 0.336 |
| 157 | 158 | 0.655 | 0.226 | 0 | 0.834 | 0.74 |
| 177 | 178 | 0.144 | 0.197 | 0 | 0.314 | 0.634 |
| 178 | 179 | 0.034 | 0.047 | 0 | 0.075 | 0.151 |
| 179 | 180 | 0.387 | 0.134 | 0 | 0.493 | 0.437 |
| 180 | 181 | 0.715 | 0.246 | 0 | 0.91 | 0.807 |
| 181 | 182 | 0.089 | 0.031 | 0 | 0.114 | 0.101 |
| 182 | 183 | 0.387 | 0.134 | 0 | 0.493 | 0.437 |
| 183 | 184 | 0.149 | 0.051 | 0 | 0.189 | 0.168 |
| 184 | 185 | 0.328 | 0.113 | 0 | 0.417 | 0.37 |
| 185 | 186 | 0.924 | 0.318 | 0 | 1.175 | 1.042 |
| 186 | 187 | 0.417 | 0.144 | 0 | 0.531 | 0.471 |
| 187 | 188 | 0.477 | 0.164 | 0 | 0.606 | 0.538 |
| 188 | 189 | 0.417 | 0.144 | 0 | 0.531 | 0.471 |
| 189 | 190 | 0.216 | 0.175 | 0 | 0.353 | 0.528 |
| 189 | 195 | 0.953 | 0.329 | 0 | 1.213 | 1.076 |
| 190 | 191 | 0.152 | 0.123 | 0 | 0.249 | 0.373 |
| 191 | 192 | 0.025 | 0.021 | 0 | 0.042 | 0.062 |
| 192 | 194 | 0.342 | 0.277 | 0 | 0.561 | 0.838 |
| 195 | 196 | 0.894 | 0.308 | 0 | 1.137 | 1.009 |
| 196 | 197 | 0.447 | 0.154 | 0 | 0.568 | 0.504 |
| 267 | 268 | 0.417 | 0.144 | 0 | 0.531 | 0.471 |
| 268 | 269 | 0.328 | 0.113 | 0 | 0.417 | 0.37 |
| 269 | 270 | 0.209 | 0.072 | 0 | 0.265 | 0.235 |
| 270 | 271 | 0.655 | 0.226 | 0 | 0.834 | 0.74 |
| 271 | 272 | 0.953 | 0.329 | 0 | 1.213 | 1.076 |
| 272 | 273 | 0.238 | 0.082 | 0 | 0.303 | 0.269 |
| 273 | 274 | 0.119 | 0.041 | 0 | 0.152 | 0.135 |

**Table I-2**
**Line Data for Power Distribution System II.  Note:  There is a 30 Degree Phase Shift between Buses 1000 and 1 (Continued)**

| From Bus | To Bus | R (+) | X (+) | Line Charg. (+) | R (0) | X (0) |
|---|---|---|---|---|---|---|
| | | (%) | (%) | (%) | (%) | (%) |
| 274 | 275 | 0.864 | 0.298 | 0 | 1.099 | 0.975 |
| 275 | 276 | 0.209 | 0.072 | 0 | 0.265 | 0.235 |
| 276 | 277 | 0.216 | 0.175 | 0 | 0.353 | 0.528 |
| 277 | 278 | 0.342 | 0.277 | 0 | 0.561 | 0.838 |
| 278 | 279 | 0.127 | 0.103 | 0 | 0.208 | 0.31 |
| 279 | 280 | 0.279 | 0.226 | 0 | 0.457 | 0.683 |
| 280 | 281 | 0.393 | 0.318 | 0 | 0.644 | 0.962 |
| 281 | 282 | 0.406 | 0.329 | 0 | 0.665 | 0.993 |
| 282 | 283 | 0.279 | 0.226 | 0 | 0.457 | 0.683 |
| 283 | 284 | 0.228 | 0.185 | 0 | 0.374 | 0.559 |
| 284 | 285 | 0.393 | 0.318 | 0 | 0.644 | 0.962 |
| 344 | 345 | 0.387 | 0.134 | 0 | 0.493 | 0.437 |
| 345 | 346 | 0.447 | 0.154 | 0 | 0.568 | 0.504 |
| 394 | 395 | 0.358 | 0.123 | 0 | 0.455 | 0.404 |
| 395 | 396 | 0.477 | 0.164 | 0 | 0.606 | 0.538 |
| 414 | 415 | 0.953 | 0.329 | 0 | 1.213 | 1.076 |

# J
# APPENDIX J – BUS AND LINE DATA FOR POWER DISTRIBUTION NETWORK III

**Table J-1**
**Bus Data for Power Distribution Network III**

| Bus Number | Bus Type | P Load (%) | Q Load (%) | Bus Voltage (%) | Shunt Load (%) |
|---|---|---|---|---|---|
| 2 | 3 | 0 | 0 | | 0 |
| 3 | 3 | 0 | 0 | | 0 |
| 4 | 3 | 0 | 0 | | 0 |
| 5 | 3 | 0.02 | 0.01 | | 0 |
| 6 | 3 | 0.09 | 0.05 | | 0 |
| 7 | 3 | 0 | 0 | | 0 |
| 8 | 3 | 0.65 | 0.36 | | 0 |
| 9 | 3 | 0.56 | 0.32 | | 0 |
| 10 | 3 | 0.22 | 0.13 | | 0 |
| 11 | 3 | 0.24 | 0.13 | | 0 |
| 12 | 3 | 0 | 0 | | 0 |
| 13 | 3 | 0 | 0 | | 0 |
| 14 | 3 | 0.02 | 0.01 | | 0 |
| 15 | 3 | 0 | 0 | | 0 |
| 16 | 3 | 0 | 0 | | 0 |
| 17 | 3 | 0 | 0 | | 0 |
| 18 | 3 | 0 | 0 | | -6 |
| 19 | 3 | 0 | 0 | | 0 |
| 20 | 3 | 0 | 0 | | 0 |
| 21 | 3 | 0.19 | 0.12 | | 0 |
| 22 | 3 | 0.23 | 0.14 | | 0 |
| 23 | 3 | 0.65 | 0.4 | | 0 |
| 24 | 3 | 0.52 | 0.32 | | 0 |
| 25 | 3 | 0 | 0 | | 0 |
| 26 | 3 | 0.29 | 0.18 | | 0 |
| 28 | 3 | 0 | 0 | | 0 |
| 29 | 3 | 0 | 0 | | 0 |
| 30 | 3 | 0.23 | 0.13 | | 0 |
| 31 | 3 | 0.05 | 0.03 | | 0 |
| 32 | 3 | 0.04 | 0.02 | | 0 |

**Table J-1**
**Bus Data for Power Distribution Network III (Continued)**

| Bus Number | Bus Type | P Load (%) | Q Load (%) | Bus Voltage (%) | Shunt Load (%) |
|---|---|---|---|---|---|
| 33 | 3 | 0.23 | 0.14 | | 0 |
| 34 | 3 | 0.19 | 0.12 | | 0 |
| 35 | 3 | 0.92 | 0.57 | | 0 |
| 36 | 3 | 0.26 | 0.15 | | 0 |
| 37 | 3 | 0.04 | 0.02 | | 0 |
| 38 | 3 | 0 | 0 | | 0 |
| 39 | 3 | 0.06 | 0.03 | | 0 |
| 40 | 3 | 0.04 | 0.02 | | 0 |
| 41 | 3 | 0 | 0 | | -12 |
| 42 | 3 | 0 | 0 | | 0 |
| 43 | 3 | 1.13 | 0.7 | | 0 |
| 44 | 3 | 0 | 0 | | 0 |
| 45 | 3 | 0.17 | 0.09 | | 0 |
| 46 | 3 | 0 | 0 | | 0 |
| 47 | 3 | 0.71 | 0.44 | | 0 |
| 48 | 3 | 0 | 0 | | 0 |
| 49 | 3 | 1.63 | 1.01 | | 0 |
| 59 | 3 | 0 | 0 | | 0 |
| 60 | 3 | 0.05 | 0.03 | | 0 |
| 61 | 3 | 0.23 | 0.14 | | 0 |
| 62 | 3 | 0.34 | 0.21 | | 0 |
| 63 | 3 | 0 | 0 | | 0 |
| 64 | 3 | 0 | 0 | | 0 |
| 65 | 3 | 0 | 0 | | 0 |
| 66 | 3 | 0 | 0 | | 0 |
| 67 | 3 | 0 | 0 | | 0 |
| 68 | 3 | 0 | 0 | | 0 |
| 69 | 3 | 0 | 0 | | 0 |
| 70 | 3 | 0.23 | 0.14 | | 0 |
| 71 | 3 | 0.59 | 0.37 | | 0 |
| 74 | 3 | 0.84 | 0.52 | | 0 |
| 75 | 3 | 0 | 0 | | 0 |
| 76 | 3 | 0.61 | 0.37 | | 0 |
| 77 | 3 | 0.88 | 0.54 | | 0 |
| 82 | 3 | 1.04 | 0.65 | | 0 |
| 83 | 3 | 0 | 0 | | 0 |
| 84 | 3 | 0 | 0 | | 0 |
| 85 | 3 | 0 | 0 | | 0 |
| 86 | 3 | 0.14 | 0.09 | | 0 |

**Table J-1**
**Bus Data for Power Distribution Network III (Continued)**

| Bus Number | Bus Type | P Load (%) | Q Load (%) | Bus Voltage (%) | Shunt Load (%) |
|---|---|---|---|---|---|
| 87 | 3 | 0 | 0 | | 0 |
| 88 | 3 | 0.27 | 0.16 | | 0 |
| 89 | 3 | 5.84 | 3.62 | | 0 |
| 93 | 3 | 0 | 0 | | -6 |
| 94 | 3 | 0 | 0 | | 0 |
| 95 | 3 | 0.04 | 0.03 | | 0 |
| 96 | 3 | 0 | 0 | | 0 |
| 98 | 3 | 0.15 | 0.09 | | 0 |
| 99 | 3 | 0.2 | 0.12 | | 0 |
| 100 | 3 | 0.08 | 0.04 | | 0 |
| 101 | 3 | 0 | 0 | | 0 |
| 102 | 3 | 0.01 | 0.01 | | 0 |
| 103 | 3 | 0 | 0 | | 0 |
| 105 | 3 | 0 | 0 | | 0 |
| 106 | 3 | 0.1 | 0.06 | | 0 |
| 107 | 3 | 0 | 0 | | 0 |
| 111 | 3 | 1.22 | 0.76 | | 0 |
| 114 | 3 | 0.1 | 0.06 | | 0 |
| 115 | 3 | 0.16 | 0.1 | | 0 |
| 118 | 3 | 0 | 0 | | 0 |
| 119 | 3 | 0.62 | 0.39 | | 0 |
| 120 | 3 | 0 | 0 | | 0 |
| 121 | 3 | 0 | 0 | | 0 |
| 122 | 3 | 0.66 | 0.41 | | 0 |
| 123 | 3 | 0.07 | 0.04 | | 0 |
| 124 | 3 | 0.77 | 0.47 | | 0 |
| 125 | 3 | 0 | 0 | | -6 |
| 126 | 3 | 0.76 | 0.47 | | 0 |
| 127 | 3 | 0 | 0 | | 0 |
| 128 | 3 | 0 | 0 | | 0 |
| 129 | 3 | 0 | 0 | | 0 |
| 130 | 3 | 1.14 | 0.7 | | 0 |
| 131 | 3 | 0.03 | 0.02 | | 0 |
| 132 | 3 | 0 | 0 | | 0 |
| 133 | 3 | 0.36 | 0.21 | | 0 |
| 134 | 3 | 0 | 0 | | 0 |
| 135 | 3 | 0 | 0 | | 0 |
| 136 | 3 | 1.01 | 0.62 | | 0 |
| 137 | 3 | 1.24 | 0.77 | | 0 |

**Table J-1**
**Bus Data for Power Distribution Network III (Continued)**

| Bus Number | Bus Type | P Load (%) | Q Load (%) | Bus Voltage (%) | Shunt Load (%) |
|---|---|---|---|---|---|
| 142 | 3 | 0 | 0 | | 0 |
| 143 | 3 | 0 | 0 | | 0 |
| 144 | 3 | 1.27 | 0.79 | | 0 |
| 145 | 3 | 0 | 0 | | 0 |
| 146 | 3 | 0.42 | 0.26 | | 0 |
| 157 | 3 | 0 | 0 | | 0 |
| 158 | 3 | 0 | 0 | | 0 |
| 159 | 3 | 0 | 0 | | 0 |
| 160 | 3 | 0.97 | 0.6 | | 0 |
| 161 | 3 | 0.06 | 0.04 | | 0 |
| 162 | 3 | 0.18 | 0.11 | | 0 |
| 163 | 3 | 1.95 | 1.2 | | 0 |
| 164 | 3 | 0.36 | 0.22 | | 0 |
| 165 | 3 | 0.09 | 0.06 | | 0 |
| 166 | 3 | 1.02 | 0.63 | | 0 |
| 167 | 3 | 0.88 | 0.54 | | 0 |
| 173 | 3 | 0 | 0 | | 0 |
| 174 | 3 | 0.25 | 0.15 | | 0 |
| 175 | 3 | 0 | 0 | | 0 |
| 176 | 3 | 0.84 | 0.49 | | 0 |
| 177 | 3 | 0 | 0 | | 0 |
| 178 | 3 | 0.34 | 0.21 | | 0 |
| 179 | 3 | 0 | 0 | | 0 |
| 180 | 3 | 0.06 | 0.03 | | 0 |
| 181 | 3 | 0 | 0 | | 0 |
| 182 | 3 | 0.41 | 0.26 | | 0 |
| 188 | 3 | 0.01 | 0.01 | | 0 |
| 189 | 3 | 0.26 | 0.15 | | 0 |
| 190 | 3 | 1 | 0.62 | | 0 |
| 195 | 3 | 0 | 0 | | 0 |
| 196 | 3 | 0.03 | 0.01 | | 0 |
| 197 | 3 | 0 | 0 | | 0 |
| 198 | 3 | 0 | 0 | | 0 |
| 199 | 3 | 0.24 | 0.15 | | 0 |
| 200 | 3 | 0.64 | 0.4 | | 0 |
| 201 | 3 | 0.45 | 0.28 | | 0 |
| 202 | 3 | 0 | 0 | | 0 |
| 203 | 3 | 0.45 | 0.28 | | 0 |
| 204 | 3 | 0 | 0 | | 0 |

**Table J-1**
**Bus Data for Power Distribution Network III (Continued)**

| Bus Number | Bus Type | P Load (%) | Q Load (%) | Bus Voltage (%) | Shunt Load (%) |
|---|---|---|---|---|---|
| 205 | 3 | 0 | 0 | | 0 |
| 206 | 3 | 1.69 | 1.04 | | 0 |
| 207 | 3 | 0 | 0 | | 0 |
| 208 | 3 | 0.24 | 0.15 | | 0 |
| 209 | 3 | 0.28 | 0.17 | | 0 |
| 210 | 3 | 0 | 0 | | 0 |
| 211 | 3 | 0 | 0 | | 0 |
| 212 | 3 | 0.93 | 0.58 | | 0 |
| 213 | 3 | 2.62 | 1.62 | | 0 |
| 214 | 3 | 0.01 | 0.01 | | 0 |
| 215 | 3 | 0 | 0 | | 0 |
| 216 | 3 | 1.16 | 0.72 | | 0 |
| 217 | 3 | 0.04 | 0.02 | | 0 |
| 218 | 3 | 0.01 | 0.01 | | 0 |
| 219 | 3 | 0.02 | 0.01 | | 0 |
| 220 | 3 | 0.01 | 0 | | 0 |
| 221 | 3 | 0.01 | 0 | | 0 |
| 222 | 3 | 0 | 0 | | 0 |
| 223 | 3 | 0.37 | 0.23 | | 0 |
| 224 | 3 | 0 | 0 | | 0 |
| 226 | 3 | 0 | 0 | | 0 |
| 227 | 3 | 0 | 0 | | 0 |
| 228 | 3 | 0.28 | 0.17 | | 0 |
| 229 | 3 | 0 | 0 | | 0 |
| 230 | 3 | 0.15 | 0.08 | | 0 |
| 231 | 3 | 0.32 | 0.18 | | 0 |
| 232 | 3 | 0.95 | 0.56 | | 0 |
| 233 | 3 | 0.1 | 0.06 | | 0 |
| 234 | 3 | 1.81 | 1.09 | | 0 |
| 235 | 3 | 0 | 0 | | 0 |
| 236 | 3 | 0.08 | 0.05 | | 0 |
| 237 | 3 | 0.07 | 0.04 | | 0 |
| 238 | 3 | 0 | 0 | | 0 |
| 239 | 3 | 2.58 | 1.6 | | 0 |
| 277 | 3 | 0.61 | 0.35 | | 0 |
| 278 | 3 | 0 | 0 | | 0 |
| 279 | 3 | 3.48 | 1.94 | | 0 |
| 327 | 3 | 0.04 | 0.02 | | 0 |
| 328 | 3 | 0.09 | 0.05 | | 0 |

**Table J-1**
**Bus Data for Power Distribution Network III (Continued)**

| Bus Number | Bus Type | P Load (%) | Q Load (%) | Bus Voltage (%) | Shunt Load (%) |
|---|---|---|---|---|---|
| 329 | 3 | 0 | 0 | | 0 |
| 330 | 3 | 0.06 | 0.03 | | 0 |
| 331 | 3 | 0.09 | 0.05 | | 0 |
| 332 | 3 | 0.09 | 0.05 | | 0 |
| 333 | 3 | 0.11 | 0.06 | | 0 |
| 334 | 3 | 0.04 | 0.02 | | 0 |
| 335 | 3 | 0.08 | 0.04 | | 0 |
| 336 | 3 | 0.12 | 0.06 | | 0 |
| 337 | 3 | 0.02 | 0.01 | | 0 |
| 338 | 3 | 0 | 0 | | 0 |
| 352 | 3 | 0 | 0 | | 0 |
| 353 | 3 | 0.04 | 0.02 | | 0 |
| 354 | 3 | 0.11 | 0.07 | | 0 |
| 355 | 3 | 0.16 | 0.1 | | 0 |
| 356 | 3 | 0.8 | 0.45 | | 0 |
| 357 | 3 | 0 | 0 | | 0 |
| 358 | 3 | 0.05 | 0.03 | | 0 |
| 359 | 3 | 0.08 | 0.05 | | 0 |
| 360 | 3 | 0.2 | 0.12 | | 0 |
| 373 | 3 | 0 | 0 | | 0 |
| 375 | 3 | 0 | 0 | | 0 |
| 376 | 3 | 1.72 | 1.07 | | 0 |
| 377 | 3 | 0 | 0 | | 0 |
| 389 | 3 | 0.65 | 0.4 | | 0 |
| 390 | 3 | 0.06 | 0.04 | | 0 |
| 391 | 3 | 0.18 | 0.11 | | 0 |
| 392 | 3 | 0 | 0 | | 0 |
| 393 | 3 | 1.77 | 1.07 | | 0 |
| 394 | 3 | 0 | 0 | | 0 |
| 395 | 3 | 0.9 | 0.49 | | 0 |
| 396 | 3 | 0.67 | 0.41 | | 0 |
| 397 | 3 | 0 | 0 | | 0 |
| 398 | 3 | 0.24 | 0.15 | | 0 |
| 399 | 3 | 0 | 0 | | 0 |
| 400 | 3 | 0.55 | 0.34 | | 0 |
| 401 | 3 | 0 | 0 | | 0 |
| 402 | 3 | 0.7 | 0.44 | | 0 |
| 404 | 3 | 0.1 | 0.06 | | 0 |
| 405 | 3 | 0.05 | 0.03 | | 0 |

**Table J-1**
**Bus Data for Power Distribution Network III (Continued)**

| Bus Number | Bus Type | P Load (%) | Q Load (%) | Bus Voltage (%) | Shunt Load (%) |
|---|---|---|---|---|---|
| 406 | 3 | 0.52 | 0.32 | | 0 |
| 407 | 3 | 0.88 | 0.54 | | 0 |
| 410 | 3 | 0.1 | 0.06 | | 0 |
| 411 | 3 | 0.52 | 0.29 | | 0 |
| 412 | 3 | 0 | 0 | | 0 |
| 413 | 3 | 0 | 0 | | 0 |
| 414 | 3 | 0 | 0 | | -12 |
| 415 | 3 | 0 | 0 | | 0 |
| 416 | 3 | 0.05 | 0.03 | | 0 |
| 417 | 3 | 0 | 0 | | 0 |
| 418 | 3 | 0.3 | 0.17 | | 0 |
| 419 | 3 | 0 | 0 | | 0 |
| 420 | 3 | 0.83 | 0.51 | | 0 |
| 421 | 3 | 0.87 | 0.51 | | 0 |
| 446 | 3 | 0.02 | 0.01 | | 0 |
| 447 | 3 | 0.22 | 0.12 | | 0 |
| 448 | 3 | 0.13 | 0.08 | | 0 |
| 449 | 3 | 0.19 | 0.1 | | 0 |
| 450 | 3 | 0 | 0 | | 0 |
| 524 | 3 | 1.41 | 0.88 | | 0 |
| 555 | 3 | 0 | 0 | | 0 |
| 1000 | 1 | | | 105 | |
| 1 | 3 | 0 | 0 | 0 | 0 |

**Table J-2**
**Line Data for Power Distribution System III. Note: There is a 30 Degree Phase Shift between Buses 1000 and 1**

| From Bus | To Bus | R (+) (%) | X(+) (%) | Line Charg. (+) | R (0) (%) | X (0) (%) |
|---|---|---|---|---|---|---|
| 1000 | 1 | 0.404 | 8.104 | 0 | 0.885 | 21.238 |
| 1 | 2 | 0.016 | 0.046 | 0 | 0.06 | 0.164 |
| 2 | 3 | 0.047 | 0.137 | 0 | 0.141 | 0.431 |
| 3 | 4 | 0.034 | 0.1 | 0 | 0.103 | 0.311 |
| 4 | 5 | 0.066 | 0.14 | 0 | 0.16 | 0.432 |
| 5 | 6 | 0.102 | 0.217 | 0 | 0.249 | 0.673 |
| 6 | 7 | 0.051 | 0.109 | 0 | 0.125 | 0.337 |
| 7 | 8 | 0.047 | 0.101 | 0 | 0.116 | 0.312 |
| 8 | 9 | 0.099 | 0.21 | 0 | 0.24 | 0.649 |
| 9 | 10 | 0.095 | 0.202 | 0 | 0.232 | 0.625 |
| 10 | 11 | 0.036 | 0.077 | 0 | 0.089 | 0.241 |
| 11 | 12 | 0.052 | 0.109 | 0 | 0.124 | 0.336 |
| 12 | 13 | 0.044 | 0.13 | 0 | 0.134 | 0.407 |
| 13 | 14 | 0.068 | 0.199 | 0 | 0.204 | 0.622 |
| 14 | 15 | 0.026 | 0.077 | 0 | 0.079 | 0.239 |
| 15 | 16 | 0.007 | 0.023 | 0 | 0.023 | 0.072 |
| 16 | 17 | 0.066 | 0.191 | 0 | 0.197 | 0.598 |
| 17 | 18 | 0.02 | 0.062 | 0 | 0.085 | 0.228 |
| 18 | 19 | 0.024 | 0.069 | 0 | 0.097 | 0.255 |
| 19 | 20 | 0.149 | 0.051 | 0 | 0.189 | 0.168 |
| 20 | 21 | 0.566 | 0.195 | 0 | 0.72 | 0.639 |
| 21 | 22 | 0.476 | 0.164 | 0 | 0.606 | 0.538 |
| 22 | 23 | 0.209 | 0.072 | 0 | 0.266 | 0.236 |
| 23 | 24 | 0.566 | 0.195 | 0 | 0.72 | 0.638 |
| 24 | 25 | 0.477 | 0.165 | 0 | 0.606 | 0.538 |
| 25 | 26 | 0.119 | 0.041 | 0 | 0.152 | 0.135 |
| 19 | 28 | 0.039 | 0.115 | 0 | 0.149 | 0.409 |
| 28 | 29 | 0.095 | 0.201 | 0 | 0.306 | 0.742 |
| 29 | 30 | 0.095 | 0.202 | 0 | 0.306 | 0.742 |
| 30 | 31 | 0.098 | 0.21 | 0 | 0.317 | 0.771 |
| 31 | 32 | 0.241 | 0.513 | 0 | 0.776 | 1.883 |
| 32 | 33 | 0.537 | 0.185 | 0 | 0.682 | 0.606 |
| 33 | 34 | 0.625 | 0.215 | 0 | 0.796 | 0.706 |
| 34 | 35 | 0.328 | 0.113 | 0 | 0.416 | 0.37 |
| 32 | 36 | 0.252 | 0.535 | 0 | 0.74 | 1.857 |
| 36 | 37 | 0.095 | 0.202 | 0 | 0.305 | 0.742 |
| 37 | 38 | 0.011 | 0.023 | 0 | 0.036 | 0.086 |
| 38 | 39 | 0.066 | 0.14 | 0 | 0.211 | 0.513 |

**Table J-2**
**Line Data for Power Distribution System III.  Note: There is a 30 Degree Phase Shift**
**between Buses 1000 and 1 (Continued)**

| From Bus | To Bus | R (+) | X(+) | Line Charg. (+) | R (0) | X (0) |
|---|---|---|---|---|---|---|
| | | (%) | (%) | | (%) | (%) |
| 39 | 40 | 0.062 | 0.132 | 0 | 0.2 | 0.486 |
| 40 | 41 | 0.037 | 0.078 | 0 | 0.118 | 0.285 |
| 41 | 42 | 0.065 | 0.139 | 0 | 0.211 | 0.514 |
| 42 | 43 | 0.567 | 0.195 | 0 | 0.72 | 0.639 |
| 43 | 44 | 0.506 | 0.175 | 0 | 0.644 | 0.571 |
| 44 | 45 | 0.268 | 0.092 | 0 | 0.341 | 0.303 |
| 45 | 46 | 0.566 | 0.195 | 0 | 0.72 | 0.639 |
| 46 | 47 | 0.447 | 0.155 | 0 | 0.569 | 0.504 |
| 46 | 48 | 0.205 | 0.046 | 0 | 0.371 | 0.073 |
| 48 | 49 | 0.123 | 0.028 | 0 | 0.222 | 0.043 |
| 42 | 59 | 0.058 | 0.124 | 0 | 0.172 | 0.431 |
| 59 | 60 | 0.084 | 0.178 | 0 | 0.271 | 0.656 |
| 60 | 61 | 0.069 | 0.148 | 0 | 0.223 | 0.542 |
| 61 | 62 | 0.146 | 0.311 | 0 | 0.47 | 1.142 |
| 62 | 63 | 0.166 | 0.331 | 0 | 0.181 | 0.373 |
| 63 | 64 | 0.04 | 0.085 | 0 | 0.13 | 0.314 |
| 64 | 65 | 0.088 | 0.26 | 0 | 0.364 | 0.966 |
| 65 | 66 | 0.042 | 0.123 | 0 | 0.171 | 0.455 |
| 66 | 67 | 0.031 | 0.092 | 0 | 0.128 | 0.341 |
| 67 | 68 | 0.367 | 0.155 | 0 | 0.511 | 0.52 |
| 68 | 69 | 0.474 | 0.201 | 0 | 0.661 | 0.674 |
| 69 | 70 | 0.238 | 0.083 | 0 | 0.303 | 0.269 |
| 70 | 71 | 0.268 | 0.092 | 0 | 0.341 | 0.302 |
| 67 | 74 | 0.096 | 0.022 | 0 | 0.173 | 0.034 |
| 66 | 75 | 0.246 | 0.056 | 0 | 0.445 | 0.087 |
| 75 | 76 | 0.328 | 0.074 | 0 | 0.594 | 0.116 |
| 76 | 77 | 0.268 | 0.092 | 0 | 0.341 | 0.303 |
| 65 | 82 | 0.068 | 0.015 | 0 | 0.124 | 0.024 |
| 64 | 83 | 0.044 | 0.13 | 0 | 0.169 | 0.464 |
| 83 | 84 | 0.089 | 0.261 | 0 | 0.364 | 0.966 |
| 84 | 85 | 0.02 | 0.061 | 0 | 0.085 | 0.228 |
| 85 | 86 | 0.206 | 0.282 | 0 | 0.449 | 0.905 |
| 86 | 87 | 0.425 | 0.582 | 0 | 0.927 | 1.87 |
| 87 | 88 | 0.474 | 0.201 | 0 | 0.661 | 0.674 |
| 88 | 89 | 0.218 | 0.05 | 0 | 0.396 | 0.078 |
| 87 | 93 | 0.185 | 0.254 | 0 | 0.404 | 0.815 |
| 93 | 94 | 0.343 | 0.47 | 0 | 0.748 | 1.509 |
| 94 | 95 | 0.13 | 0.178 | 0 | 0.284 | 0.573 |

**Table J-2**
**Line Data for Power Distribution System III.  Note: There is a 30 Degree Phase Shift between Buses 1000 and 1 (Continued)**

| From Bus | To Bus | R (+) (%) | X(+) (%) | Line Charg. (+) | R (0) (%) | X (0) (%) |
|---|---|---|---|---|---|---|
| 95 | 96 | 0.219 | 0.301 | 0 | 0.479 | 0.965 |
| 96 | 98 | 0.151 | 0.206 | 0 | 0.329 | 0.664 |
| 98 | 99 | 0.117 | 0.16 | 0 | 0.254 | 0.513 |
| 99 | 100 | 0.116 | 0.16 | 0 | 0.254 | 0.513 |
| 100 | 101 | 0.13 | 0.178 | 0 | 0.284 | 0.573 |
| 101 | 102 | 0.083 | 0.113 | 0 | 0.18 | 0.362 |
| 102 | 103 | 0.068 | 0.094 | 0 | 0.149 | 0.302 |
| 101 | 105 | 0.228 | 0.185 | 0 | 0.374 | 0.559 |
| 105 | 106 | 0.228 | 0.185 | 0 | 0.374 | 0.558 |
| 106 | 107 | 0.203 | 0.164 | 0 | 0.333 | 0.497 |
| 105 | 111 | 0.026 | 0.006 | 0 | 0.048 | 0.009 |
| 96 | 114 | 0.179 | 0.062 | 0 | 0.227 | 0.202 |
| 94 | 115 | 0.566 | 0.195 | 0 | 0.72 | 0.639 |
| 84 | 118 | 0.044 | 0.13 | 0 | 0.169 | 0.464 |
| 118 | 119 | 0.095 | 0.021 | 0 | 0.173 | 0.034 |
| 118 | 120 | 0.034 | 0.1 | 0 | 0.129 | 0.354 |
| 120 | 121 | 0.01 | 0.031 | 0 | 0.043 | 0.114 |
| 121 | 122 | 0.123 | 0.028 | 0 | 0.222 | 0.044 |
| 121 | 123 | 0.22 | 0.652 | 0 | 0.846 | 2.318 |
| 123 | 124 | 0.05 | 0.145 | 0 | 0.203 | 0.54 |
| 124 | 125 | 0.047 | 0.138 | 0 | 0.193 | 0.512 |
| 125 | 126 | 0.039 | 0.115 | 0 | 0.16 | 0.426 |
| 126 | 127 | 0.094 | 0.276 | 0 | 0.386 | 1.024 |
| 127 | 128 | 0.177 | 0.144 | 0 | 0.291 | 0.434 |
| 128 | 129 | 0.178 | 0.143 | 0 | 0.29 | 0.435 |
| 129 | 130 | 0.298 | 0.103 | 0 | 0.379 | 0.336 |
| 129 | 131 | 0.152 | 0.123 | 0 | 0.249 | 0.372 |
| 131 | 132 | 0.215 | 0.174 | 0 | 0.353 | 0.528 |
| 132 | 133 | 0.477 | 0.164 | 0 | 0.606 | 0.538 |
| 133 | 134 | 0.536 | 0.185 | 0 | 0.682 | 0.605 |
| 134 | 135 | 0.268 | 0.093 | 0 | 0.341 | 0.303 |
| 135 | 136 | 0.685 | 0.236 | 0 | 0.872 | 0.773 |
| 136 | 137 | 0.209 | 0.072 | 0 | 0.265 | 0.235 |
| 135 | 142 | 0.179 | 0.062 | 0 | 0.227 | 0.202 |
| 142 | 143 | 0.209 | 0.072 | 0 | 0.265 | 0.236 |
| 143 | 144 | 0.625 | 0.216 | 0 | 0.796 | 0.706 |
| 144 | 145 | 0.209 | 0.072 | 0 | 0.265 | 0.235 |
| 145 | 146 | 0.054 | 0.011 | 0 | 0.099 | 0.019 |

**Table J-2**
**Line Data for Power Distribution System III.  Note: There is a 30 Degree Phase Shift between Buses 1000 and 1 (Continued)**

| From Bus | To Bus | R (+) (%) | X(+) (%) | Line Charg. (+) | R (0) (%) | X (0) (%) |
|---|---|---|---|---|---|---|
| 132 | 157 | 1.102 | 0.38 | 0 | 1.402 | 1.244 |
| 157 | 158 | 0.119 | 0.041 | 0 | 0.152 | 0.135 |
| 158 | 159 | 0.238 | 0.082 | 0 | 0.303 | 0.268 |
| 159 | 160 | 0.209 | 0.072 | 0 | 0.265 | 0.236 |
| 160 | 161 | 0.566 | 0.195 | 0 | 0.72 | 0.639 |
| 161 | 162 | 0.804 | 0.278 | 0 | 1.023 | 0.907 |
| 162 | 163 | 0.923 | 0.318 | 0 | 1.175 | 1.043 |
| 163 | 164 | 0.298 | 0.103 | 0 | 0.379 | 0.336 |
| 164 | 165 | 0.566 | 0.195 | 0 | 0.719 | 0.639 |
| 165 | 166 | 0.09 | 0.03 | 0 | 0.114 | 0.101 |
| 165 | 167 | 0.055 | 0.012 | 0 | 0.099 | 0.019 |
| 157 | 173 | 0.357 | 0.123 | 0 | 0.455 | 0.403 |
| 129 | 174 | 0.357 | 0.123 | 0 | 0.455 | 0.403 |
| 127 | 175 | 0.01 | 0.044 | 0 | 0.06 | 0.173 |
| 175 | 176 | 0.021 | 0.095 | 0 | 0.131 | 0.374 |
| 176 | 177 | 0.03 | 0.139 | 0 | 0.192 | 0.547 |
| 177 | 178 | 0.027 | 0.125 | 0 | 0.171 | 0.49 |
| 178 | 179 | 0.019 | 0.088 | 0 | 0.121 | 0.345 |
| 179 | 180 | 0.007 | 0.029 | 0 | 0.04 | 0.115 |
| 180 | 181 | 0.268 | 0.093 | 0 | 0.341 | 0.303 |
| 181 | 182 | 0.357 | 0.123 | 0 | 0.455 | 0.403 |
| 180 | 188 | 0.238 | 0.082 | 0 | 0.303 | 0.269 |
| 188 | 189 | 0.596 | 0.206 | 0 | 0.758 | 0.673 |
| 189 | 190 | 0.566 | 0.195 | 0 | 0.72 | 0.638 |
| 178 | 195 | 0.01 | 0.044 | 0 | 0.06 | 0.173 |
| 195 | 196 | 0.017 | 0.081 | 0 | 0.111 | 0.317 |
| 196 | 197 | 0.06 | 0.02 | 0 | 0.076 | 0.067 |
| 197 | 198 | 0.119 | 0.041 | 0 | 0.152 | 0.135 |
| 196 | 199 | 0.014 | 0.066 | 0 | 0.091 | 0.259 |
| 199 | 200 | 0.268 | 0.092 | 0 | 0.341 | 0.303 |
| 200 | 201 | 0.257 | 0.011 | 0 | 0.051 | 0.07 |
| 201 | 202 | 0.016 | 0.073 | 0 | 0.101 | 0.288 |
| 202 | 203 | 0.005 | 0.022 | 0 | 0.03 | 0.086 |
| 203 | 204 | 0.02 | 0.095 | 0 | 0.131 | 0.374 |
| 204 | 205 | 0.032 | 0.147 | 0 | 0.202 | 0.576 |
| 205 | 206 | 0.022 | 0.103 | 0 | 0.141 | 0.403 |
| 206 | 207 | 0.005 | 0.022 | 0 | 0.03 | 0.087 |
| 207 | 208 | 0.024 | 0.11 | 0 | 0.151 | 0.432 |

**Table J-2**
**Line Data for Power Distribution System III.  Note: There is a 30 Degree Phase Shift**
**between Buses 1000 and 1 (Continued)**

| From Bus | To Bus | R (+) (%) | X(+) (%) | Line Charg. (+) | R (0) (%) | X (0) (%) |
|---|---|---|---|---|---|---|
| 208 | 209 | 0.026 | 0.117 | 0 | 0.162 | 0.46 |
| 209 | 210 | 0.054 | 0.249 | 0 | 0.342 | 0.979 |
| 210 | 211 | 0.032 | 0.147 | 0 | 0.202 | 0.576 |
| 211 | 212 | 0.033 | 0.154 | 0 | 0.211 | 0.605 |
| 212 | 213 | 0.149 | 0.051 | 0 | 0.19 | 0.168 |
| 213 | 214 | 0.09 | 0.031 | 0 | 0.113 | 0.101 |
| 214 | 215 | 0.029 | 0.01 | 0 | 0.038 | 0.033 |
| 212 | 216 | 0.06 | 0.021 | 0 | 0.076 | 0.067 |
| 212 | 217 | 0.01 | 0.044 | 0 | 0.06 | 0.173 |
| 217 | 218 | 0.067 | 0.307 | 0 | 0.423 | 1.209 |
| 218 | 219 | 0.027 | 0.125 | 0 | 0.171 | 0.489 |
| 219 | 220 | 0.019 | 0.088 | 0 | 0.121 | 0.346 |
| 220 | 221 | 0.029 | 0.132 | 0 | 0.181 | 0.518 |
| 221 | 222 | 0.04 | 0.183 | 0 | 0.252 | 0.72 |
| 222 | 223 | 0.088 | 0.072 | 0 | 0.146 | 0.217 |
| 223 | 224 | 0.19 | 0.154 | 0 | 0.311 | 0.466 |
| 222 | 226 | 0.19 | 0.154 | 0 | 0.311 | 0.465 |
| 226 | 227 | 0.038 | 0.031 | 0 | 0.062 | 0.093 |
| 227 | 228 | 0.298 | 0.103 | 0 | 0.379 | 0.336 |
| 228 | 229 | 0.536 | 0.185 | 0 | 0.682 | 0.605 |
| 229 | 230 | 0.238 | 0.082 | 0 | 0.303 | 0.269 |
| 230 | 231 | 0.447 | 0.154 | 0 | 0.569 | 0.504 |
| 231 | 232 | 0.179 | 0.061 | 0 | 0.227 | 0.202 |
| 232 | 233 | 0.417 | 0.144 | 0 | 0.531 | 0.471 |
| 233 | 234 | 0.387 | 0.134 | 0 | 0.492 | 0.437 |
| 234 | 235 | 0.149 | 0.051 | 0 | 0.19 | 0.168 |
| 235 | 236 | 0.089 | 0.031 | 0 | 0.113 | 0.101 |
| 236 | 237 | 0.864 | 0.297 | 0 | 1.099 | 0.975 |
| 237 | 238 | 0.566 | 0.196 | 0 | 0.72 | 0.639 |
| 238 | 239 | 0.078 | 0.017 | 0 | 0.145 | 0.028 |
| 226 | 277 | 0.101 | 0.082 | 0 | 0.166 | 0.248 |
| 277 | 278 | 0.343 | 0.278 | 0 | 0.561 | 0.838 |
| 278 | 279 | 0.076 | 0.061 | 0 | 0.125 | 0.186 |
| 278 | 327 | 0.254 | 0.205 | 0 | 0.415 | 0.621 |
| 327 | 328 | 0.19 | 0.154 | 0 | 0.311 | 0.465 |
| 328 | 329 | 0.152 | 0.123 | 0 | 0.25 | 0.373 |
| 329 | 330 | 0.051 | 0.041 | 0 | 0.083 | 0.124 |
| 330 | 331 | 0.026 | 0.021 | 0 | 0.041 | 0.062 |

**Table J-2**
**Line Data for Power Distribution System III.  Note: There is a 30 Degree Phase Shift between Buses 1000 and 1 (Continued)**

| From Bus | To Bus | R (+) (%) | X(+) (%) | Line Charg. (+) | R (0) (%) | X (0) (%) |
|---|---|---|---|---|---|---|
| 331 | 332 | 0.266 | 0.215 | 0 | 0.436 | 0.652 |
| 332 | 333 | 0.228 | 0.185 | 0 | 0.374 | 0.558 |
| 333 | 334 | 0.228 | 0.185 | 0 | 0.374 | 0.559 |
| 334 | 335 | 0.216 | 0.175 | 0 | 0.354 | 0.528 |
| 335 | 336 | 0.253 | 0.205 | 0 | 0.415 | 0.62 |
| 336 | 337 | 0.115 | 0.092 | 0 | 0.187 | 0.28 |
| 337 | 338 | 0.088 | 0.072 | 0 | 0.145 | 0.217 |
| 208 | 352 | 0.775 | 0.267 | 0 | 0.985 | 0.874 |
| 352 | 353 | 0.298 | 0.102 | 0 | 0.378 | 0.336 |
| 353 | 354 | 0.506 | 0.175 | 0 | 0.645 | 0.572 |
| 354 | 355 | 0.507 | 0.174 | 0 | 0.644 | 0.571 |
| 355 | 356 | 0.054 | 0.161 | 0 | 0.225 | 0.597 |
| 356 | 357 | 0.044 | 0.13 | 0 | 0.182 | 0.483 |
| 357 | 358 | 0.045 | 0.131 | 0 | 0.182 | 0.484 |
| 358 | 359 | 0.036 | 0.107 | 0 | 0.149 | 0.398 |
| 359 | 360 | 0.039 | 0.115 | 0 | 0.161 | 0.426 |
| 355 | 373 | 0.149 | 0.051 | 0 | 0.189 | 0.168 |
| 207 | 375 | 0.096 | 0.022 | 0 | 0.173 | 0.034 |
| 375 | 376 | 0.136 | 0.031 | 0 | 0.248 | 0.048 |
| 206 | 377 | 0.01 | 0.044 | 0 | 0.06 | 0.173 |
| 127 | 389 | 0.044 | 0.13 | 0 | 0.169 | 0.464 |
| 389 | 390 | 0.028 | 0.084 | 0 | 0.118 | 0.313 |
| 390 | 391 | 0.034 | 0.1 | 0 | 0.139 | 0.369 |
| 391 | 392 | 0.024 | 0.069 | 0 | 0.096 | 0.256 |
| 392 | 393 | 0.017 | 0.08 | 0 | 0.111 | 0.317 |
| 393 | 394 | 0.019 | 0.088 | 0 | 0.121 | 0.345 |
| 394 | 395 | 0.045 | 0.206 | 0 | 0.282 | 0.807 |
| 395 | 396 | 0.328 | 0.113 | 0 | 0.417 | 0.37 |
| 396 | 397 | 0.268 | 0.092 | 0 | 0.341 | 0.302 |
| 397 | 398 | 0.298 | 0.103 | 0 | 0.379 | 0.336 |
| 398 | 399 | 0.208 | 0.072 | 0 | 0.265 | 0.236 |
| 399 | 400 | 0.358 | 0.123 | 0 | 0.455 | 0.403 |
| 400 | 401 | 0.465 | 0.16 | 0 | 0.596 | 0.532 |
| 401 | 402 | 0.815 | 0.281 | 0 | 1.044 | 0.931 |
| 395 | 404 | 0.054 | 0.249 | 0 | 0.342 | 0.979 |
| 404 | 405 | 0.566 | 0.195 | 0 | 0.719 | 0.638 |
| 405 | 406 | 0.239 | 0.082 | 0 | 0.304 | 0.269 |
| 406 | 407 | 0.417 | 0.144 | 0 | 0.53 | 0.471 |

**Table J-2**
**Line Data for Power Distribution System III.  Note: There is a 30 Degree Phase Shift between Buses 1000 and 1 (Continued)**

| From Bus | To Bus | R (+) (%) | X(+) (%) | Line Charg. (+) | R (0) (%) | X (0) (%) |
|---|---|---|---|---|---|---|
| 404 | 410 | 0.045 | 0.205 | 0 | 0.282 | 0.806 |
| 410 | 411 | 0.011 | 0.051 | 0 | 0.07 | 0.201 |
| 411 | 412 | 0.024 | 0.11 | 0 | 0.151 | 0.432 |
| 412 | 413 | 0.03 | 0.14 | 0 | 0.192 | 0.547 |
| 413 | 414 | 0.011 | 0.051 | 0 | 0.07 | 0.202 |
| 414 | 415 | 0.04 | 0.183 | 0 | 0.252 | 0.72 |
| 415 | 416 | 0.01 | 0.044 | 0 | 0.061 | 0.173 |
| 416 | 417 | 0.238 | 0.082 | 0 | 0.303 | 0.269 |
| 417 | 418 | 0.953 | 0.329 | 0 | 1.212 | 1.075 |
| 418 | 419 | 0.209 | 0.072 | 0 | 0.266 | 0.236 |
| 419 | 420 | 0.328 | 0.113 | 0 | 0.416 | 0.37 |
| 419 | 421 | 1.102 | 0.38 | 0 | 1.402 | 1.244 |
| 415 | 446 | 0.026 | 0.117 | 0 | 0.161 | 0.461 |
| 446 | 447 | 0.021 | 0.096 | 0 | 0.131 | 0.374 |
| 447 | 448 | 0.043 | 0.198 | 0 | 0.272 | 0.777 |
| 448 | 449 | 0.019 | 0.088 | 0 | 0.121 | 0.346 |
| 449 | 450 | 0.019 | 0.087 | 0 | 0.121 | 0.345 |
| 83 | 524 | 0.464 | 0.105 | 0 | 0.841 | 0.165 |
| 15 | 555 | 0.016 | 0.046 | 0 | 0.06 | 0.164 |

*Target:*

End-Use Power Quality Mitigation Systems

**About EPRI**

EPRI creates science and technology solutions for the global energy and energy services industry. U.S. electric utilities established the Electric Power Research Institute in 1973 as a nonprofit research consortium for the benefit of utility members, their customers, and society. Now known simply as EPRI, the company provides a wide range of innovative products and services to more than 1000 energy-related organizations in 40 countries. EPRI's multidisciplinary team of scientists and engineers draws on a worldwide network of technical and business expertise to help solve today's toughest energy and environmental problems.

EPRI. Electrify the World

1000664